

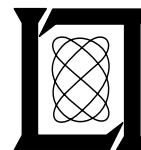
**Project Report
ATC-37**

An Analysis of Aircraft L-Band Beacon Antenna Patterns

G.J. Schlieckert

15 January 1975

Lincoln Laboratory
MASSACHUSETTS INSTITUTE OF TECHNOLOGY
LEXINGTON, MASSACHUSETTS



Prepared for the Federal Aviation Administration,
Washington, D.C. 20591

This document is available to the public through
the National Technical Information Service,
Springfield, VA 22161

This document is disseminated under the sponsorship of the Department of Transportation in the interest of information exchange. The United States Government assumes no liability for its contents or use thereof.

1. Report No. FAA-RD-74-144		2. Government Accession No.		3. Recipient's Catalog No.	
4. Title and Subtitle An Analysis of Aircraft L-Band Beacon Antenna Patterns				5. Report Date 15 January 1975	
				6. Performing Organization Code	
7. Author(s) G.J. Schlieckert				8. Performing Organization Report No. ATC-37	
9. Performing Organization Name and Address Massachusetts Institute of Technology Lincoln Laboratory P.O. Box 73 Lexington, Massachusetts 02173				10. Work Unit No. (TRAIS) 45364 Project No. 034-241-012	
				11. Contract or Grant No. DOT-FA-72-WAI-261	
12. Sponsoring Agency Name and Address Department of Transportation Federal Aviation Administration Systems Research and Development Service Washington, D.C. 20591				13. Type of Report and Period Covered Project Report	
				14. Sponsoring Agency Code	
15. Supplementary Notes The work reported in this document was performed at Lincoln Laboratory, a center for research operated by Massachusetts Institute of Technology under Air Force Contract F19628-73-C-0002.					
16. Abstract Radiation patterns are examined for L-Band beacon antennas mounted on aircraft ranging from small, single-engine, general aviation aircraft to the Boeing 747. The data analyzed consists of antenna gain values taken in two degree (2°) steps over a spherical surface centered at the antenna location. Data from three representative scale model aircraft are studied in detail and show the effects of various airframe structural members on the radiation lobe patterns and the relative performance of antennas located at a number of positions on each scale model aircraft. Significant observations were that:					
17. Key Words Aircraft antenna patterns Shielding Maneuvers Statistics General-aviation Air-carrier				18. Distribution Statement Document is available to the public through the National Technical Information Service, Springfield, Virginia 22151.	
20. Security Classif. (of this page) Unclassified		21. No. of Pages 116			

TABLE OF CONTENTS

<u>Section</u>	<u>Page</u>
1. INTRODUCTION	1
2. AIRCRAFT TYPES AND TEST CONFIGURATIONS	1
3. PATTERN COORDINATES	3
4. AIRFRAME STRUCTURAL EFFECTS (BASED ON UNPROCESSED PATTERN DATA)	4
4.1 CESSNA 150	4
4.2 PIPER CHEROKEE ARROW	16
4.3 BOEING 727	19
5. EFFECTS OF AIRFRAME STRUCTURE AND ANTENNA LOCATION UPON AIRBORNE ANTENNA PERFORMANCE (BASED ON PROCESSED PATTERN DATA)	23
5.1 STATISTICAL TREATMENT OF PATTERN DATA	26
5.2 EFFECT OF DATA INACCURACIES	31
5.3 EFFECTS OF LANDING GEAR AND FLAPS	32
5.3.1 Cessna 150	35
5.3.2 Piper Cherokee Arrow	35
5.3.3 Boeing 727	41
5.4 ROLL MANEUVERS	41
5.4.1 Cessna 150	41
5.4.2 Piper Cherokee Arrow	43
5.4.3 Boeing 727	43
5.5 PITCH MANEUVERS	46
5.6 EFFECTS OF ANTENNA LOCATION	49
6. EFFECTS OF STRUCTURE AND ANTENNA LOCATION OBSERVED ON OTHER AIRCRAFT TYPES	62
7. SUMMARY AND CONCLUSIONS	74
APPENDIX A Photos and Drawings of Aircraft Showing Antenna and Landing Gear Locations	76
APPENDIX B Aircraft-Ground Sensor Coordinate Relationships	106
APPENDIX C Effect of Depression Angle on Radiation Statistics	110

1. INTRODUCTION

The performance of an air traffic control beacon system is affected by the occurrence of very low aircraft antenna gain at certain aspect angles. At these angles the received signal energy is insufficient for reliable link performance between the aircraft and the ground station. This report presents pattern data for L-band antennas mounted at several locations on a number of aircraft. An examination of the statistics of these patterns has enabled the effects of various physical structures, such as the landing gear, flaps, fuselage, and wings, to be determined and comparisons of overall antenna-airframe radiation performance to be made. Such comparisons are presented in this report.

2. AIRCRAFT TYPES AND TEST CONFIGURATIONS

Antenna pattern data has been obtained for a variety of aircraft models, as listed in Table 1. Since a large portion of general-aviation traffic is made up of single-engine aircraft, of which the Cessna 150 (high wing) and the Piper Cherokee Arrow (low wing) aircraft are typical, and since the Boeing 727 is a widely used air carrier, aircraft pattern data from these aircraft form the primary data for this report. Photos or drawings of these aircraft are given in Appendix A.

Because the antenna patterns cannot reasonably be made on full size aircraft, scale model aircraft were used.* Several general-aviation aircraft

* Scale model measurements were made by Lincoln Laboratory at their Bedford Antenna Test Range or supplied by contract with the Boeing Commercial Airplane Company. Pattern measurements were taken at an appropriately scaled-up frequency (20-40 GHz) corresponding to the L-band frequency used in beacon operations (1030 MHz/1090 MHz).

TABLE 1
SCALE MODEL AIRCRAFT TESTED

<u>Aircraft Type</u>	<u>Aircraft Class</u>	<u>Scale</u>	<u>Extendable</u>	
			<u>Wheels</u>	<u>Flaps</u>
Cessna 150	Single engine high wing; G/A	1/20	yes	yes
Helio U10	Single engine high wing; G/A	1/20	yes	yes
Cherokee Arrow	Single engine low wing; G/A	1/20	yes	yes
Beech Baron	Twin engine low wing; G/A	1/20	yes	yes
Beech B99	Twin engine low wing; G/A	1/20	yes	yes
Grumman Gulstream	Small jet; G/A	1/20	yes	yes
Gates Lear Jet	Small jet; G/A	1/20	yes	yes
Boeing 727	Large jet; A/C	1/25	yes	no
Boeing 737	Large jet; A/C	1/20	yes	no
Boeing 707	Large jet; A/C	1/20	yes	no
Boeing 747	Jumbo jet; A/C	1/40	yes	no

models were built to 1/20th scale and air carrier models from 1/20th to 1/40th scale. The general-aviation models were made from wood and coated with a silver paint, while the air carrier models were made from molded plastic covered with thin copper sheeting. For aircraft with retractable landing gear, the landing gear structures of the models are removable to simulate the wheels in the retracted or stowed condition. The general-aviation aircraft models also have flap structures which can be placed in the retracted or fully-extended positions. On the commercial airliner models, however, the flaps are fixed in the retracted position. Therefore, up to four combinations of flap and landing gear conditions can apply to each model, a separate pattern being recorded for each combination. Patterns were recorded using vertical polarization for several antenna locations, including at least one top-mounted antenna and one bottom-mounted antenna on each model. Only data on bottom-mounted antennas are presented in this report. The effects of the landing gear and flaps on the antenna patterns are discussed in later sections of this report. If patterns for several bottom-mounted antenna positions were recorded on the same aircraft, the effect of antenna location is also discussed.

3. PATTERN COORDINATES

Data used in this study consist of antenna pattern measurements taken over the entire sphere of polar coordinate aspect angles (4π steradians). The polar coordinate system used is defined in the usual sense relative to a Cartesian system whose origin is at the antenna. The X-axis is parallel to a line connecting the aircraft wing tips, with positive values in the direction of the right wing, and the Y-axis is parallel to the fuselage center line, with the positive direction toward the nose of the aircraft. The Z-axis in this right-handed coordinate

system is normal to the XY plane with the positive direction toward the top of the aircraft. This coordinate system is shown in Fig. 1 with the common polar angle relationship. The polar coordinates φ and θ are referred to as the azimuthal and vertical aspect angles.

The model is placed in a uniform radiation field and antenna patterns are measured at two-degree increments in both polar angles, with φ varying from 0 to 358 degrees and θ from 1 to 179 degrees. This results in a total of 16200 samples for each pattern.* By integrating over these samples the antenna pattern is normalized to units of decibels relative to an isotropic radiator (dBi).

4. AIRFRAME STRUCTURAL EFFECTS (BASED ON UNPROCESSED PATTERN DATA)

4.1 Cessna 150

Figure 2 shows a region in θ and φ coordinates with the gain values represented by shaded areas between constant gain contours at 10 dB intervals. This figure is for the Cessna 150. The landing gear is not retractable and, for this case, the flaps are in the up or retracted position. Only data from the central half of the θ values are shown since this is the region of the antenna pattern generally involved with ground communications.

The general shape of the spherical pattern can be shown by various planar or conical cuts through the sphere. The principal plane cuts, the XY, YZ, ZX planes, are shown in Figs. 3, 4 and 5, respectively, and are horizontal and vertical cuts from the data in Fig. 2. The gain as a function of heading is obtained, for level flight, by a horizontal cut through Fig. 6

*For the air carrier antenna patterns θ varies from 0 to 180 degrees and results in 16380 samples.

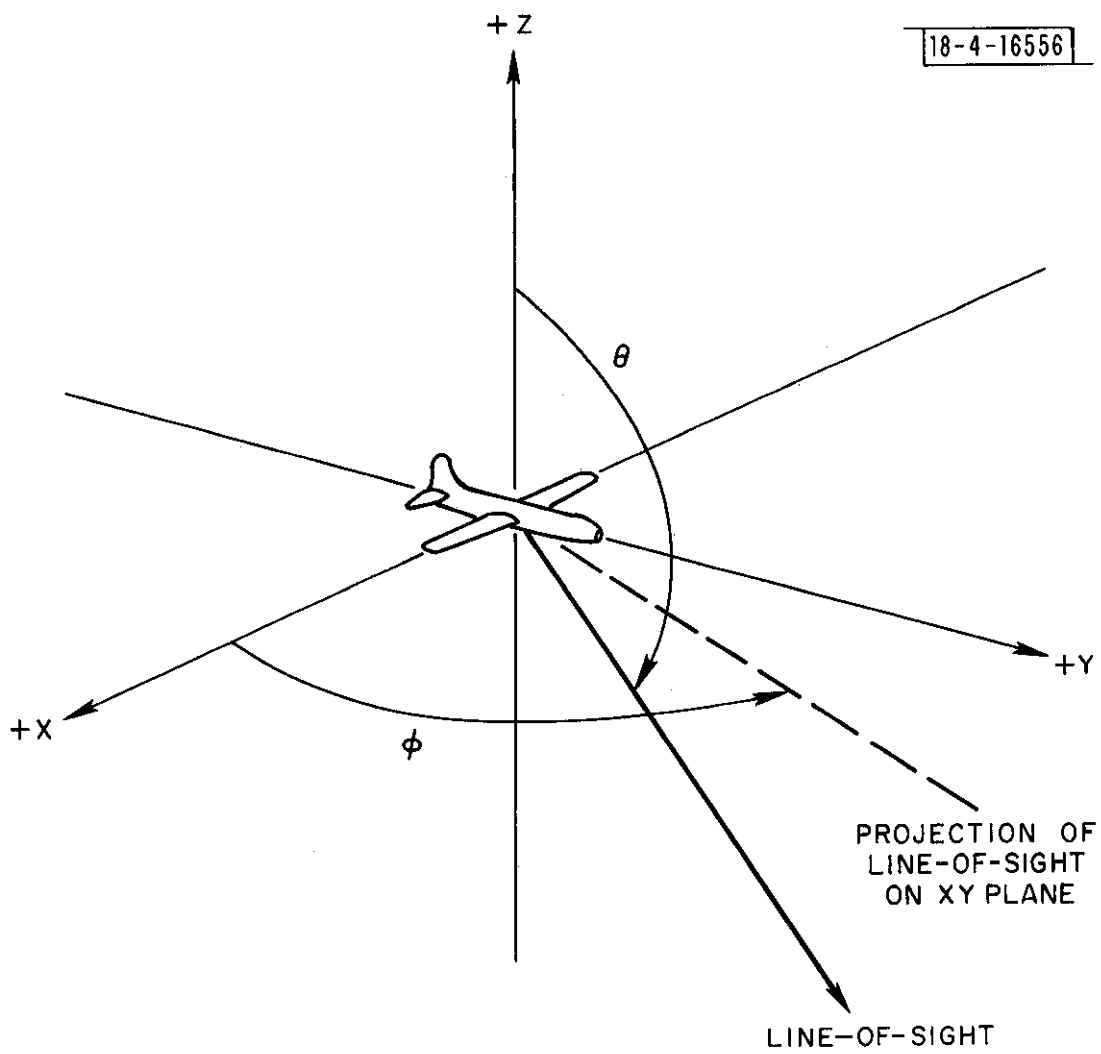


Fig. 1. Definition of aircraft aspect angles.

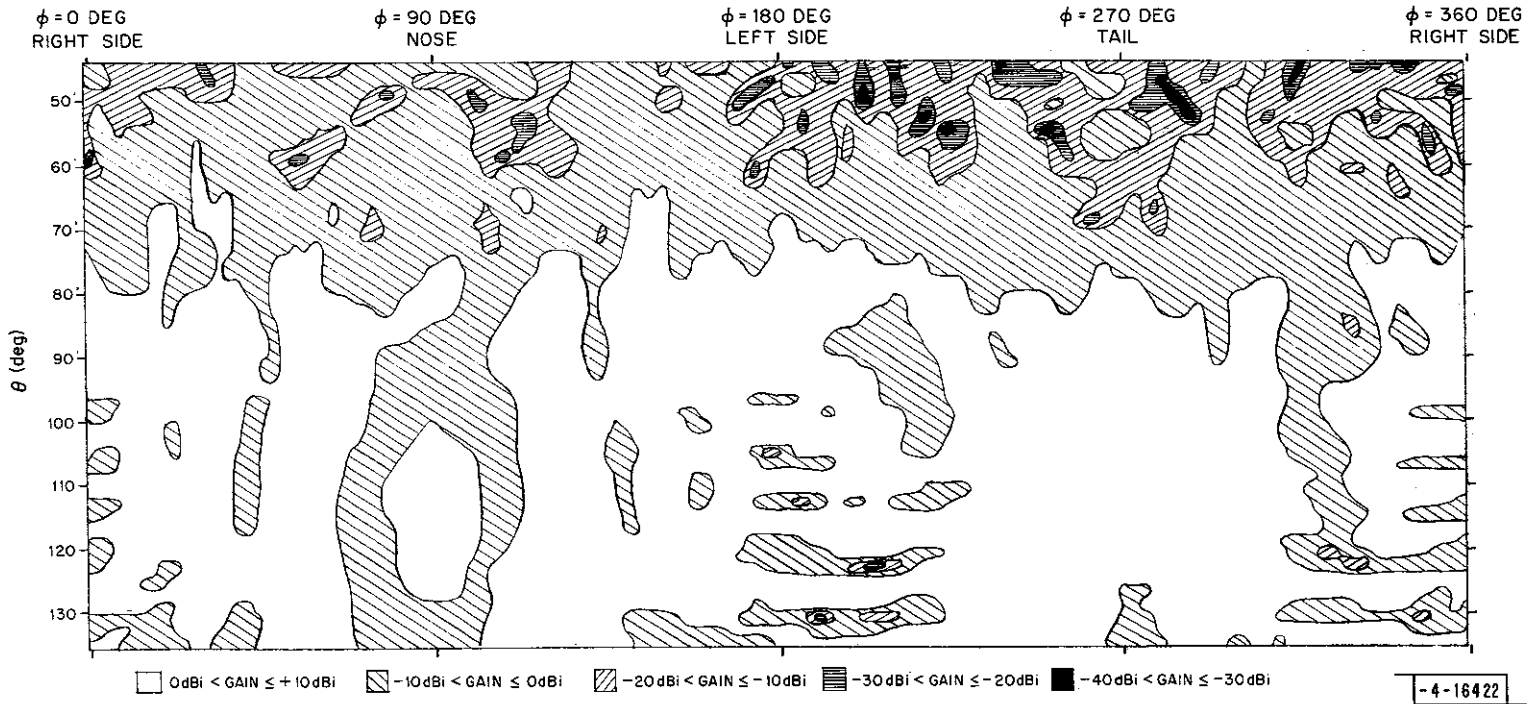


Fig. 2 Gain contours for Cessna 150 over θ, ϕ (antenna 3; flaps up).

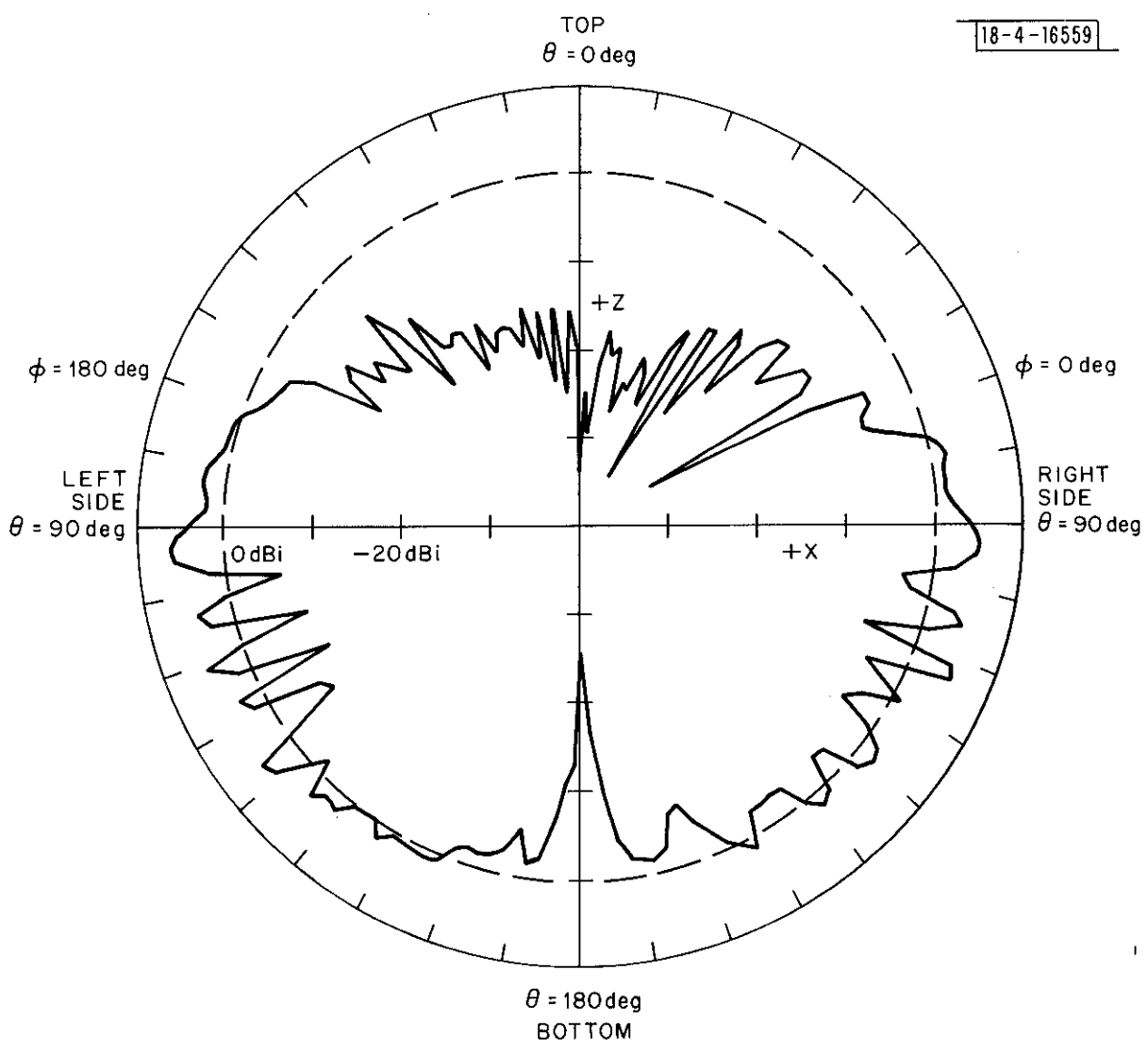


Fig. 5. Cessna 150 antenna pattern in ZX-plane (antenna 3; flaps up).

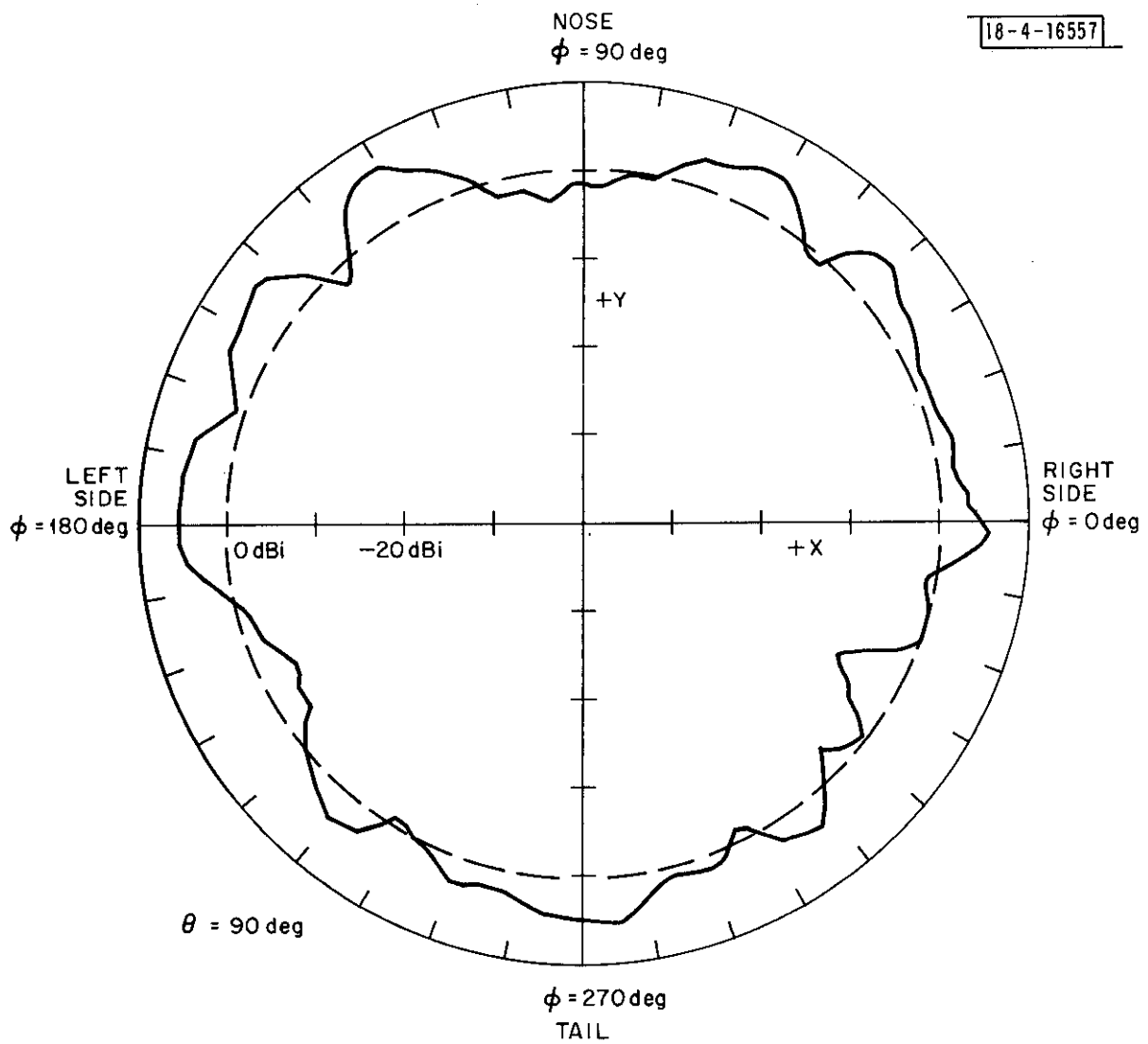


Fig. 3. Cessna 150 antenna pattern in XY-plane (antenna 3; flaps up).

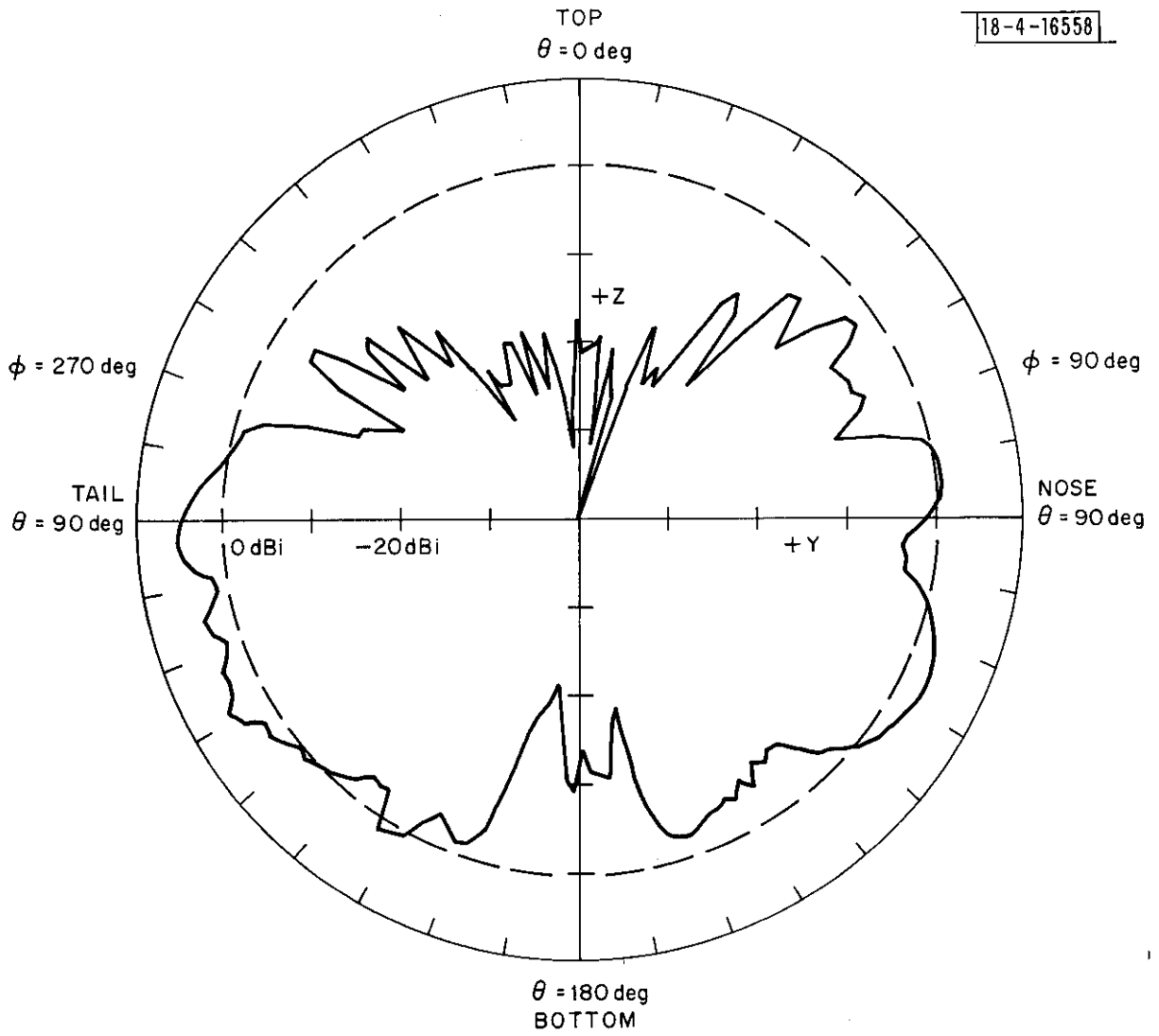


Fig. 4. Cessna 150 antenna pattern in YZ-plane (antenna 3; flaps up).

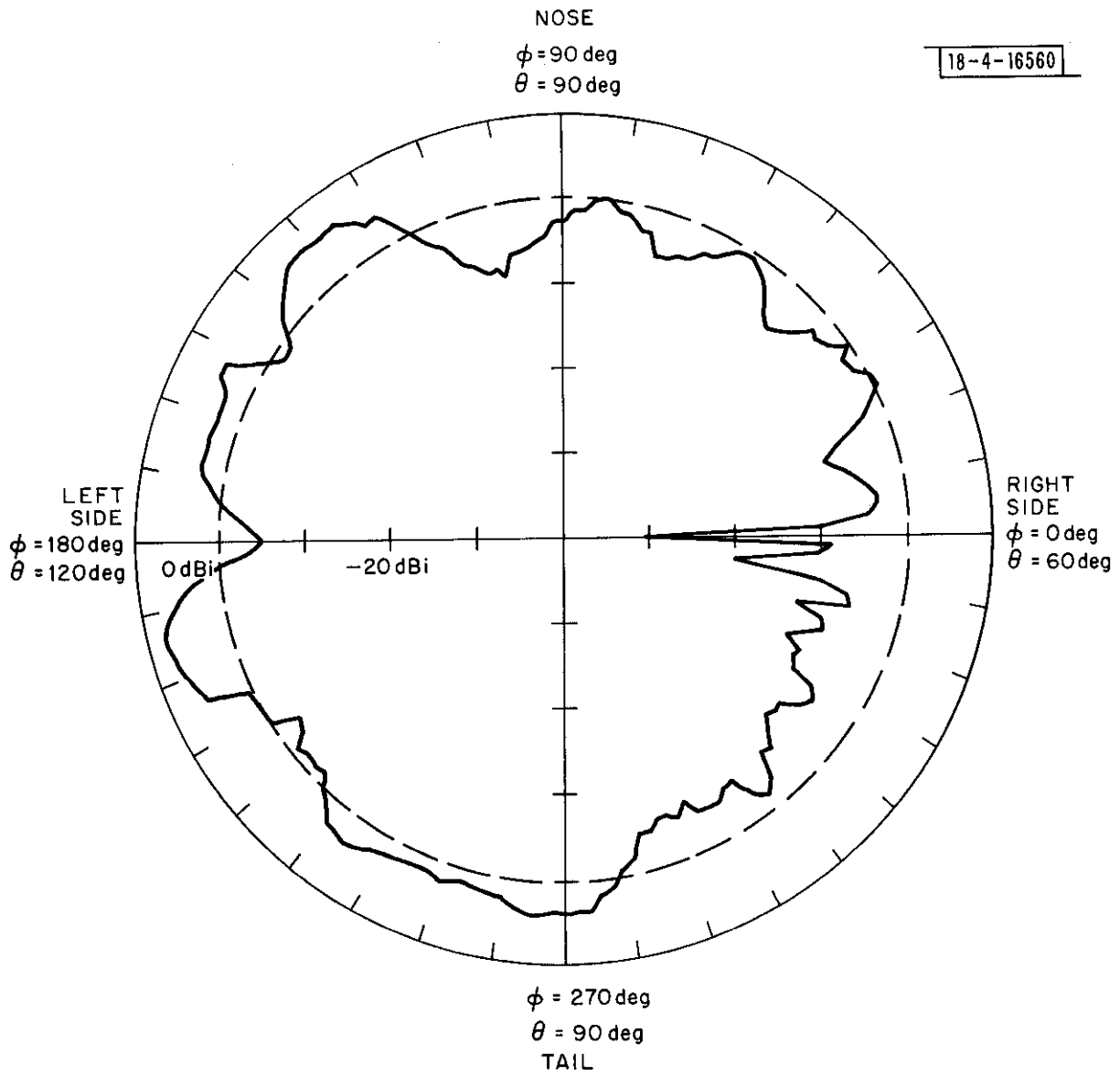


Fig. 6. Cessna 150 antenna pattern for roll = + 30° (antenna 3; flaps up).

at a fixed θ value, depending on the relative geometry between the aircraft and the ground sensor. On a spherical presentation of the pattern this is a conical cut.

For a banked or pitched aircraft the sampling is more complicated but is approximated by a cosine or sine function, respectively, on Fig. 2. Two examples of the gain versus heading for roll only and pitch only conditions are given in Figs. 6 and 7. The actual relationship between the aspect angles for a level aircraft heading north and the aspect angles for an aircraft with non-zero roll, pitch and heading angles is given in Appendix II.

There are symmetries and contour shapes in Fig. 2 which are explainable by analysis of the aircraft structure. In a (θ, φ) representation, the structural features of the Cessna 150 are distorted when viewed from the antenna position. Figure 8 shows how a number of the structural members of the aircraft appear in such a plot. Included is a sinusoidal curve which represents a flat plane tangent to the fuselage at the antenna and would be the lower limit of θ for the pattern if the fuselage was not curved or limited in extent. Because of diffraction and reflection effects, structural surfaces above this curve do affect the antenna pattern.

Although the Cessna airframe represents a complicated geometrical shape, it is possible to identify some of the diffraction and reflection mechanisms which produce the contour shapes. The most prominent feature is the doughnut-shaped region at $\varphi = 90^\circ$ corresponding to the nose-on azimuth view. Referring to Fig. 8, one observes the obvious presence of the nose-wheel strut in this region. From experience with elementary optics theory, this ring of lower gain values and the isolated curved regions at around

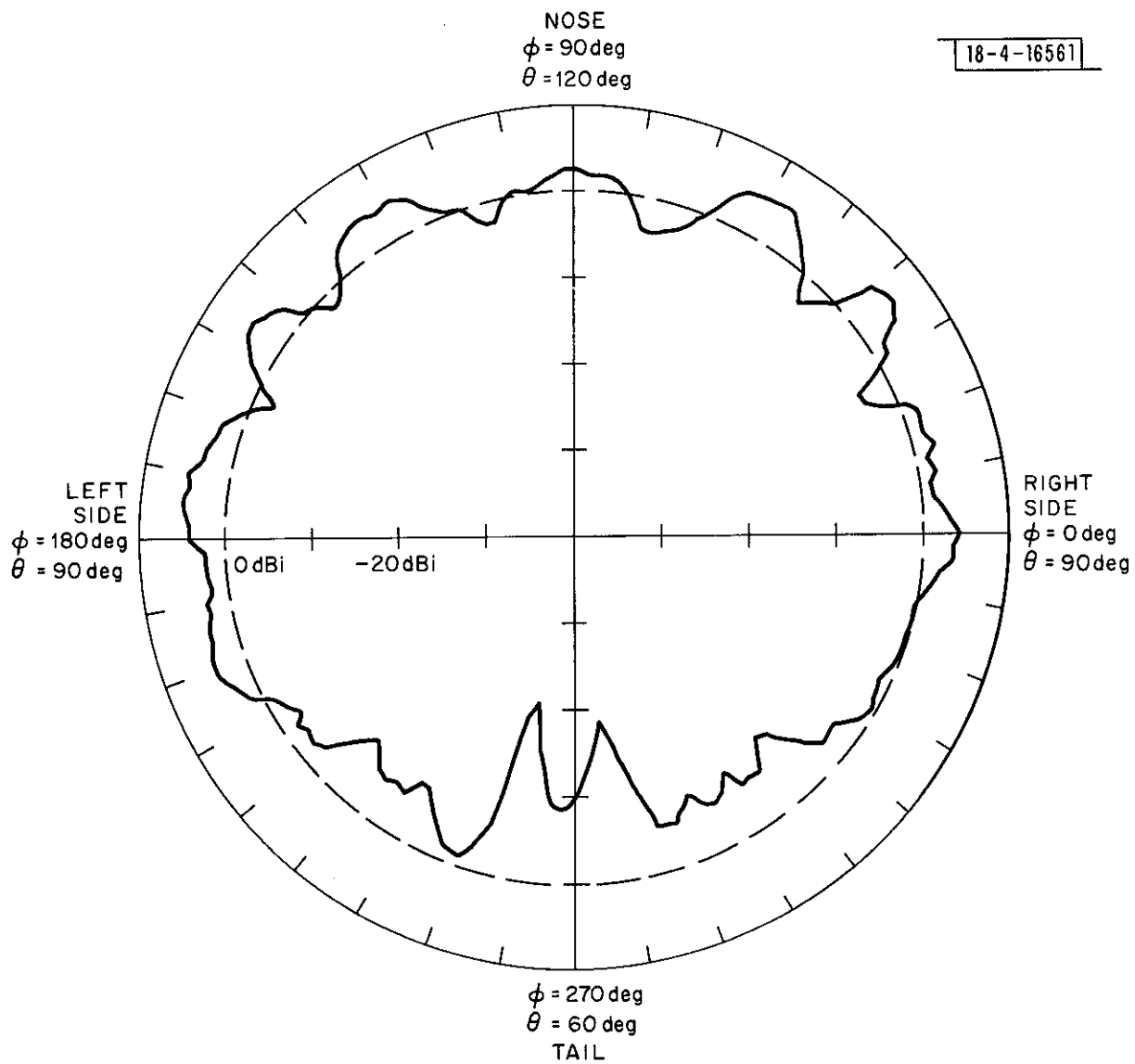


Fig. 7. Cessna 150 antenna pattern for pitch = $+30^\circ$ (antenna 3; flaps up).

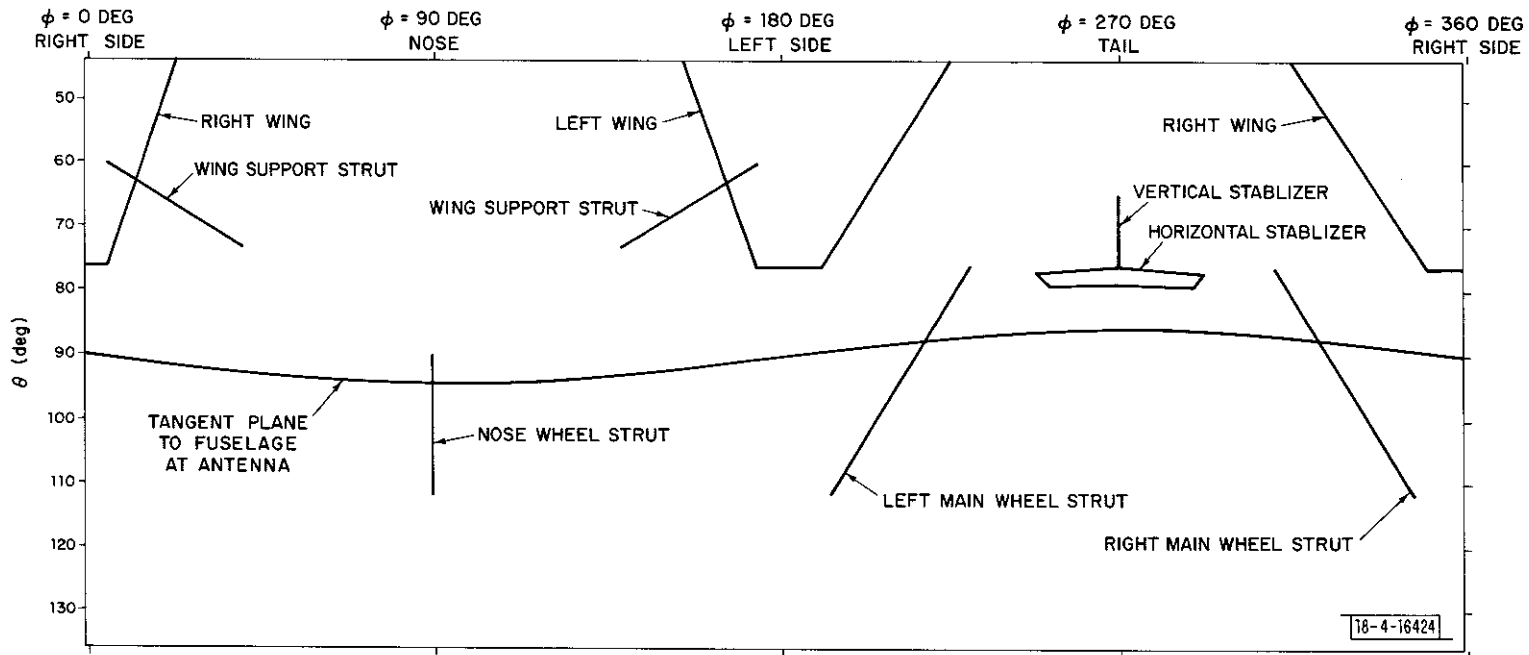


Fig. 8. θ, ϕ representation of Cessna 150 structural members and landing gear as seen from antenna position 3.

$\varphi = 40$ and $\varphi = 140$ and extending over a number of degrees in θ resemble Fresnel diffraction patterns which may be caused by the nose-wheel strut. However, based on the spacing between the antenna and the nose wheel, the resulting computation of the locations of the maxima and minima using Fresnel theory does not predict the locations of these contours very accurately. Since the basic shapes of the contours are Fresnel-like, it seems reasonable that the complex shape of the aircraft causes additional reflections which shift the Fresnel pattern caused by the primary wave and the nose wheel diffracted wave. It is these types of complex reflection problems that make prediction of aircraft antenna patterns so difficult. There are, however, a limited number of cases when theory and the data more closely agree.

Below the wing tips there is a series of maxima and minima which are also typical of a diffraction or interference pattern. Upon examining the geometry of the antenna relative to the wings, one can consider the system as an antenna on a pedestal above a reflecting plane, as shown in Fig. 9. This is the same theory used in predicting vertical lobing in the ground antenna pattern due to multipath reflections from the surrounding terrain. The value of the "pedestal height", h , in this case is the height of the fuselage. The minima will occur at those values of α , the complement of the angle of incidence, when the two ray paths differ by an odd number of half wavelengths. Therefore, the n th minimum occurs when:

$$2h \sin \alpha = \frac{\lambda}{2} (2n-1)$$

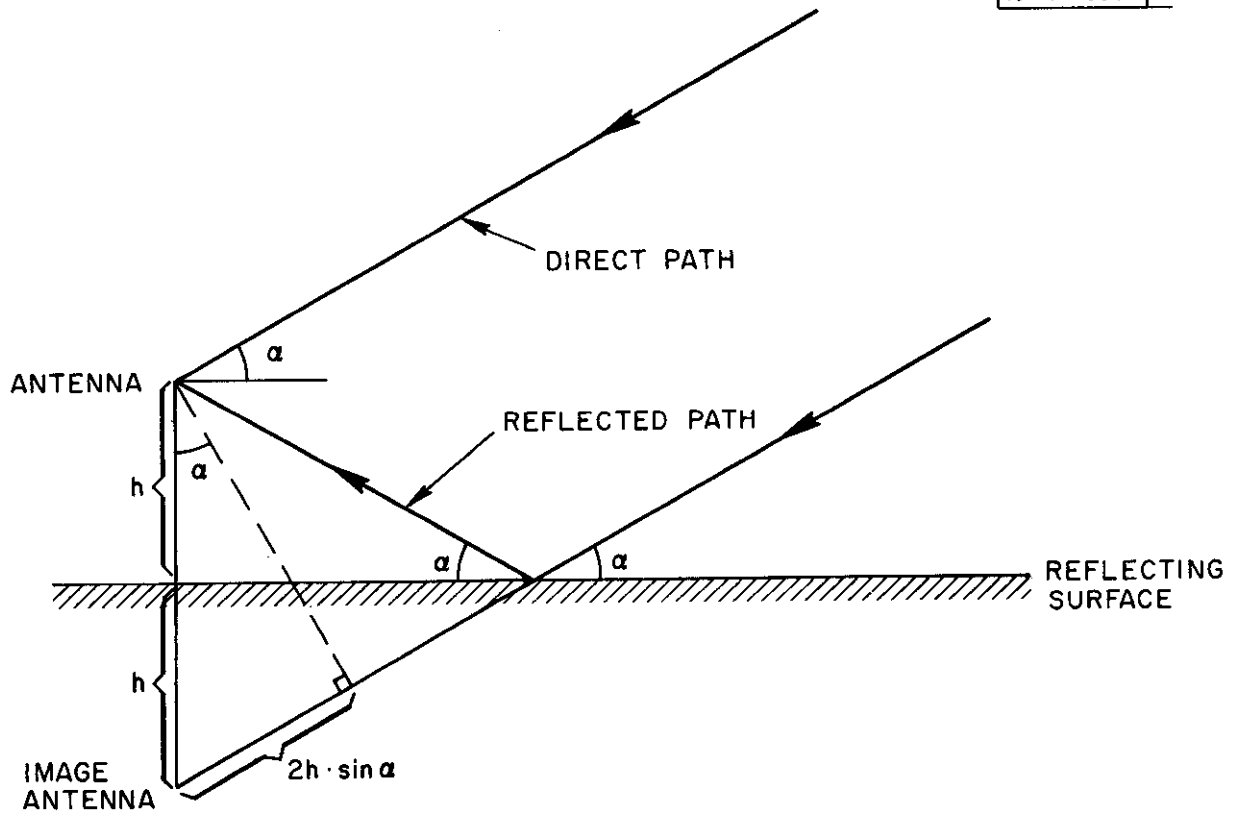


Fig. 9. Geometry of reflected signals arriving at an antenna a distance h above the reflecting surface.

For the Cessna 150 and the DABS uplink frequency of 1030 MHz, these nulls should appear at the following angles:

<u>n</u>	<u>Theoretical</u>	<u>Actual</u>	
	$\theta (= \alpha + 90^\circ)$	<u>Right Wing</u>	<u>Left Wing</u>
1	98°	98°	97°
2	105°	108°	106°
3	112°	114°	112°
4	121°	121°	122°
5	130°	132°	131°

The computed locations of the interference nulls correspond reasonably well with the actual θ values of minima in Fig. 2. The greater φ extent of the minima at larger values of θ or α is also consistent with the decreasing size of the Fresnel zones and the increasing angular extent of the reflecting wing surface as the value of θ increases.

Finally, there are lower gain values in regions around the main landing gear struts. The shapes of these regions are less explainable in terms of Fresnel theory because of the proximity of the maxima-minima patterns due to the wings, but one can clearly correlate the lower gain regions with the positions of the struts.

4.2 Piper Cherokee Arrow

The Piper Cherokee Arrow aircraft is a low-wing, single-engine, general-aviation aircraft, with antenna gain pattern as shown in Fig. 10. This pattern is for a flaps-up and landing-gear-up condition. By comparison, the next figure, Fig. 11, shows the same aircraft with the landing gear extended. Both figures are for the same antenna position which is on the fuselage bottom centerline, under the wings and exactly between the main landing gear. Note that here also a nose wheel may be observed at $\varphi = 90^\circ$.

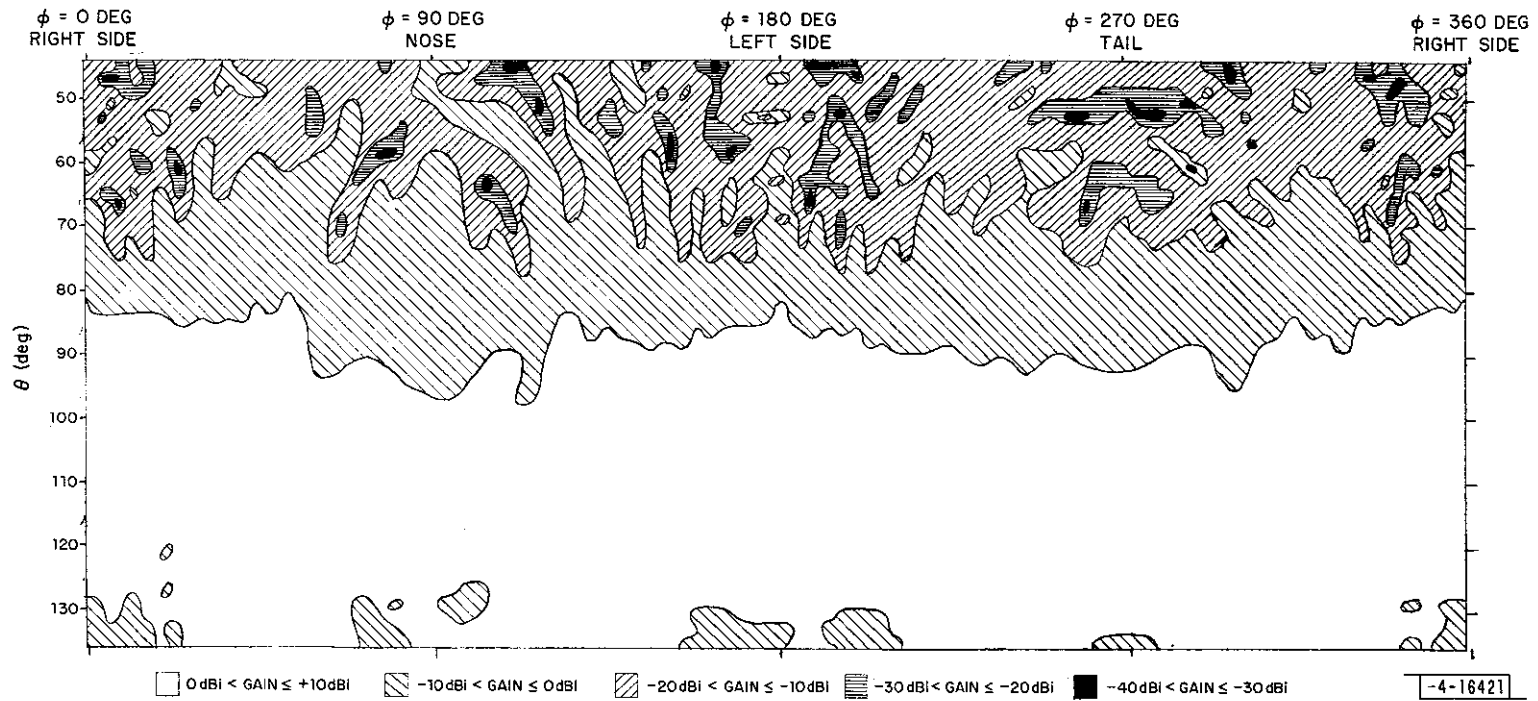


Fig. 10. Gain contours for Piper Cherokee Arrow over θ, ϕ (antenna 3; gear up; flaps up).

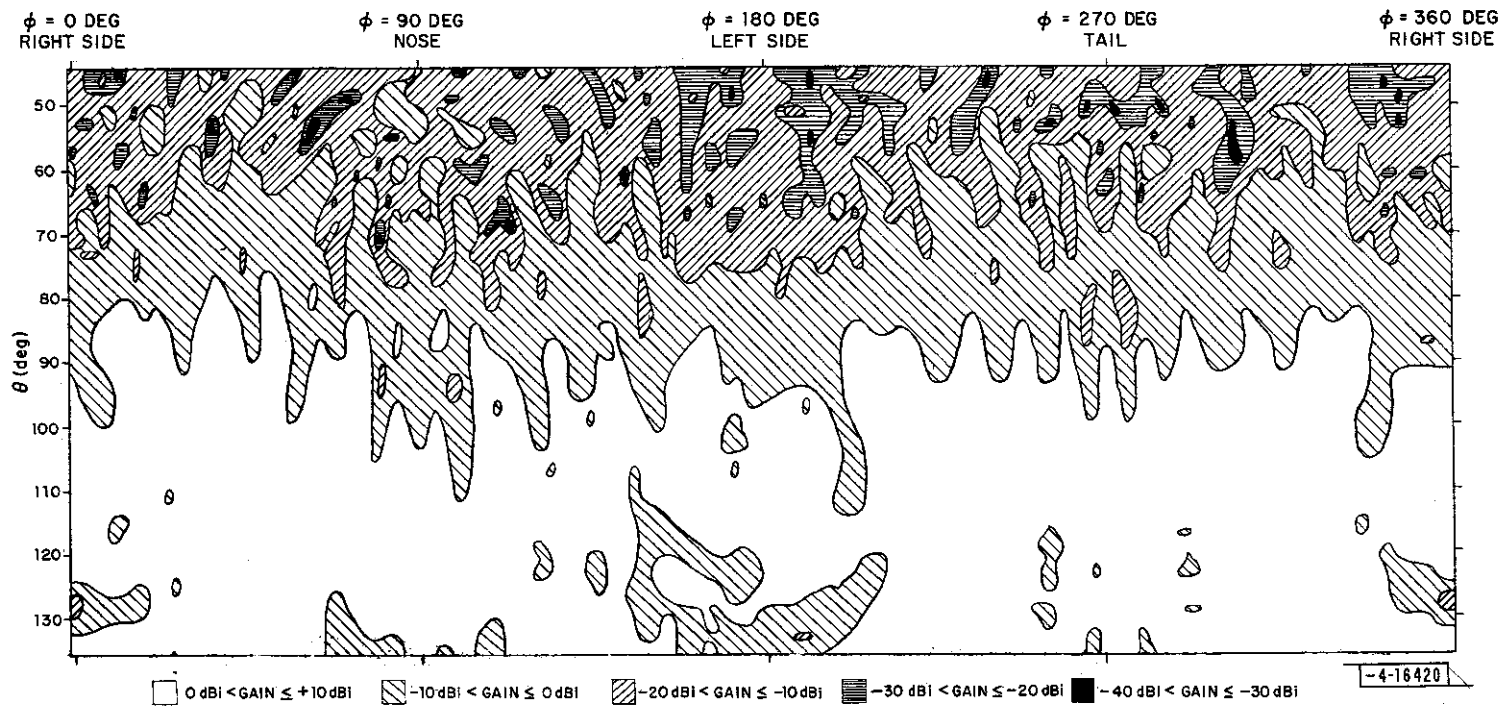


Fig. 11. Gain contours for Piper Cherokee Arrow over θ, ϕ (antenna 3; gear down; flaps up).

As with the Cessna data, the landing gear creates ring-shaped contours which suggest some form of diffraction/interference effect. In this case, however, it is the main landing gear and not the nose wheel which shows the more prominent patterns. Even at the tail-on or $\varphi = 270^\circ$ view, there are small regions of less than isotropic gain. These suggest a certain amount of sharper angle scattering (90° to 180°) off the wheel struts. For this example aircraft the contour shapes are less predictable although still generally symmetrical about the fuselage center line angles of $\varphi = 90^\circ$ and $\varphi = 270^\circ$. The short finger-like protrusions of negative gain values into the positive gain region along $\theta = 90^\circ$ is also characteristic of an interference pattern for several secondary radiators.

Since the Piper Cherokee Arrow has a retractable landing gear, the effects of the flaps can be examined independent of the wheel strut effects. Figure 12 shows constant gain contours for the Piper aircraft with the landing gear retracted and the flaps extended. In comparison with Fig. 10 for gear and flaps both up, one notices very little difference. At the φ angles corresponding to the locations of the flaps (approximately from 210° to 240° and from 300° to 330°), the 0 dBi contour only extends about $4-6^\circ$ down to larger θ values. The small effect of the flaps for the Piper and the Cessna will also be shown in the antenna gain statistics described in a later subsection.

4.3 Boeing 727

Figures 13 and 14 show the various gain levels for the Boeing 727 aircraft with the landing gear retracted and extended, respectively. This aircraft has low-mounted wings like the Piper aircraft except the dimensions are

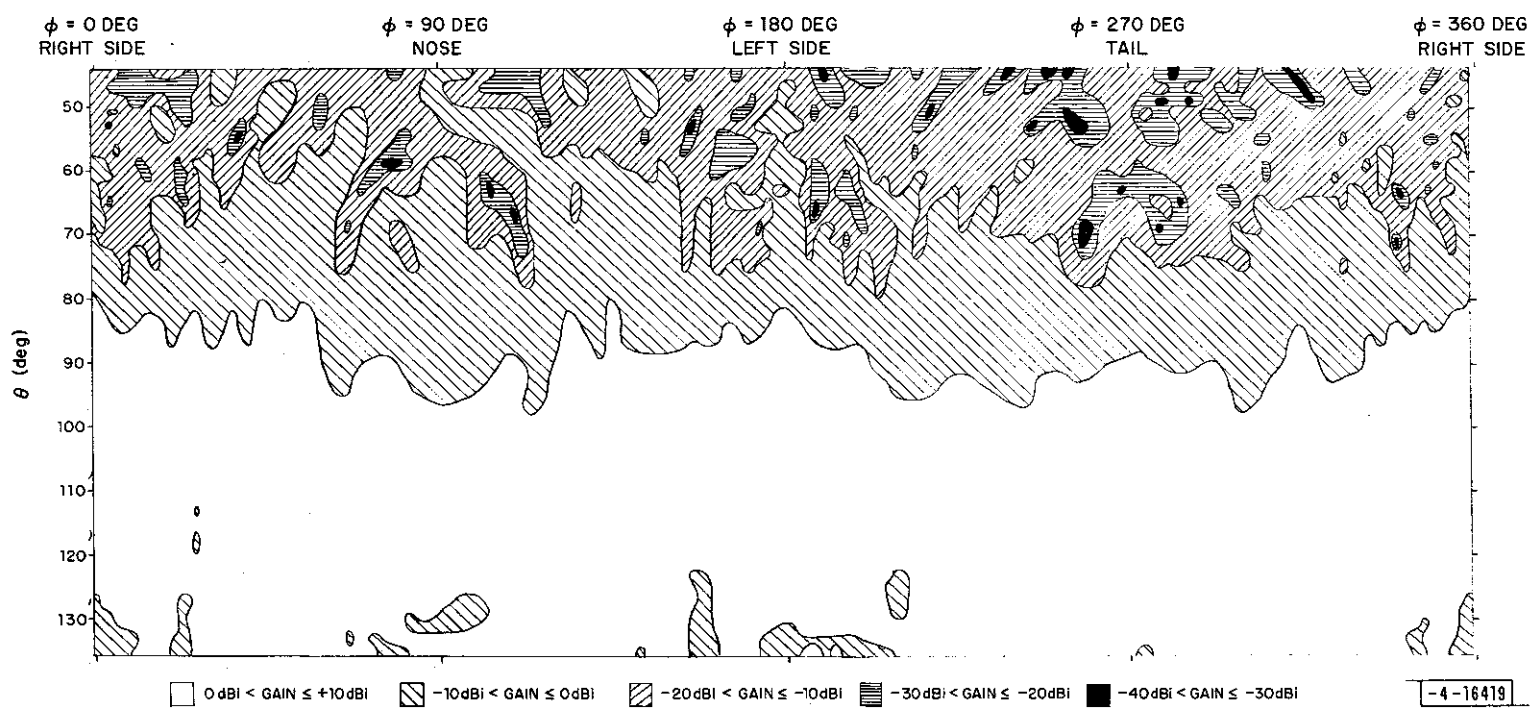


Fig. 12. Gain contours for Piper Cherokee Arrow over θ, ϕ (antenna 3; gear up; flaps down).

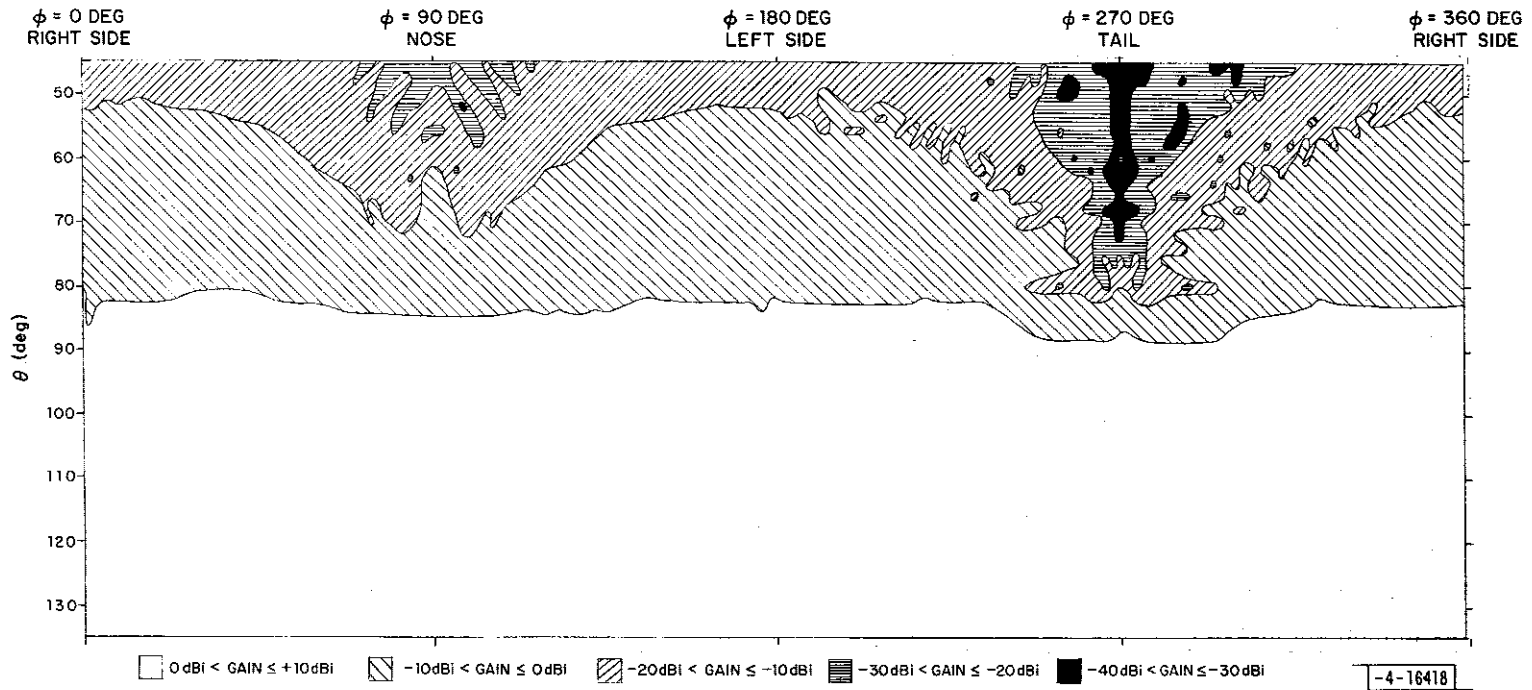


Fig. 13. Gain contours for Boeing 727 over θ, ϕ (antenna 2; gear up)

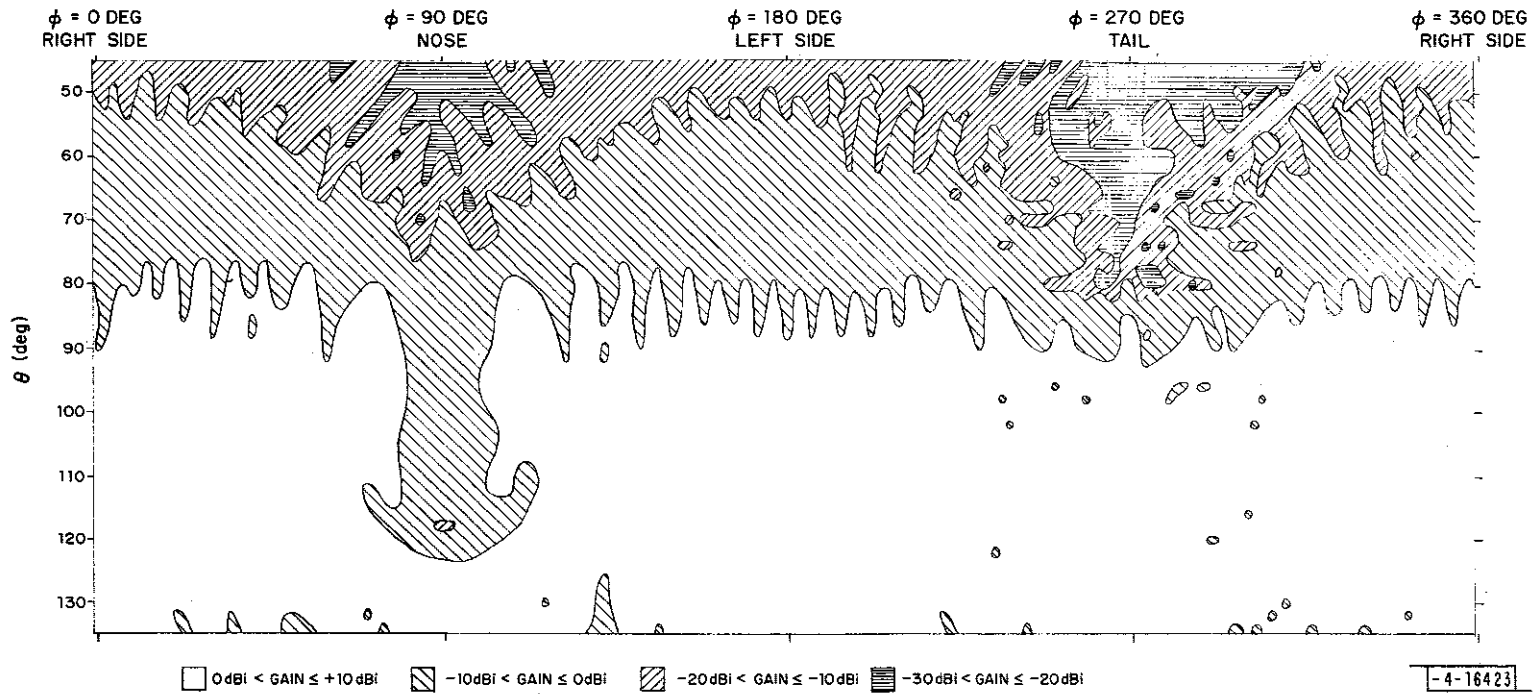


Fig. 14. Gain contours for Boeing 727 over θ, ϕ (antenna 2; gear down).

significantly greater and the antenna is located farther forward. The greater fuselage size results in low gain values directly above the nose and particularly above the tail.

The presence of the landing gear again modifies the pattern, improving the gain in some areas and degrading it in others. The nose wheel has caused a region of lower than isotropic in the forward ($\varphi = 90^\circ$) direction but with only a small indication of a Fresnel ring. Also, there are no obvious lower gain regions due to the main landing-gear struts. This is probably due to the greater spacing between the antenna and the main gear.

As with the low wing Piper aircraft, however, the presence of landing gear struts creates a series of finger-like contour projections around the $\theta = 90^\circ$ viewing plane. This is shown also by the XY planar cuts in Figures 15 and 16 for the two gear conditions. This is typical of an interference pattern from multiple scatterers or secondary radiators. It is also interesting to note how the very low gain region over the tail has been improved by the landing gear. The gain in that region is still below -20 dBi and explains why the present interrogators occasionally fail to interrogate aircraft during climbout.

5. EFFECTS OF AIRFRAME STRUCTURE AND ANTENNA LOCATION UPON AIRBORNE ANTENNA PERFORMANCE (BASED ON PROCESSED PATTERN DATA)

The preceding analysis is useful in understanding the mechanisms which lead to low-gain regions in the aircraft antenna pattern, but the performance quality of an antenna from a link reliability point of view really depends on the proportion of the radiation pattern which exhibits these low-gain characteristics. The performance quality, in fact, varies inversely with the quantity

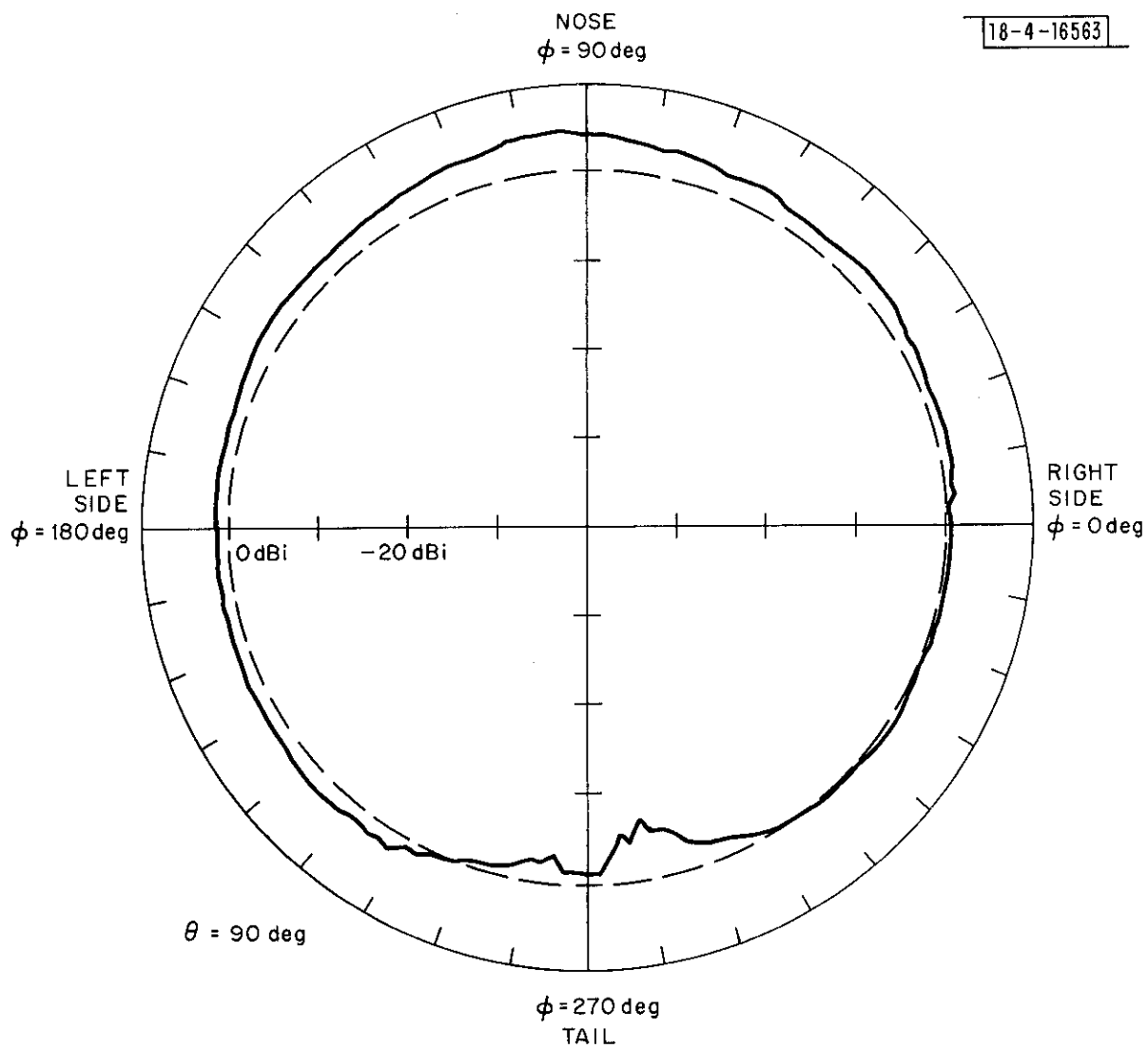


Fig. 15. Boeing 727 antenna pattern in XY-plane (antenna 2; gear up).

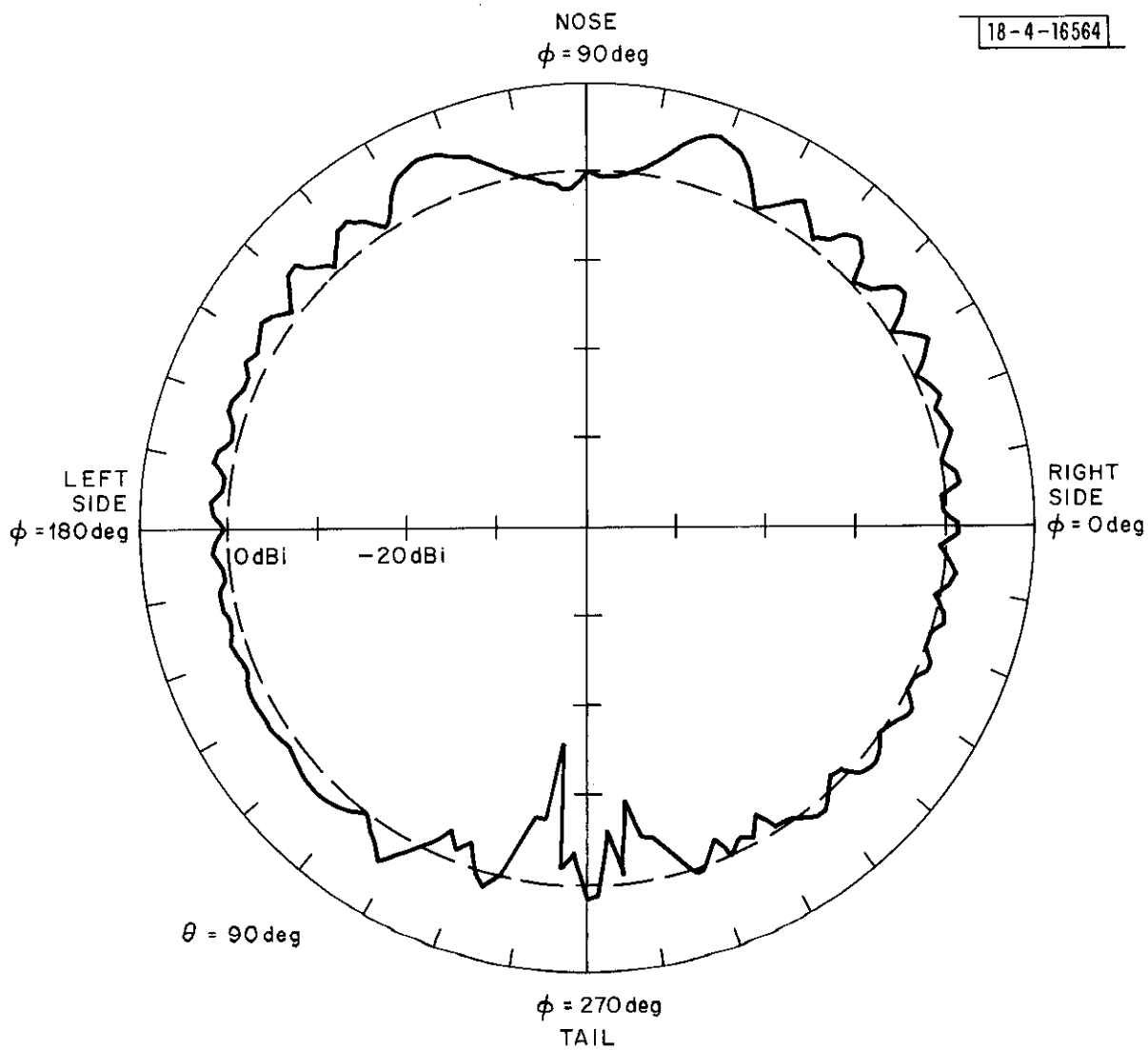


Fig. 16. Boeing 727 antenna pattern in XY-plane (antenna 2; gear down).

of low-gain values. As will be described, this fraction is not computed on the basis of the entire pattern but only on that portion which is in effect during various expected flight conditions. The statistical sample space and calculations provide the appropriate results to measure the performance quality not in an absolute scale but in a comparative fashion. From these results the landing gear, flaps, antenna location and aircraft maneuvers are examined in terms of their effect on the performance quality of airborne beacon antennas.

5.1 Statistical Treatment of Pattern Data

The techniques used in this report to determine pattern quality involve the calculation of density functions which express the spread of gains over a selected portion of the antenna pattern. An example of such a density function is shown in Fig. 17. Figure 18 shows the corresponding cumulative distribution function for this antenna. When comparing antenna patterns, the low-gain tail of the density function is somewhat more difficult to work with than the distribution function, but the density function is useful for some analysis discussions.

From a probability view the cumulative distribution function is interpreted as the probability that the gain observed is worse than a given value. The logarithmic probability scale permits the study of the more significant low-probability region. The effect of erroneous data in the rare, deep, narrow nulls is reduced by limiting how much of the low-gain tail of the distribution function one considers reasonably void of these kinds of errors. The distribution functions generally have a smooth shape for the upper 99% of the gain samples and take on a more erratic step-function shape within the lowest one percent of the distribution. For large sample spaces as

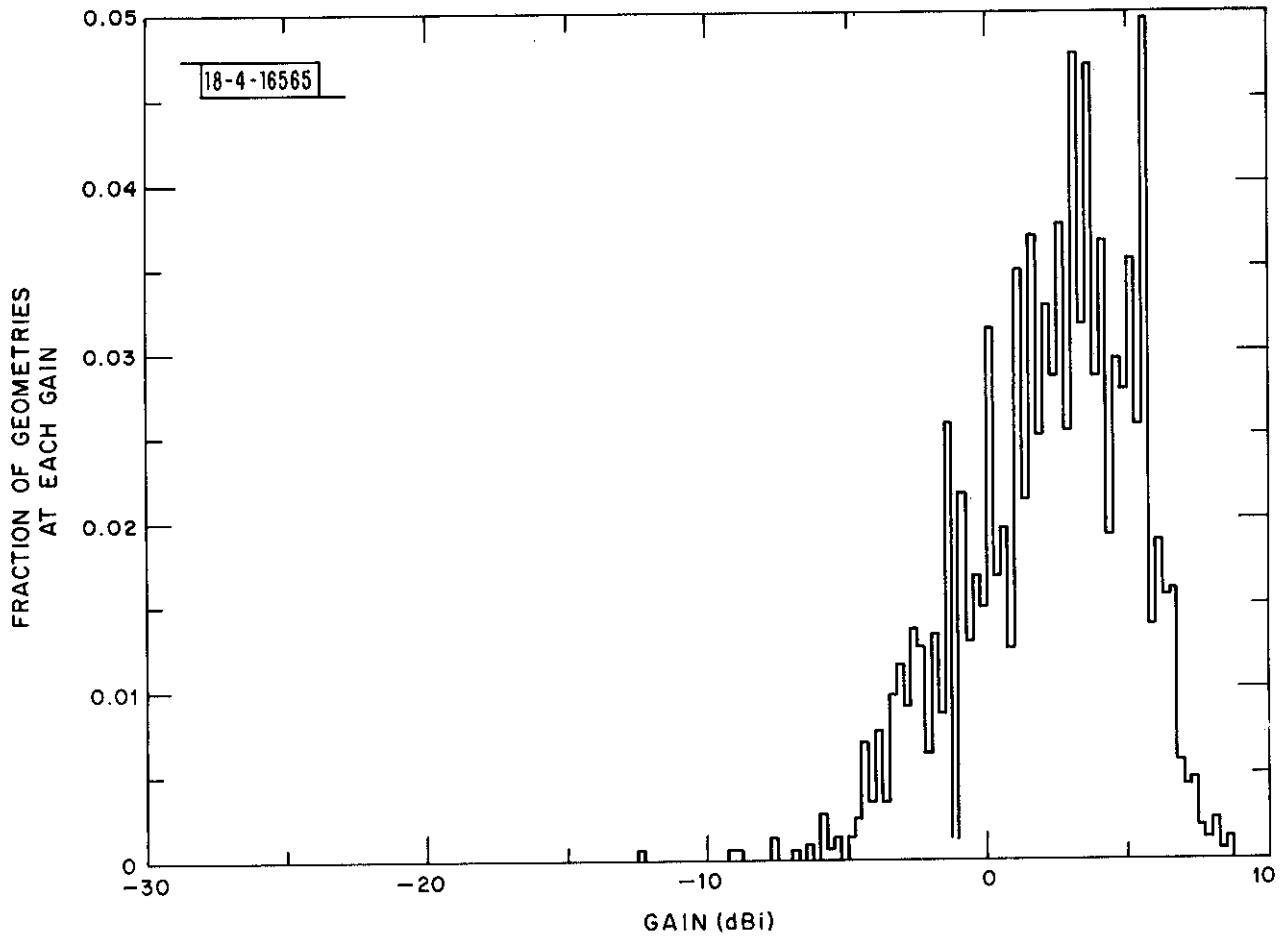


Fig. 17. Example of a density function of antenna gains.

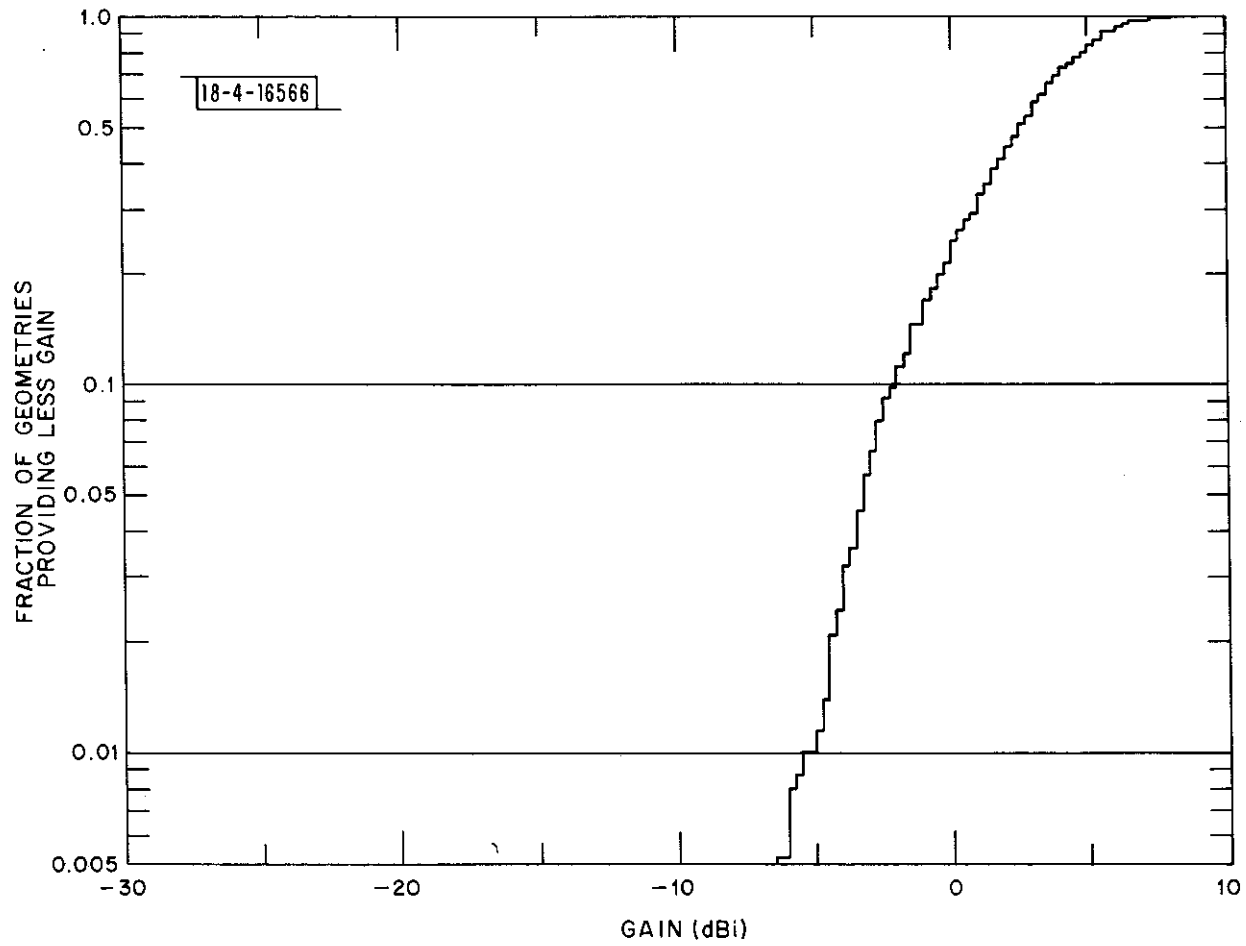


Fig. 18. Example of a cumulative distribution of antenna gains

described below, the one-percent level of the distribution function is considered safe to use in assessing the quality of an antenna without making substantial errors due to the two-degree sampling step.

Each density or distribution function is computed over a sample space of gain values which result from different combinations of attitude angles. The attitude angle combinations are defined by the type and severity of the various aircraft maneuvers and are based on pilot experiences and opinions. For example, in the case of level flight, it is not unusual for some small wandering in roll and pitch angles due to vertical air drafts, winds or various pilot corrections on the controls. These wanderings are assumed limited to $\pm 3^\circ$ in either attitude angle. Thus, when either or both of these attitude angles are described as "level" flight conditions, the statistical sample space actually includes a band of data from the pattern samples. For "shallow" banking conditions, a band of roll angles between 1° and 15° in either direction from zero is included in the statistical sample. Similarly, for "moderate" banking conditions, the band covers roll angles between 16° and 30° in either direction. These and other band definitions with their descriptive adjectives are given in Table 2. Also, pitch-attitude angles up to 15° are described as "moderate" and up to 30° are described as "steep". Sharper pitch conditions do occur occasionally, but generally are restricted to jet aircraft during take off or during unusual maneuvers which are not considered in this report.

The third angle which describes the aircraft orientation is the heading angle. Since relative heading between the ground-station antenna beam and the direction of flight of the aircraft can take on any value, all heading values are included in determining the statistical sample space. For the 2° sampling

TABLE 2

DEFINITIONS OF MANEUVER CATEGORIES

CATEGORY OF MANEUVER	LIMITS OF MANEUVER	
	ROLL	PITCH
Level	-3° to $+3^{\circ}$	-3° to $+3^{\circ}$
Shallow	-15° to $+15^{\circ}$	—
Moderate	-30° to -15° $+15^{\circ}$ to $+30^{\circ}$	-15° to $+15^{\circ}$
Steep	-45° to -30° $+30^{\circ}$ to $+45^{\circ}$	-30° to -15° $+15^{\circ}$ to 30°
Very Steep	-60° to -45° $+45^{\circ}$ to $+60^{\circ}$	—

in the data there are a total of 180 samples added to the statistical sample space for each combination of roll and pitch angle values. Changes in the roll and pitch angles modify the 180 heading-dependent samples very slowly, so these two attitude angles are changed in 2° steps to select the data samples used in the statistics. Thus, if one wishes to set up a sample space, for example, for an aircraft in a level pitch condition (-3° to $+3^\circ$; 4 values), moderate roll angles (-30° to -16° and $+16^\circ$ to 30° ; 16 values) and all headings (0° to 360° ; 180 values), the sample space would contain 11,520 data samples. Note that the data samples included in the statistical sample space are not all different. Some samples are included several times such as the "nose-on" view during all roll angle values. If this is not done, then the heading angle is not a uniformly-distributed random variable as has been assumed.

5.2 Effect of Data Inaccuracies

Data are recorded at 2° angular steps. This step size, of course, limits the amount of detail recorded for each pattern. The accuracy of the recorded gain level for each measurement sample is placed at 0.25 dB for the equipment according to the equipment manufacturer, but the angular step size also affects the accuracy of the recorded levels. In particular, the patterns have regions of low gain, (nulls) which can be much narrower than 2° and significant in depth compared to the surrounding antenna gain values. These deep, narrow nulls can introduce two types of errors which have offsetting effects. When using the data, each measurement is considered valid for as much as four square degrees on the pattern whereas some of the nulls are actually much narrower. On the other hand, the lowest gain value in these narrow nulls

is often missed because the measurement is not taken when the exact aspect angles of the lowest value within the null are in effect. The resulting amplitude recorded is then several dB larger than the actual minimum gain in that region but can be considered a reasonable value since the null does not extend over the entire θ, ϕ sample point. Fortunately, based on examination of continuous analog plots of the antenna patterns such as in Fig. 19, most pattern features, including nulls, are of sufficient angular extent to give reliable results at most aspect angles. Also, those errors which occur at a few deep, narrow nulls do not significantly affect the normalization of the gain relative to an isotropic antenna.

5.3 Effects of Landing Gear and Flaps

Using the statistical techniques described above, the effects of the landing gear and flaps are examined first. Each aircraft is assumed in a level flight condition, as described by Table 2, but the geometry between the aircraft and the ground-based beacon interrogator also influences which portion of the pattern is in view. Models of aircraft spatial distributions based on actual aircraft flight data indicate that a large majority of the aircraft are at low viewing angles as seen from the ground station. For level flight conditions these low angles correspond to viewing that portion of the aircraft antenna slightly below the XY (wing-fuselage) plane. The XY plane in this case is parallel to the earth tangent plane but is translated by the aircraft altitude above the earth. As the aircraft maneuvers the XY plane moves with the aircraft while the translated earth tangent plane remains fixed. The angle between this fixed plane and the line-of-sight vector, therefore, stays the same. Because the line-of-sight vector is always slightly below the tangent plane at the aircraft location, the angle is called the depression angle, δ , as shown in Fig. 20.

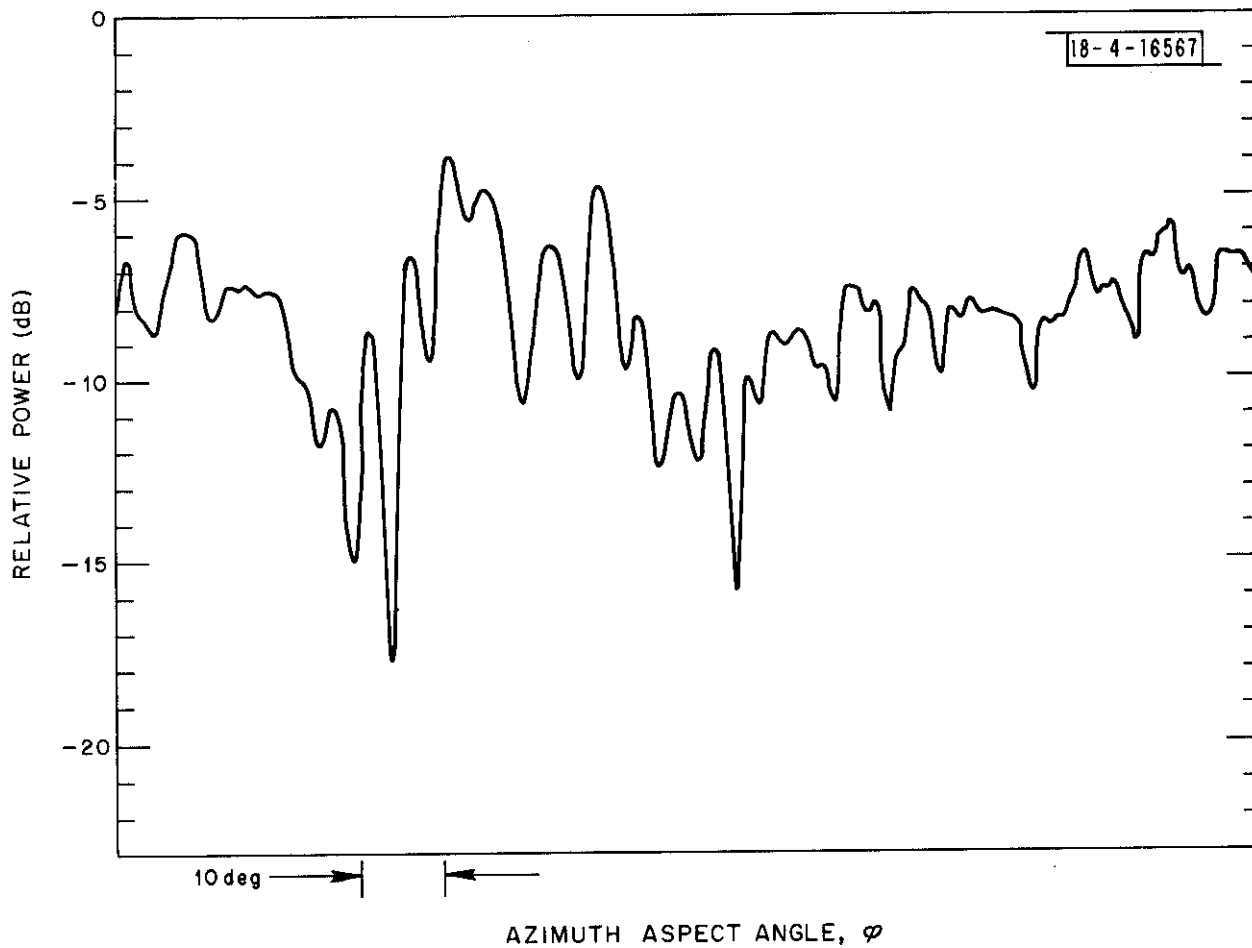


Fig. 19. Example analog output of antenna gain fluctuations.

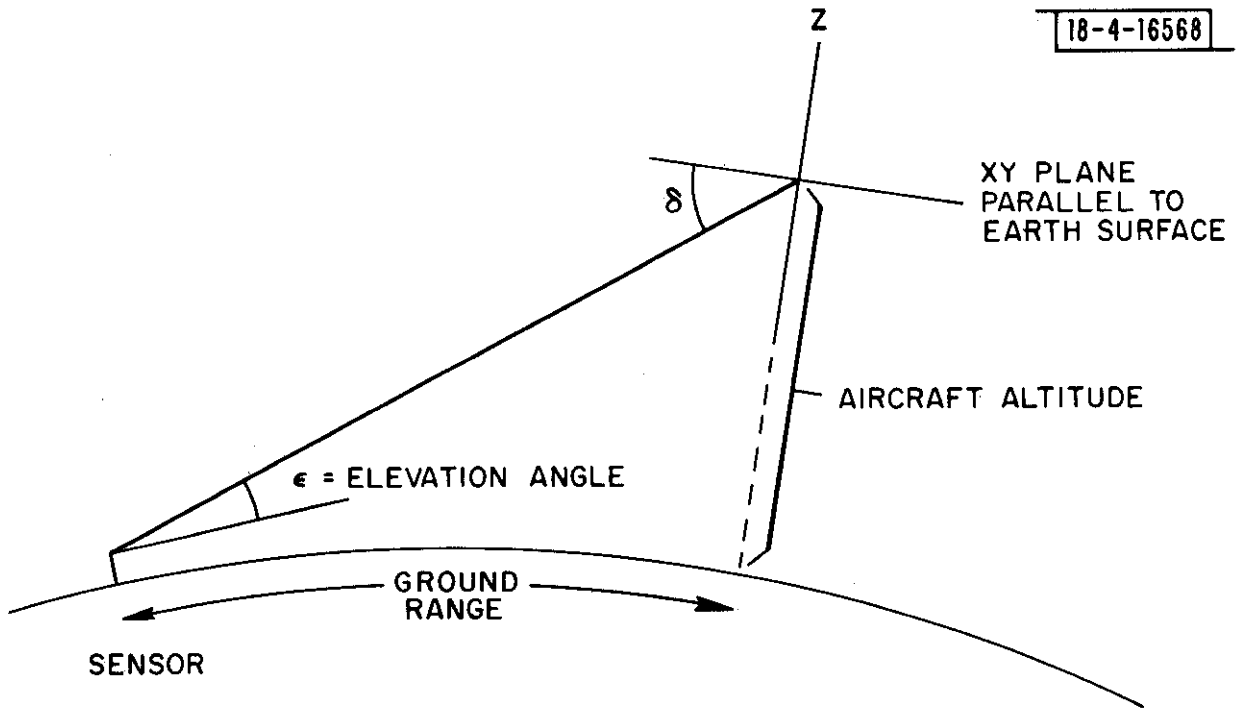


Fig. 20. Definition of depression angle, δ , in terms of sensor-aircraft geometry.

5.3.1 Cessna 150

Since the Cessna 150 does not have retractable landing gear, only the effect of flaps can be studied for that aircraft. Figure 21 shows two distributions of aircraft antenna gain patterns for the Cessna 150: one for flaps up; one for flaps down. (The antenna position for this data is different from the one used in the previous subsection because the flaps-down data for the earlier position appears erroneous and has been rejected. The third bottom-mounted antenna produced similar results as described here so the conclusions are considered valid for all the antennas on the C-150.) As can be seen, the flaps have very little effect on the distribution function for a high-wing aircraft. This is a logical result since the flaps are close to the fuselage, and the fuselage blocks the view of the flaps from the antenna position. A comparative examination of the unprocessed patterns for these two conditions shows the flaps-down condition actually improves the gain in some regions while degrading it in other regions. It is difficult to say whether the improvement is a statistical fluctuation in the data measurements or whether the flaps are providing scattering surfaces which improve the pattern at previously poor viewing angles. In either case, the general conclusion is still valid that the flaps have little effect on the distribution of antenna gain.

5.3.2 Piper Cherokee Arrow

For the low-wing Piper Cherokee Arrow, Fig. 22 shows the comparison of flaps up versus flaps down. This time the flaps do cause a small degradation in antenna quality by having a greater fraction of the geometric conditions result in a lower gain value. For a low-wing aircraft the extended flaps actually come directly between the aircraft antenna and the ground transmitting/receiving antenna at some aspect angles.

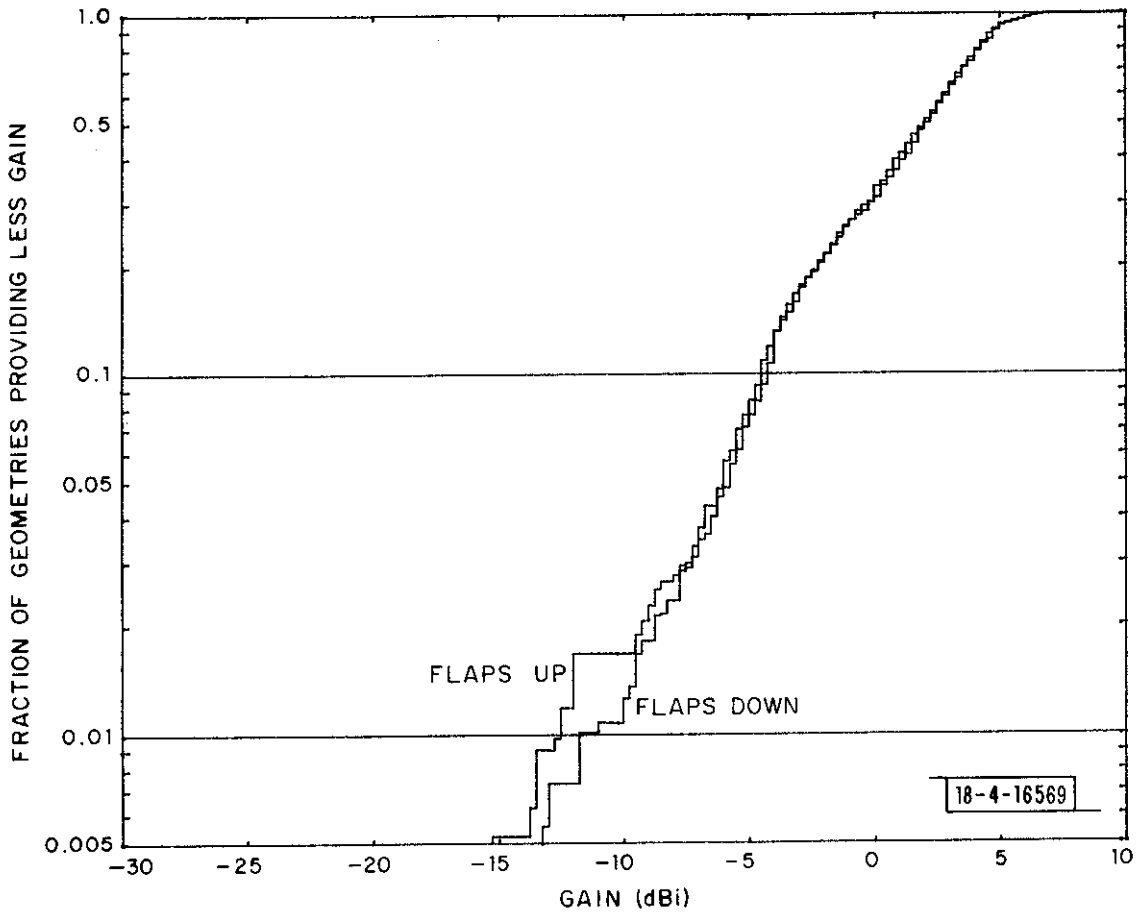


Fig. 21. Effect of flaps on distribution of gains for Cessna 150 (antenna 2; level flight).

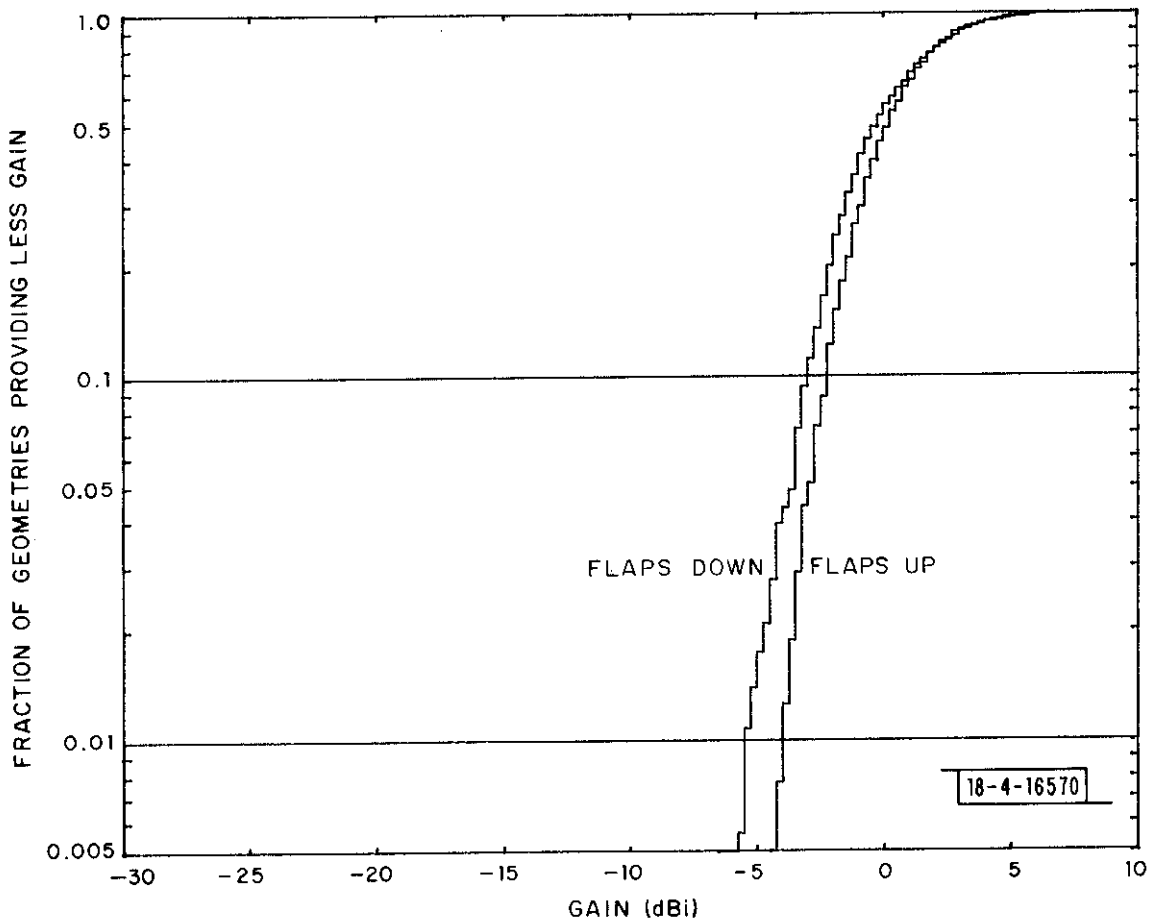


Fig. 22. Effect of flaps on distribution of gains for Piper Cherokee Arrow (antenna 3; gear up; level flight).

When examining curves on semilogarithmic scales as the above results are presented, it is important to interpret the differences between two curves in terms of which scale corresponds to the independent variable and which to the dependent variable. If the fraction of geometric conditions resulting in poor communications is restricted to less than some value such as 1%, then the communication link should ideally have enough power to achieve this for the worst expected flight conditions. For the example in Fig. 22, the power budget must have enough power to result in successful communications with the flaps down and will thereby have 1.5 dB residual power for the flaps-up condition. However, if there is no residual power in the link and if exactly 1% of the geometric conditions provide sufficient gain for successful communication when the flaps are up, then the minimum antenna gain which allows successful communication is fixed at -4 dBi. While only 1% of the geometric conditions result in an antenna gain worse than this value for the flaps up, 4% of the geometries yield a gain below -4 dBi for the flaps-down condition. One could pessimistically say the chance of not having gain has increased by a factor of four or optimistically say the chance of having sufficient gain is 96%, which is still very good. This latter, optimistic interpretation is considered by the author as the more reasonable interpretation because the success or failure of a communication is, in this study, strictly geometry-dependent and 4% is still a small fraction of the possible geometric conditions which can exist. Both viewpoints are used, however, in the discussion of the remaining results in this report. As later results will show, it is unrealistic to expect the power budget to provide such a high success

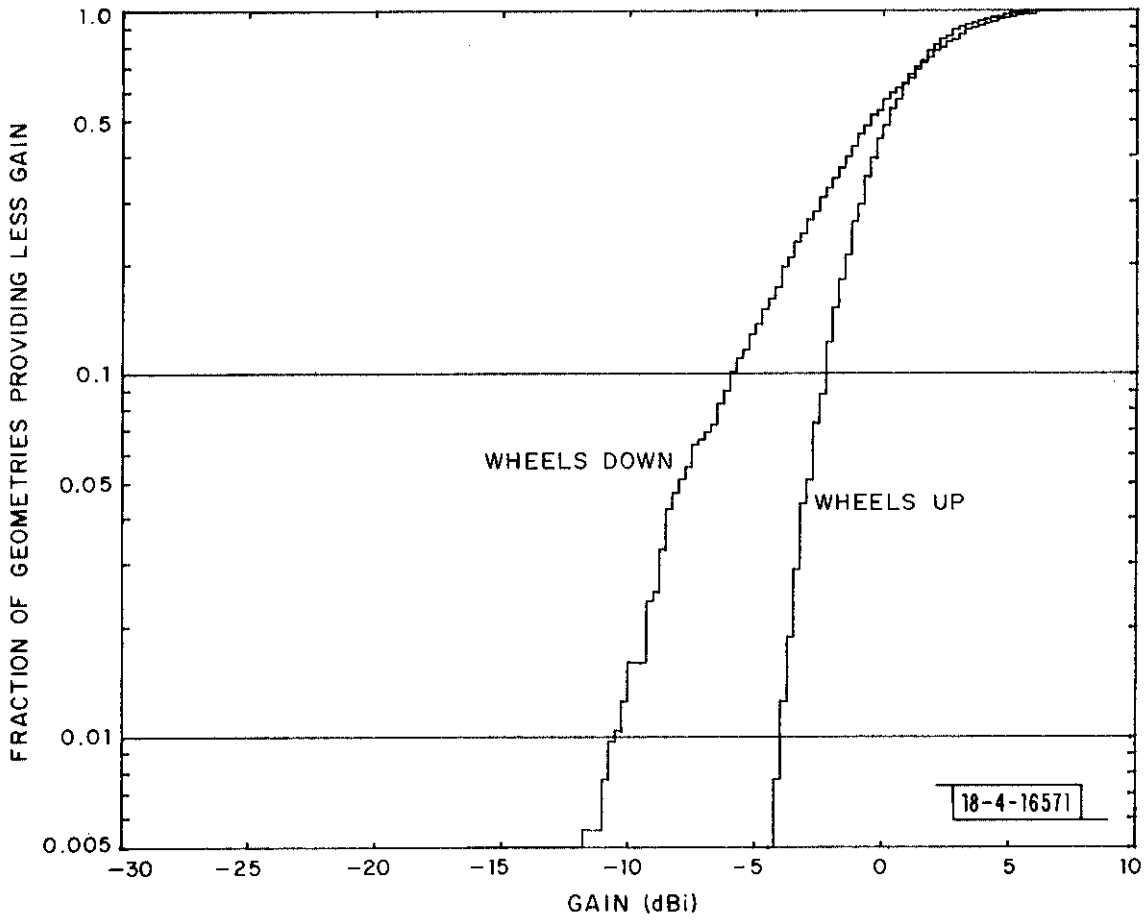


Fig. 23. Effect of landing gear on distribution of gains for Piper Cherokee Arrow (antenna 3; flaps up; level flight).

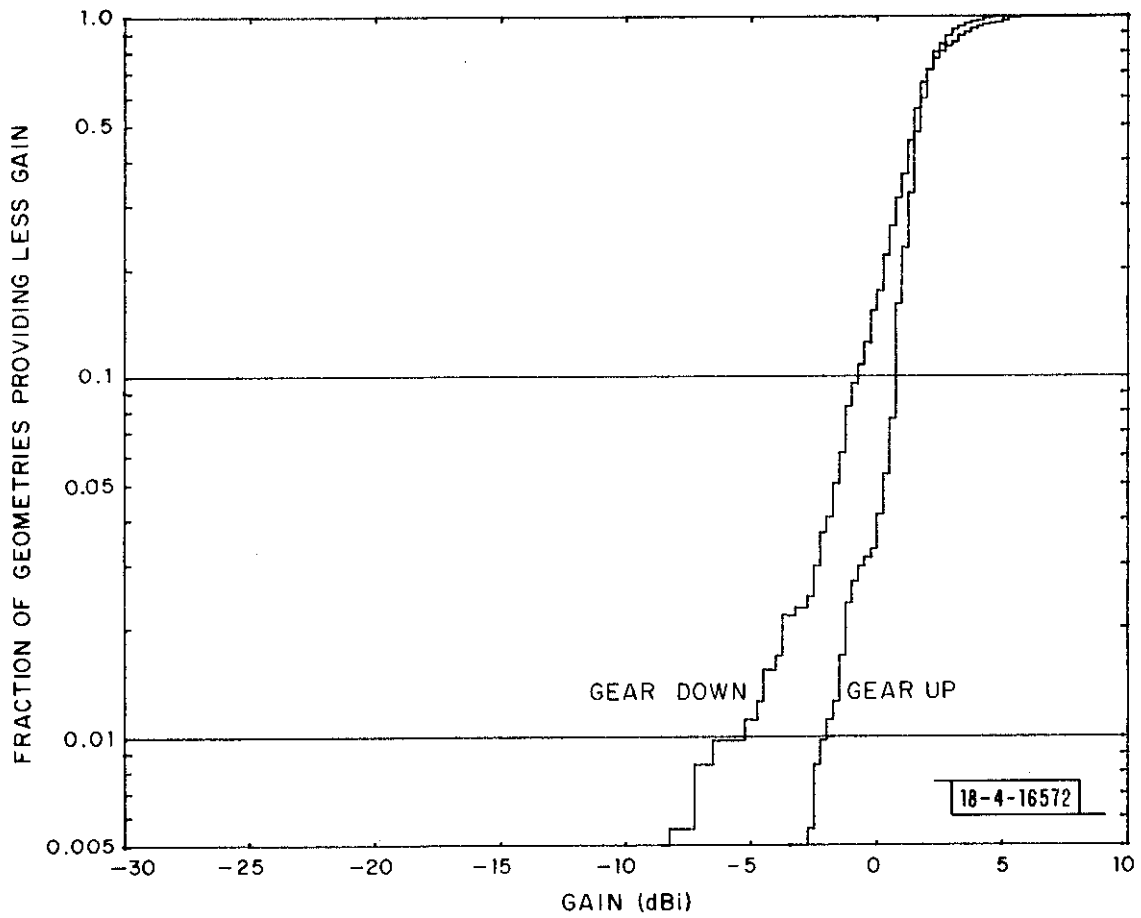


Fig. 24. Effects of landing gear on distribution of gains for Boeing 727 (antenna 2; level flight).

likelihood for all flight conditions since the number of low-gain conditions can increase dramatically.

Returning to the data analysis, one concludes that the presence of landing gear tends to degrade the performance quality even more than the flaps do. Figure 23 shows this quite vividly for the Piper aircraft. For the retracted-gear condition the performance level defined by 1% worse gain or 99% better gain occurs at a gain of -4 dBi, as stated before. The gear down condition requires 6.5 dBi more power in the link to give the same performance, or only an 81% chance of having sufficient gain will exist if -4 dBi is the minimum usable gain. Clearly, the presence of the landing gear has seriously reduced the performance quality of this aircraft antenna.

5.3.3 Boeing 727

The distribution of gains for the Boeing 727 in gear-up and gear-down conditions are given in Fig. 24. The conclusions are similar to those for the small, low-wing Piper aircraft.

5.4 Roll Maneuvers

5.4.1 Cessna 150

When an aircraft goes through various maneuvers, the gain distribution changes as more or less of the wing and fuselage structures obstruct the wave at each viewing angle. The effects of different roll-angle conditions are shown in Fig. 25 for the Cessna 150. The shallow rolls have very little effect, consistent with Fig. 8 which shows the wings obstructing the direct ray path at around 14° above the horizontal plane. For greater roll angles the wing begins to obstruct the direct ray path at some headings and any

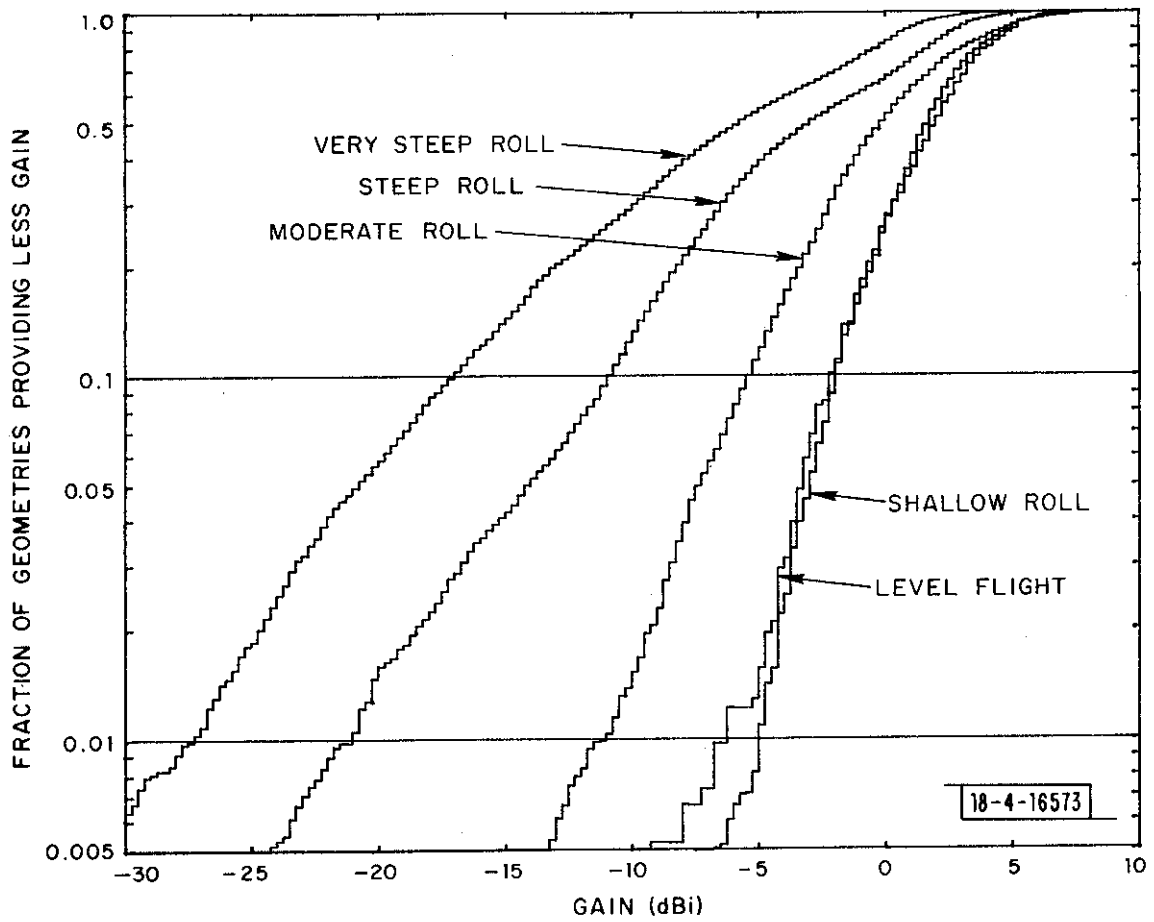


Fig. 25. Effects of roll on distribution of gains for Cessna 150 (antenna 3; flaps up).

signal received must be from diffraction around the wings or reflection of the wave off other parts of the aircraft. In order to have no more than a 1% chance of having insufficient gain at moderate roll angles, the link must have 4.5 dB more power than is required to achieve the same performance while the aircraft is in level flight. Otherwise the fraction of the geometric conditions which can lead to communication failure increases from 1% to 7%. For even greater roll angles, these values are greater still.

5.4.2 Piper Cherokee Arrow

There is a greater change in the gain distribution for banking conditions over level flight conditions when the aircraft wings are mounted low on the fuselage and with the antenna between them. Although the wings generally have a slightly upward slope from the fuselage, even shallow roll angles degrade the performance of the antenna. Figure 26 shows this for the Piper Cherokee Arrow where even a shallow roll produces a -5.5 dB shift and a moderate roll produces a very large -18.25 dB shift for the poorest 1% of the sample space. Physically this result is reasonable because the wing is very close to the antenna and during roll maneuvers the wing obstructs the signal over a number of degrees in ϕ which makes the diffracted signal intensity very low.

5.4.3 Boeing 727

Because the Boeing 727 has a long fuselage, the wing-shielding problem can be reduced by placing the antenna well forward of the wings. The results of maneuvering under various roll-angle conditions for this example are shown in Fig. 27. Whereas the wings shield the antenna for the Piper aircraft, in this case the fuselage is causing the lower gain values. This

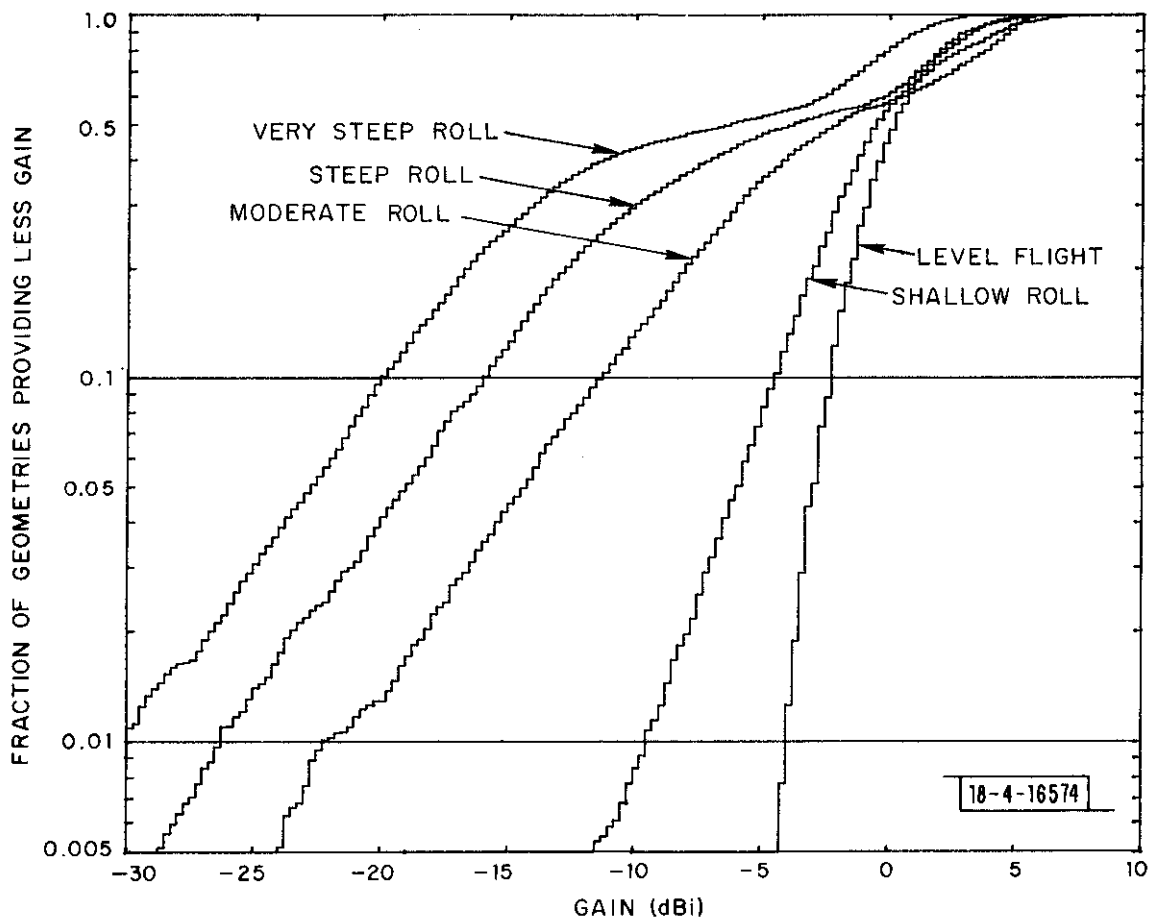


Fig. 26. Effects of roll on distribution of gains for Piper Cherokee Arrow (antenna 3; gear up, flaps up).

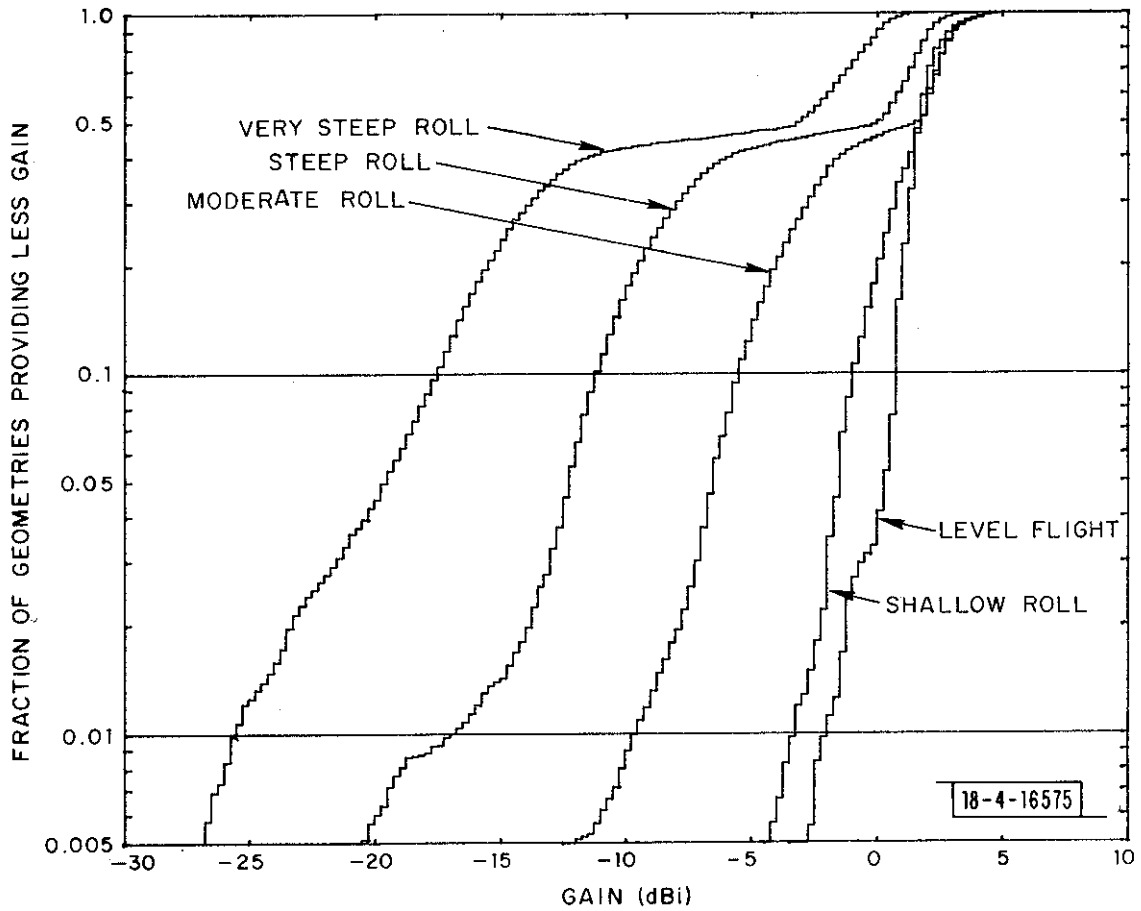


Fig. 27. Effects of roll on distribution of gains for Boeing 727 (antenna 2; gear up).

difference in the effect of the wings was discussed previously when presenting the unprocessed data.

The two step staircase shape of the functions at larger roll angles for both low-wing aircraft is the result of a density function having two peaks, as in Fig. 28 for the 727. This double-peak density function is indicative of sampling an antenna pattern primarily over geometries producing extremes in shielded and unshielded conditions. The lower gain peak is due to geometries which cause obstruction of the direct ray path while the top of the aircraft is observed from the ground station. The higher gain peak corresponds to geometric conditions which tend to reduce shielding, and the belly of the aircraft is directed more at the ground station. This higher gain peak is taller and more narrow than the lower peak, which is consistent with observing a smooth, nearly constant, unobstructed gain pattern for almost half of the heading values.

5.5 Pitch Maneuvers

As the aircraft pitches up or down the occurrence of low gain values increases also. Figure 29 provides a comparison of the gain distributions for level flight conditions and for moderate and steep pitch-angle values using the Piper antenna data. In the case of moderate pitch angles the fuselage is obstructing the direct ray path at some of the heading values, and there is a -5.25 dB shift in the gain corresponding to 1% of the sample space. For a minimum usable gain constraint of -4dBi, the fraction of geometric conditions which can provide successful communication drops from 0.99 to 0.86. These results show that even at only moderate pitch angles, the performance of the antenna can be severely degraded.

For sharper pitch-angle conditions more severe degradation of the gain distribution is observed in comparison to the level flight conditions.

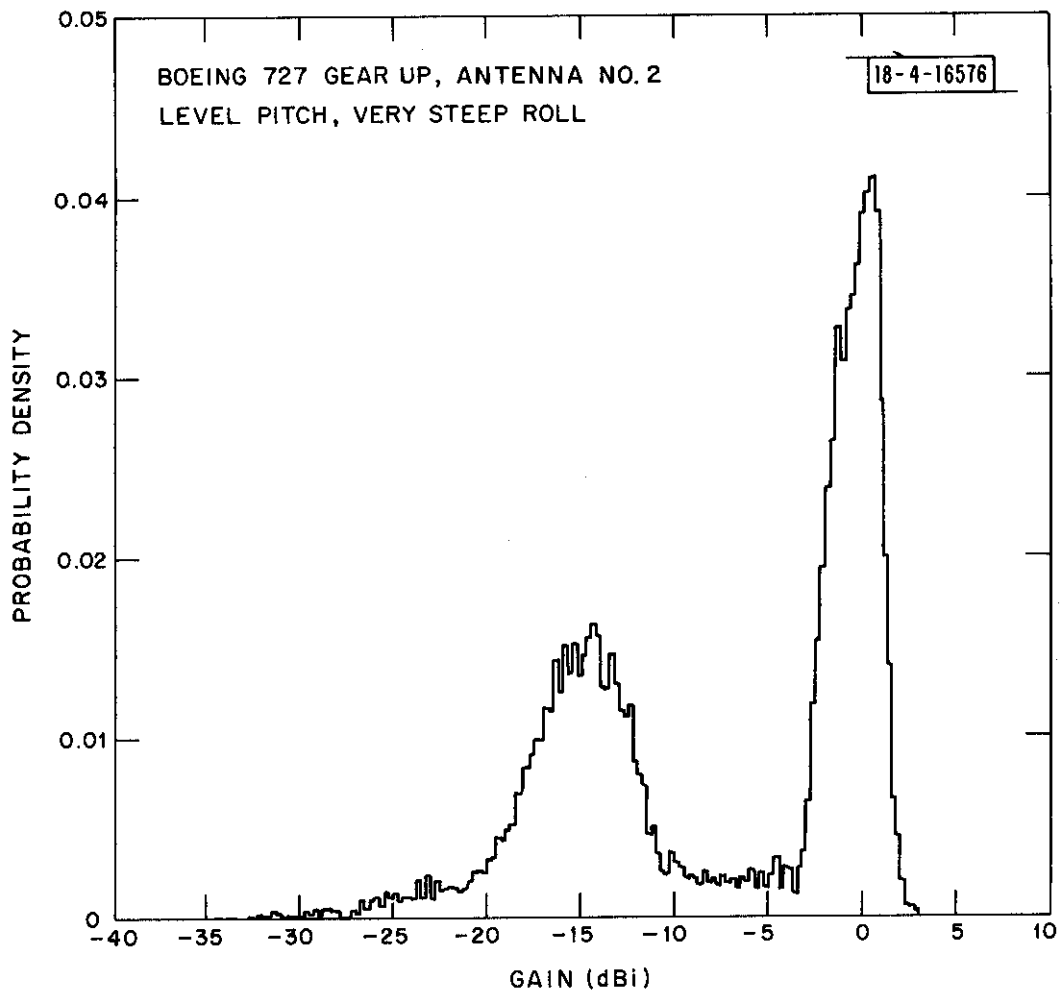


Fig. 28. Example of a double peak density function.

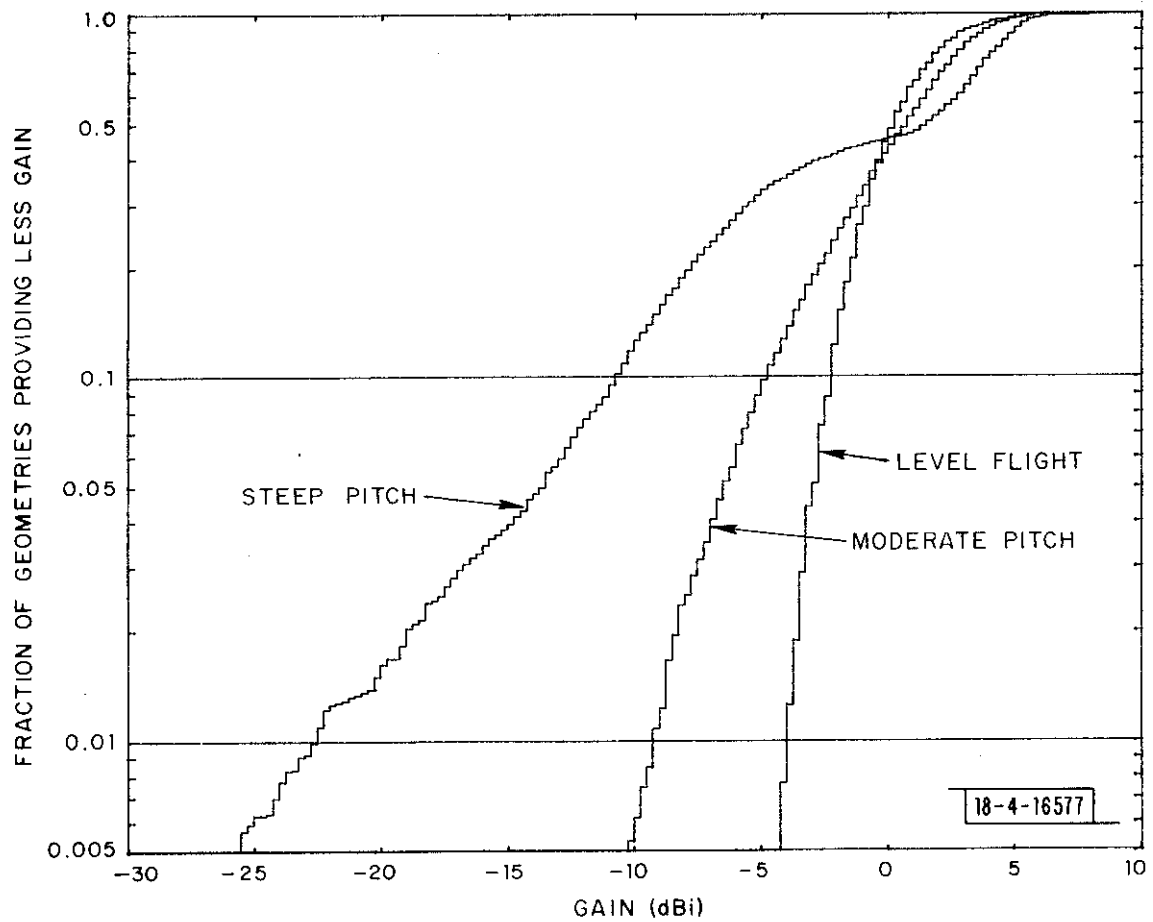


Fig. 29. Effects of pitch on distribution of gains for Piper Cherokee Arrow (antenna 3; gear up; flaps up).

Under steep pitch-angle conditions the distribution function of the Piper data again takes on a staircase shape as the fuselage obstructs the signal in a manner similar to the way the wings do during larger roll angles. However, under the same pitch maneuvers, the distribution functions for the Cessna 150, shown in Figure 30, and for the Boeing 727, shown in Figure 31, do not result in a staircase shape. As one would expect, the larger 727 aircraft does exhibit more very low gain values compared to the Piper aircraft data. The high wing Cessna, however, shows fewer low gain values. Apparently there are some heading values when the low wings of the Piper obstruct the signal during pitch maneuvers, while a similar situation does not exist for the high-wing Cessna aircraft. The shape of the fuselage may also affect the degree of shielding. These results again reflect the effects of the size and proximity of obstructing surfaces on the performance of airborne antennas.

5.6 Effects of Antenna Location

The location of the antenna on the aircraft also affects the gain distribution functions. This is demonstrated to only a limited extent because patterns exist for only a small number of locations on any one aircraft. Therefore, this study does not optimize the antenna location but provides evidence for establishing some antenna placement guidelines.

The Cessna 150 data includes three antenna locations. The gain distribution curves for level and moderately banked flight conditions for these three antennas are shown in Figs. 32 and 33, respectively. Relating these results to the physical placement of the antennas, antennas 2 and 3 are on the fuselage centerline and have very similar distribution curves over 60 percent of the higher gain values during level flight. Antenna 4 is mounted off center and has

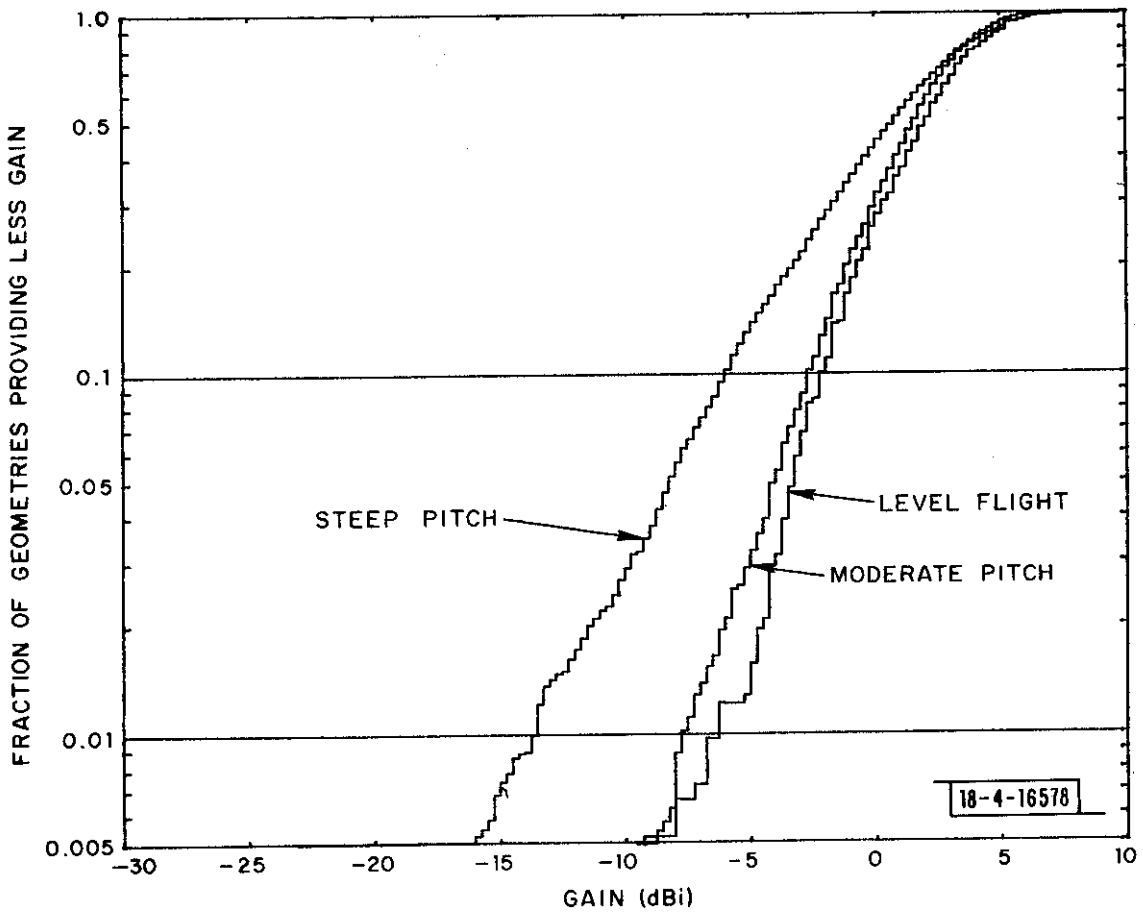


Fig. 30. Effects of pitch on distribution of gains for Cessna 150 (antenna 3; flaps up).

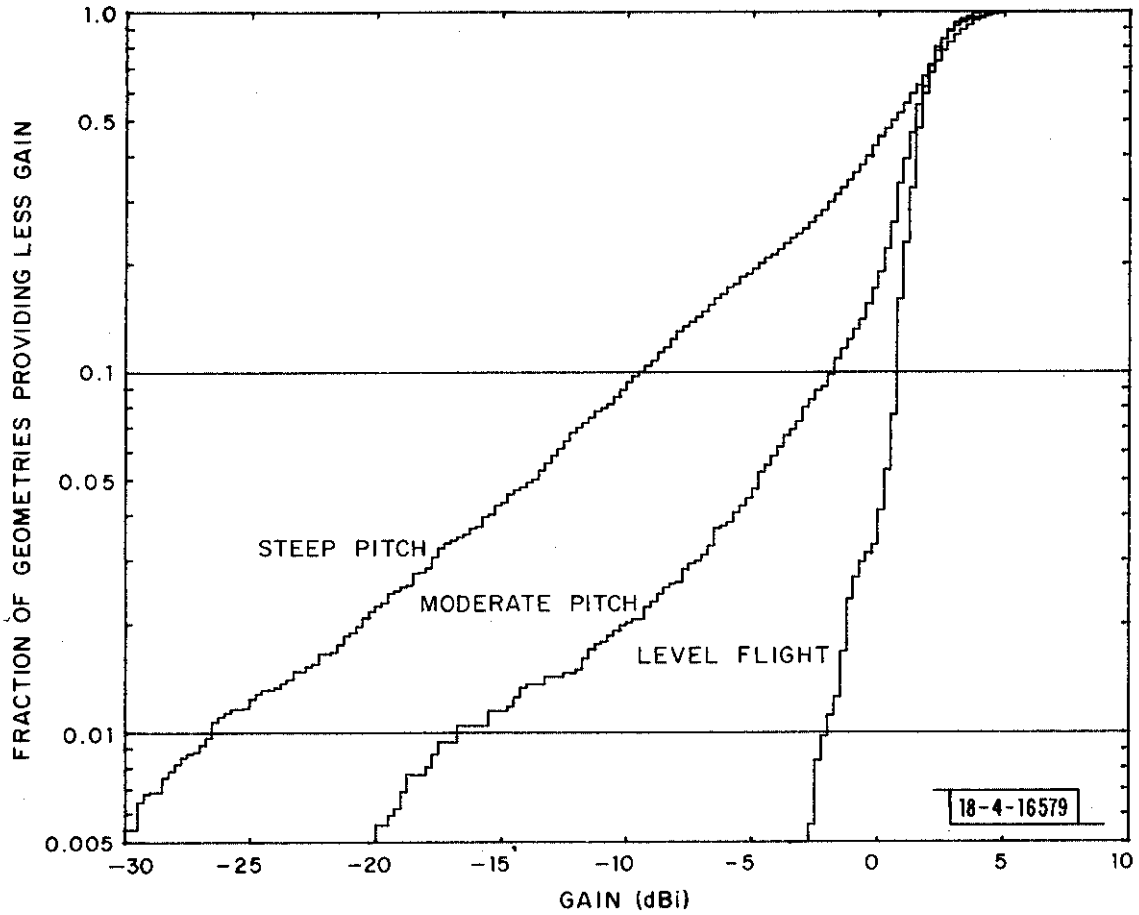


Fig. 31. Effects of pitch on distribution of gains for Boeing 727 (antenna 2; gear up).

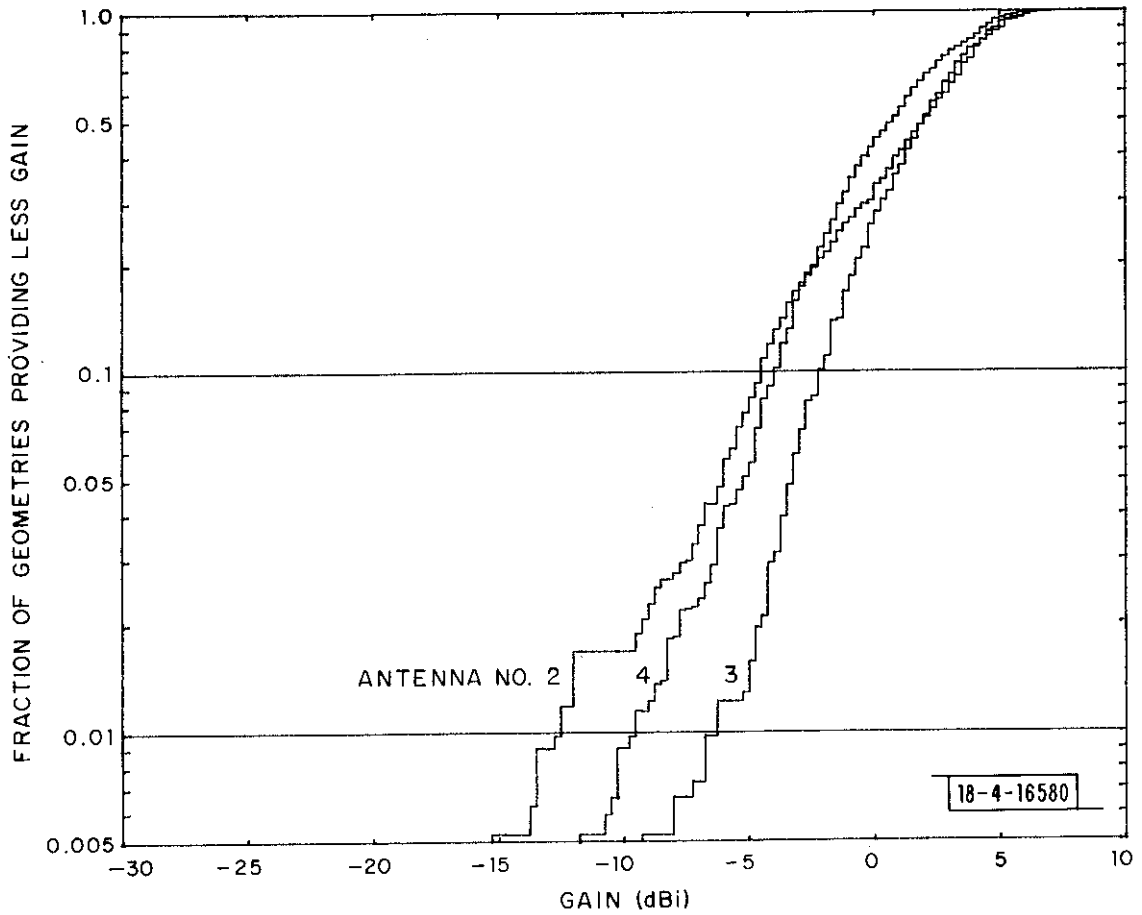


Fig. 32. Distribution of gains for three antenna positions on a Cessna 150 in level flight (flaps up).

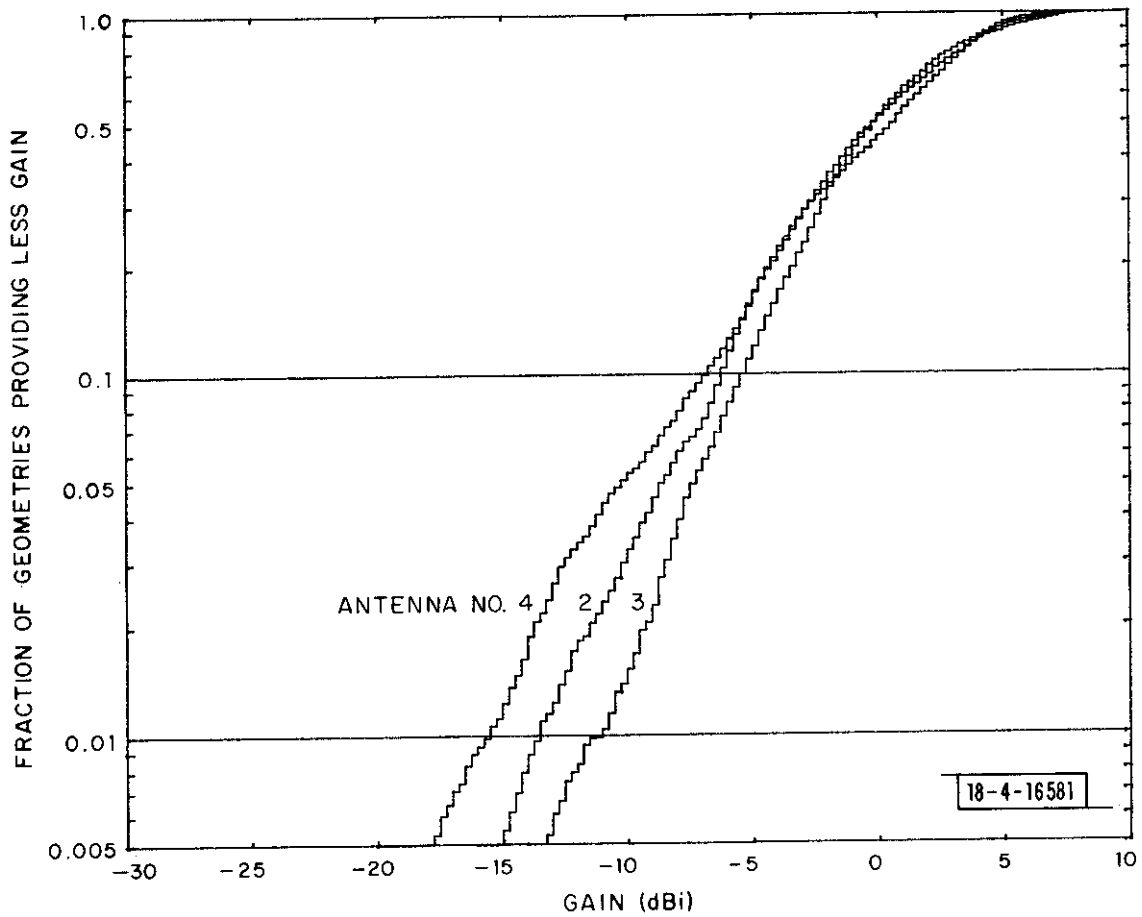


Fig. 33. Distribution of gains for three antenna positions on a Cessna 150 in a moderate roll (flaps up).

an overall lower gain distribution except for a few poor gain values for antenna 2. Similar results hold for moderate roll conditions.

As an additional measure of the comparative qualities of these antennas, Figs. 34 and 35 show the mean and standard deviation as a function of roll angle for each antenna. The mean and standard deviation are computed in dBi rather than in linear units in order to preserve the influence of the small gain values. From the first figure one observes that the mean gain values for the two antennas on the fuselage centerline are symmetric about the zero roll-angle condition with antenna 3 having a higher mean gain for small roll angles. The mean gain for antenna 4, which is to the left of the fuselage centerline, has a definite unsymmetric shape around the zero roll-angle value, and is at a maximum value for a roll to the left of around 14° . This is consistent with the location of the antenna since a roll to left reduces fuselage shielding of the antenna as viewed from the right of the aircraft. Positive roll angles tend to increase this shielding and reduce the average gain of the antenna. One also notices a definite change in slope of the data as the wings begin to obstruct the line of sight to the antenna at a roll angle of 16° in either direction.

Similar observations hold for the standard deviation or spread in the gain distributions with a larger σ indicating more data at the extremes or tails of the gain density curves. Since the density curve for higher gains tends to generally drop sharply to zero, the larger σ is indicative of more low or poor gain values. Again antenna 3 gives the best overall results.

Figures 36 through 39 show similar curves for the Piper aircraft and the same general conclusion holds. The conclusion is that antennas located

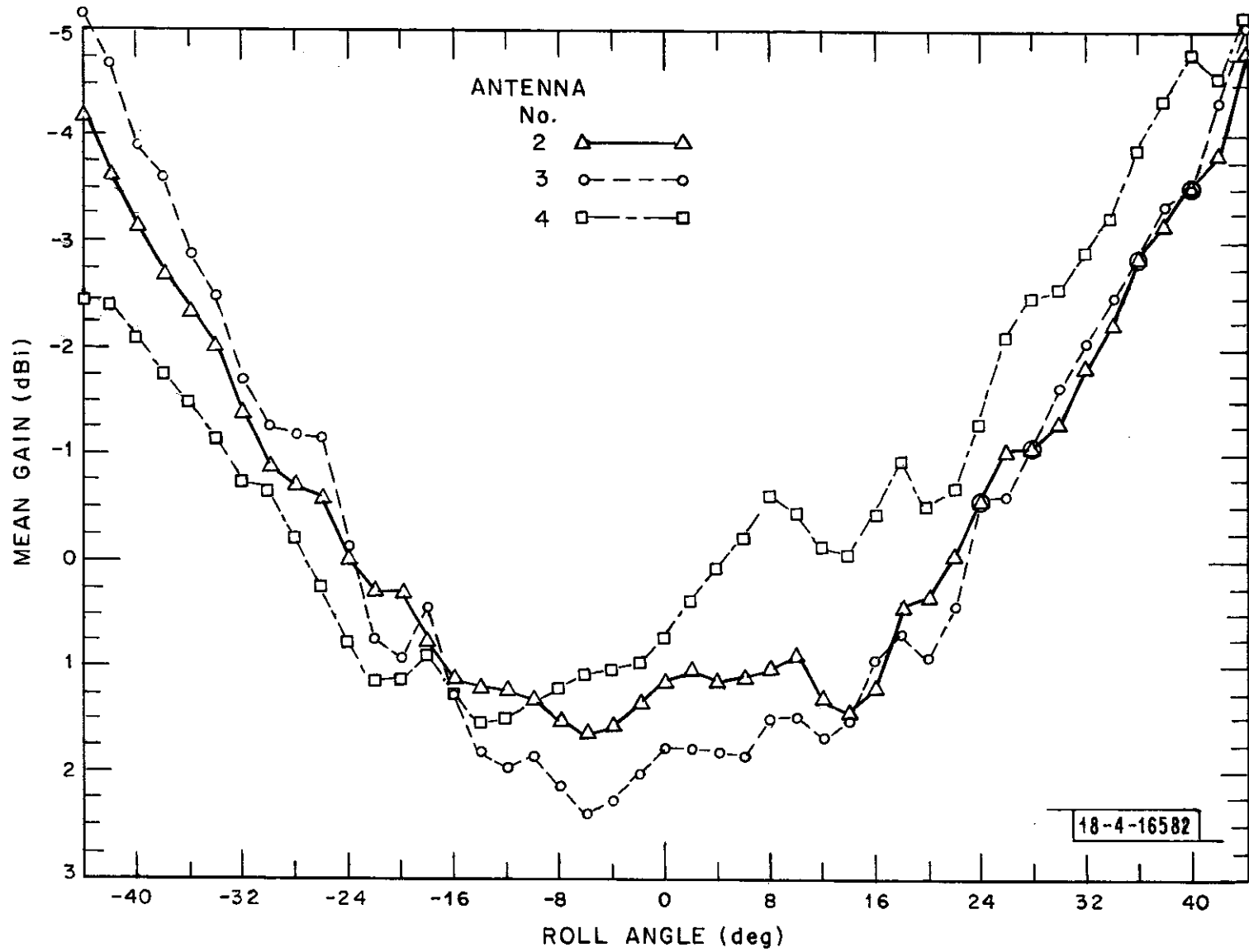


Fig. 34. Mean gain as a function of roll angle for three antenna positions on a Cessna 150 (flaps up).

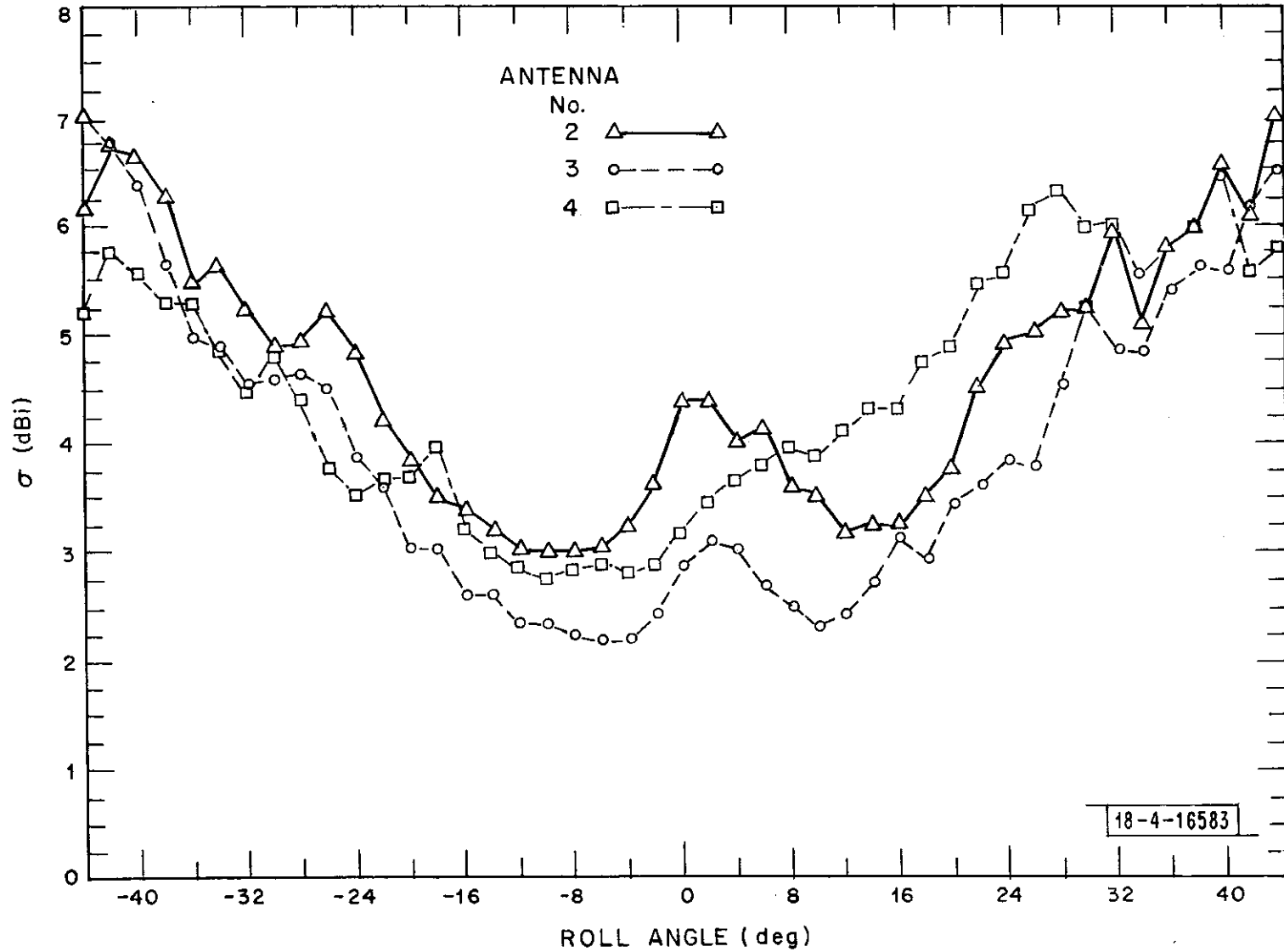


Fig. 35. RMS spread of gains as a function of roll angle for three antenna positions on a Cessna 150 (flaps up).

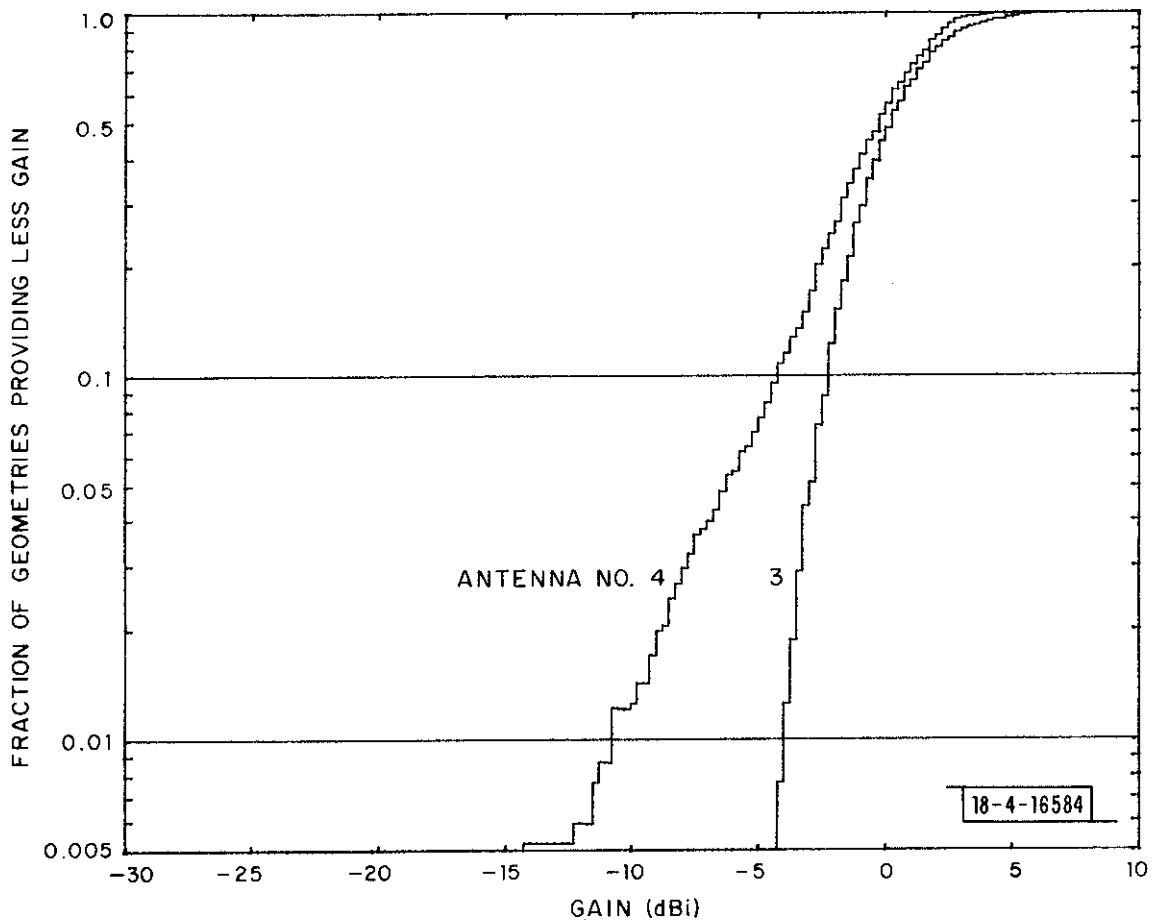


Fig. 36. Distribution of gains for two antenna positions on a Piper Cherokee Arrow in level flight (gear up; flaps up).

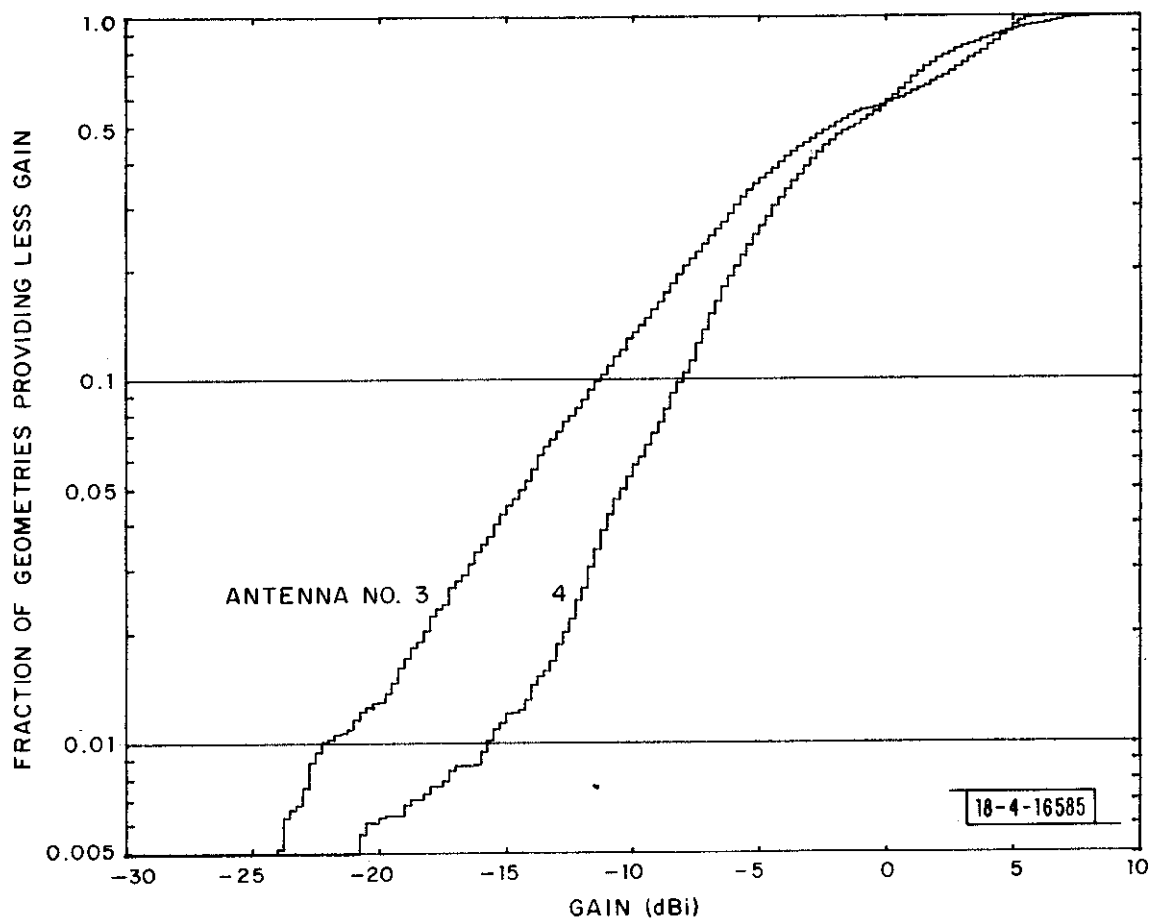


Fig. 37. Distribution of gains for two antenna positions on a Piper Cherokee Arrow in a moderate roll (gear up; flaps up).

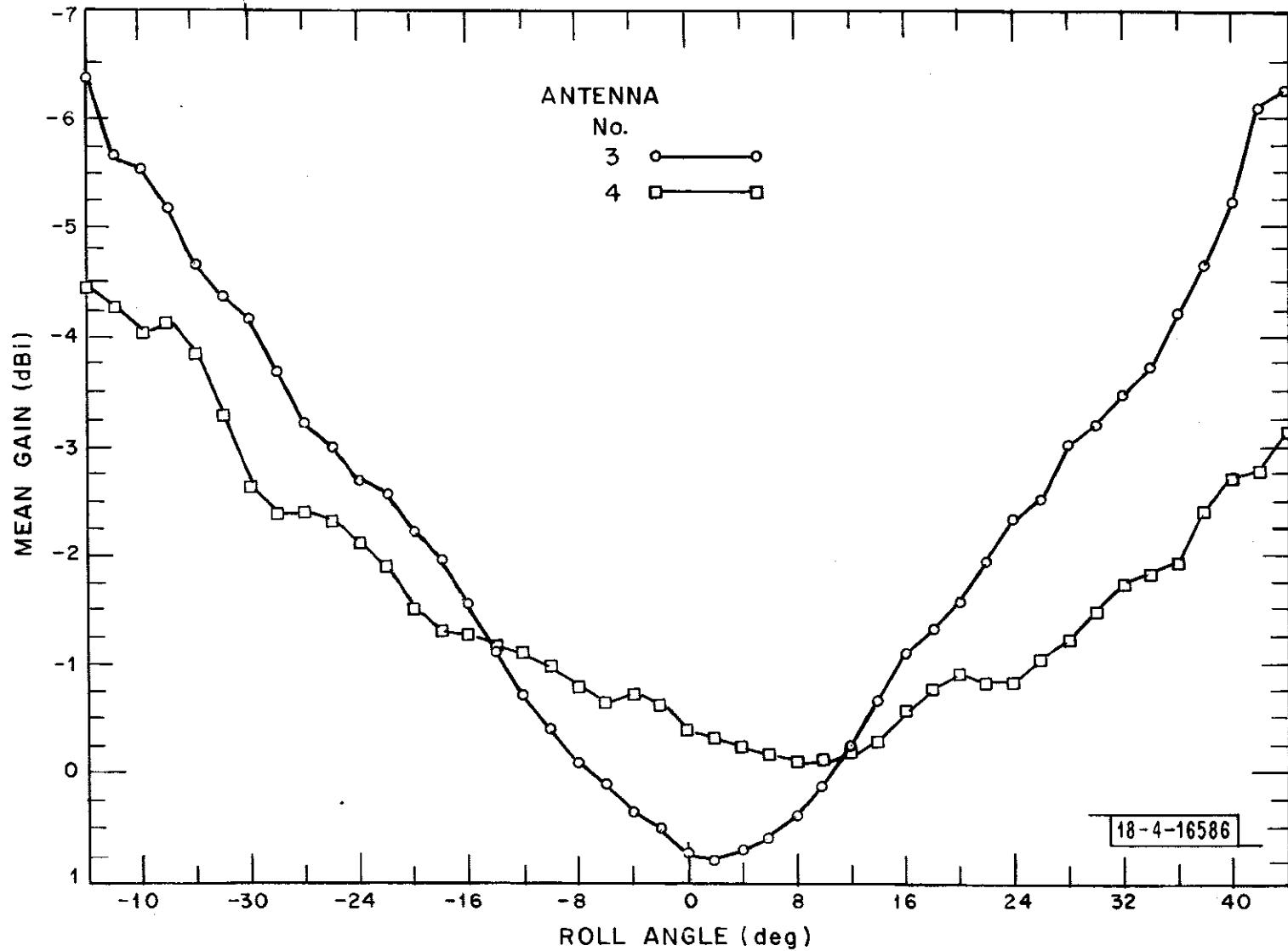


Fig. 38. Mean gain as a function of roll angle for two antenna positions on a Piper Cherokee Arrow (gear up; flaps up).

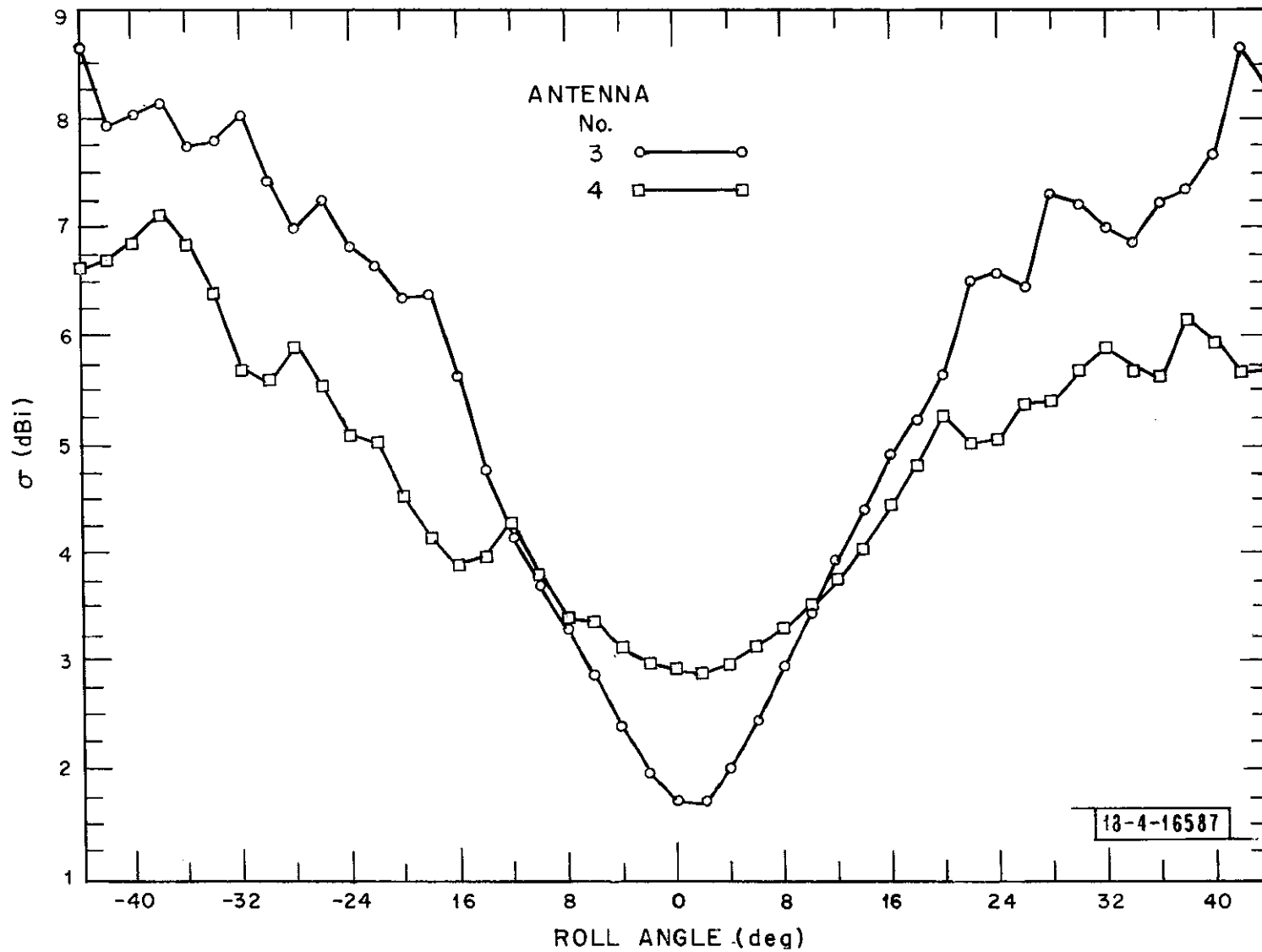


Fig. 39. RMS spread of gains as a function of roll angle for two antenna positions on a Piper Cherokee Arrow (gear up; flaps up).

on the fuselage centerline tend to have better gain distributions for most flight conditions. The better performance of the off center antenna (#4) in Figure 37 and for large roll angles in Figures 38 and 39 is attributed to the forward mounting of the antenna which reduces the wing shielding. During the more predominant level and shallow roll flight conditions however, the antenna on the fuselage center line is superior.

6. EFFECTS OF STRUCTURE AND ANTENNA LOCATION OBSERVED ON OTHER AIRCRAFT TYPES

Data on eight other aircraft are presented in this section as analyzed using the statistical methods previously employed. These additional aircraft include two twin-engine, low-wing, general-aviation aircraft (Beech Baron and Beech B99), two small jetliners (Grumman Gulfstream and Gates Lear Jet), one additional small, single-engine, high-wing aircraft (Helio U10D), and three additional commercial airliners of various sizes (Boeing 737, 707, 747). Photos showing the locations of the various bottom-mounted antenna stations are included in Appendix A. Figures 40 through 48 show the gain values at which 1% of the geometric conditions provide less gain and 99% provide equal or better gain for each type of aircraft, including the three previously analyzed, under varying flight conditions. The number in each data symbol indicates the antenna position. Summary comments on the data in these figures follow.

During level flight conditions most antennas provide gain values (see Fig. 40) between 0 and -10 dBi regardless of aircraft size. The Beech B99 performs slightly worse than the other small, low-wing aircraft because the engine housings extend below the wing and partially obstruct the antenna. Similarly, the Boeing 727 has a higher gain value than the other commercial airliners and is the only such aircraft without engines suspended below the wings.

As a roll angle is introduced, the two small jet aircraft, the four commercial airliners and, to a lesser extent, the high-wing aircraft react similarly and give a higher gain value than the three small, low-wing,

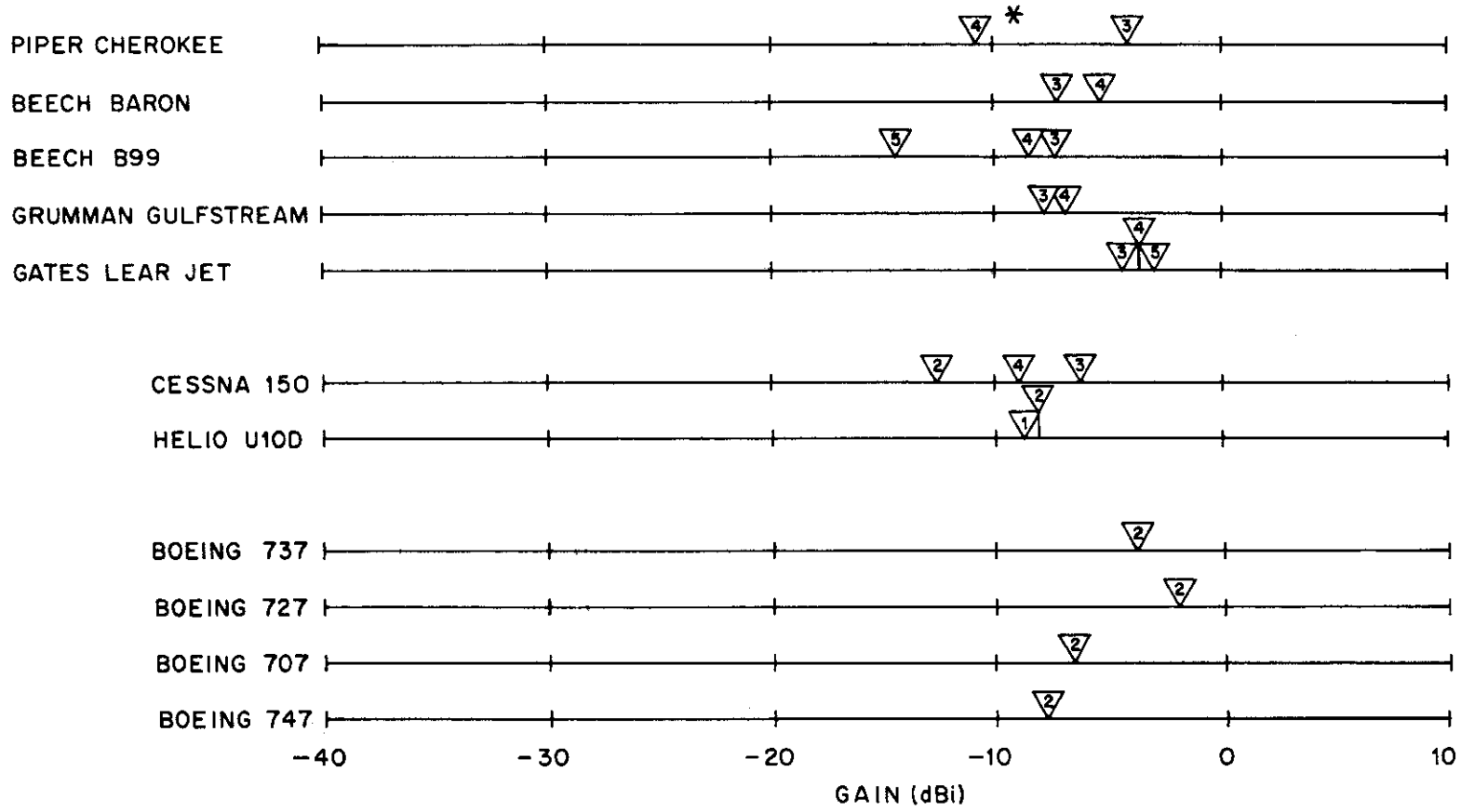
propeller aircraft. This is explainable by the degree of obstruction introduced by the wings. It has already been mentioned how the high-wing aircraft experiences less of a wing obstruction problem. For the large, low-wing aircraft the long fuselage permits placement of the antenna far enough forward along the bottom centerline to reduce the wing shielding effects during a roll. As the roll angle increases, the most forward antenna position gives consistently higher gain than the more aft antennas. Finally, at very steep roll angles the fuselage becomes an important obstruction and all the small aircraft give a similar gain value. The rounded shape of the underside of the commercial aircraft or the very far forward mounting of their antennas may explain why three of them give slightly better results than the small aircraft. The Boeing 747, however, has a flatter underside and experiences more shielding at large roll angles.

The effects of pitch are related to the fuselage diameter and one concludes that the wider the fuselage is, the greater obstruction it poses during pitch maneuvers. The five small, low-wing aircraft first listed in the figures are in increasing order of fuselage diameter and the gain value marking the worst 1% of the geometric conditions degrades in the same order. Only the Boeing 707 seems to violate the stated rule, although the 727 exaggerates the anomaly by shielding the antenna with its tail-mounted engines. As noted earlier for the Cessna 150 and verified here by the Helio U10D, the high-wing aircraft have less shielding problems during pitch maneuvers.

The effects of landing-gear and flap structures for the additional aircraft are consistent with the previously examined aircraft. The extended landing gear reduces antenna performance by shifting the gain at the 1% point

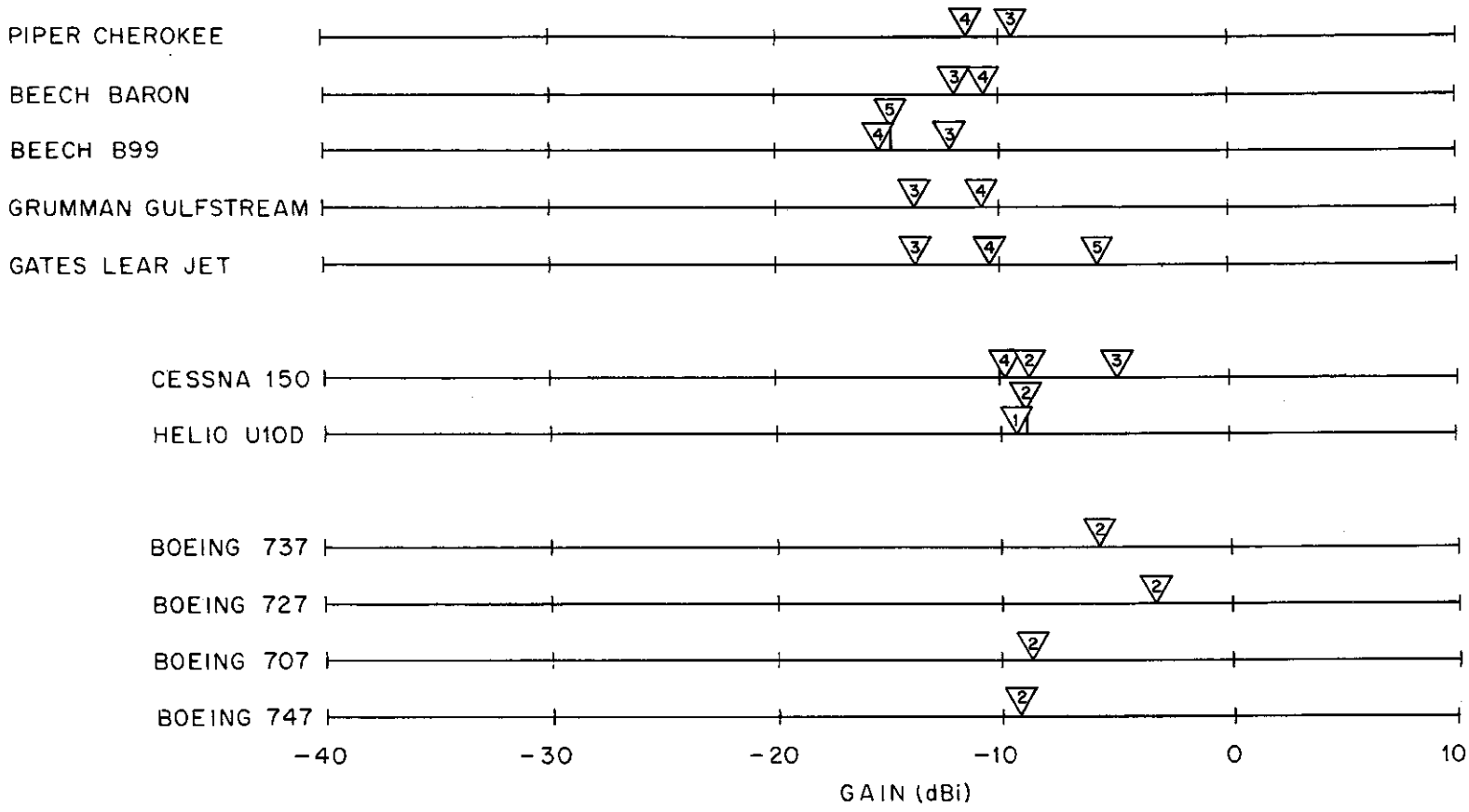
down by 2 to 6 dBi. The extended flaps give less predictable results although most pattern statistics are only slightly affected. Some antennas perform worse and a couple perform better than without flaps. This result again demonstrates the complicated nature of the reflections and diffractions which cause the antenna lobing structure. For most cases, however, the gain marking the worst 1% of the geometric conditions is shifted less than 2 dBi.

Since the presence of landing-gear struts degrades the performance of an antenna, it is important not to locate the antenna too close to any of the landing-gear struts. While the random heading statistics may show good overall performance for an antenna located very far forward, the poor gain values introduced by the nose wheel, as observed in Figs. 2 and 11, occur for nose-on aspect angles. It is at these angles that an airport-located ground station normally observes the aircraft on final approach. For constant receiver/transmitter characteristics this is generally not a problem since propagation losses are greatly reduced at such close ranges. But, if the ground sensor receiver sensitivity or transmit power are varied with aircraft range, the nulls introduced by the nose wheel can become a problem. This point should be considered when trying for the best enroute and terminal performance with only one antenna on the aircraft.



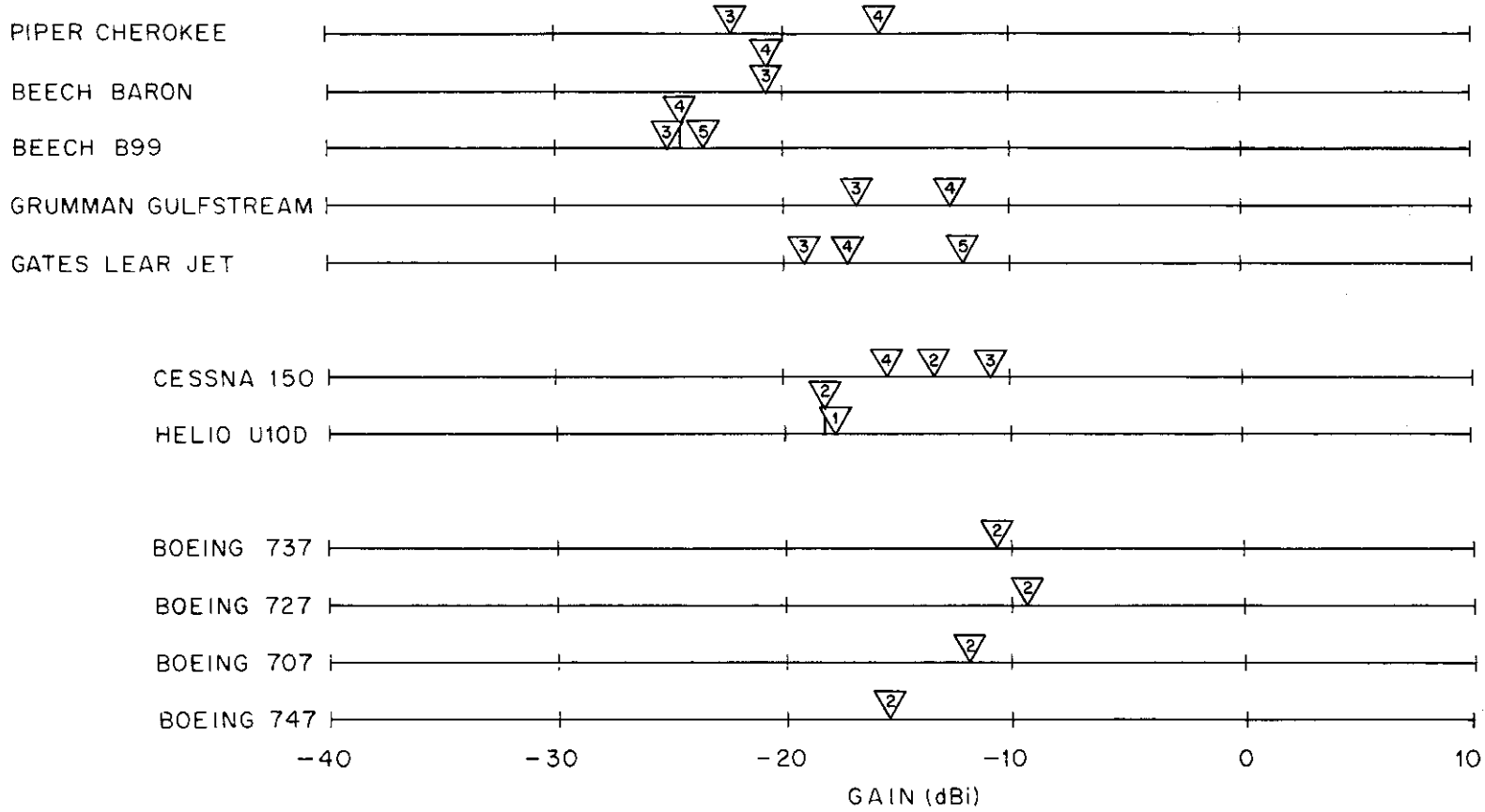
* THE NUMBER IN EACH DATA SYMBOL IS ANTENNA POSITION CODE.

Fig. 40. 99% gain values for various aircraft in level flight (various antennas; gear up; flaps up).



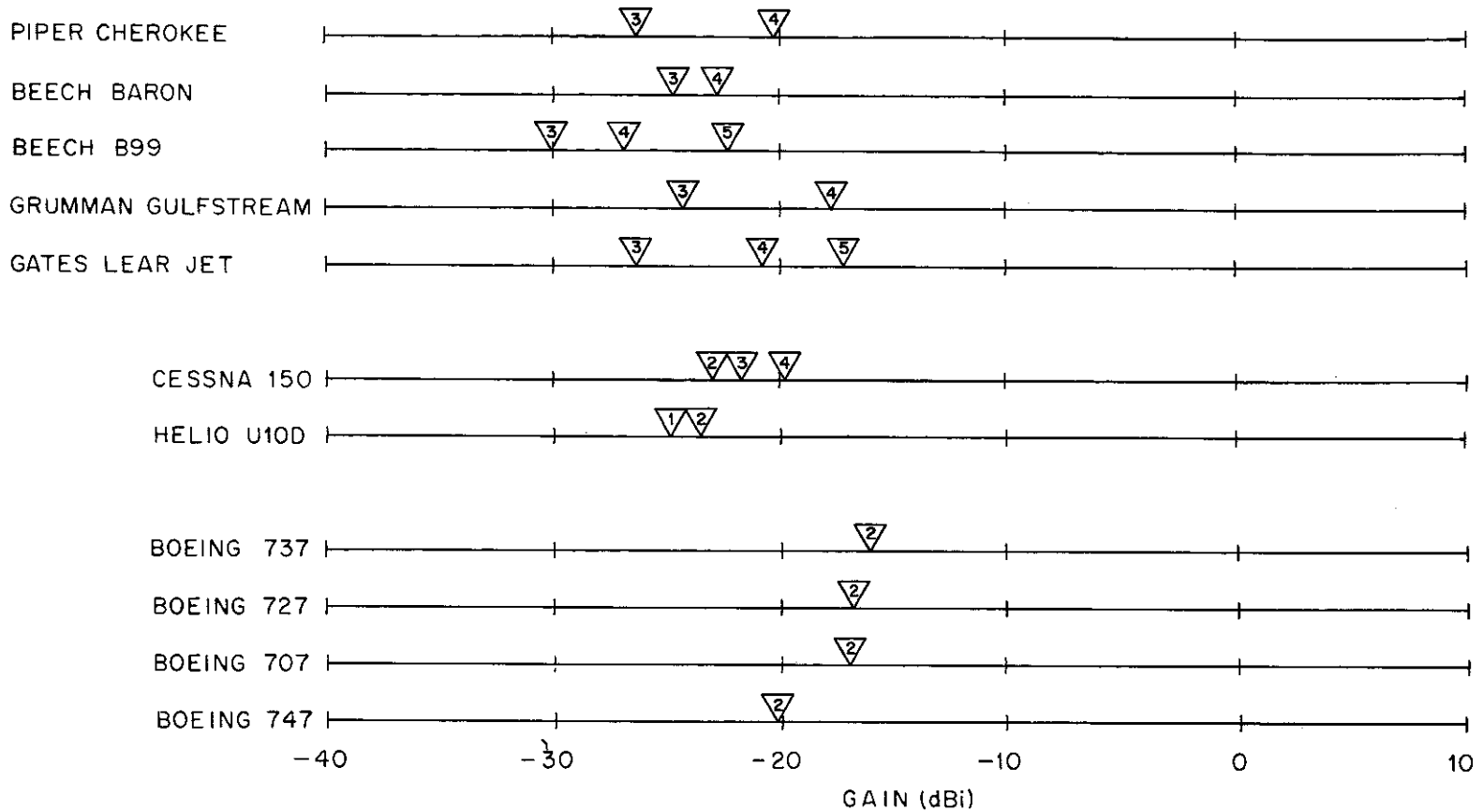
* THE NUMBER IN EACH DATA SYMBOL IS ANTENNA POSITION CODE.

Fig. 41. 99% gain values for various aircraft in a shallow roll (various antennas; gear up; flaps up).



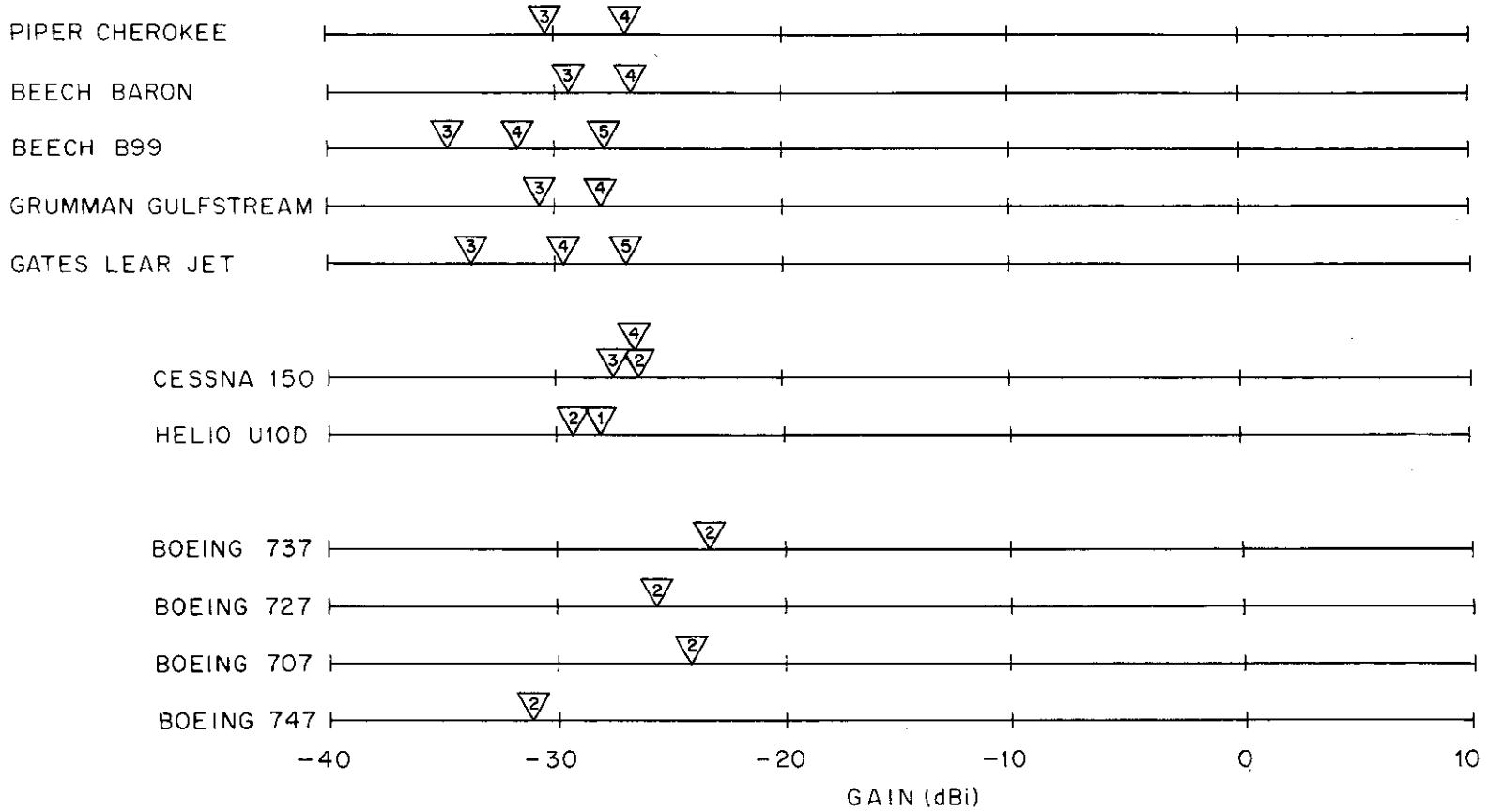
* THE NUMBER IN EACH DATA SYMBOL IS ANTENNA POSITION CODE.

Fig. 42. 99% gain values for various aircraft in a moderate roll (various antennas; gear up; flaps up).



* THE NUMBER IN EACH DATA SYMBOL IS ANTENNA POSITION CODE.

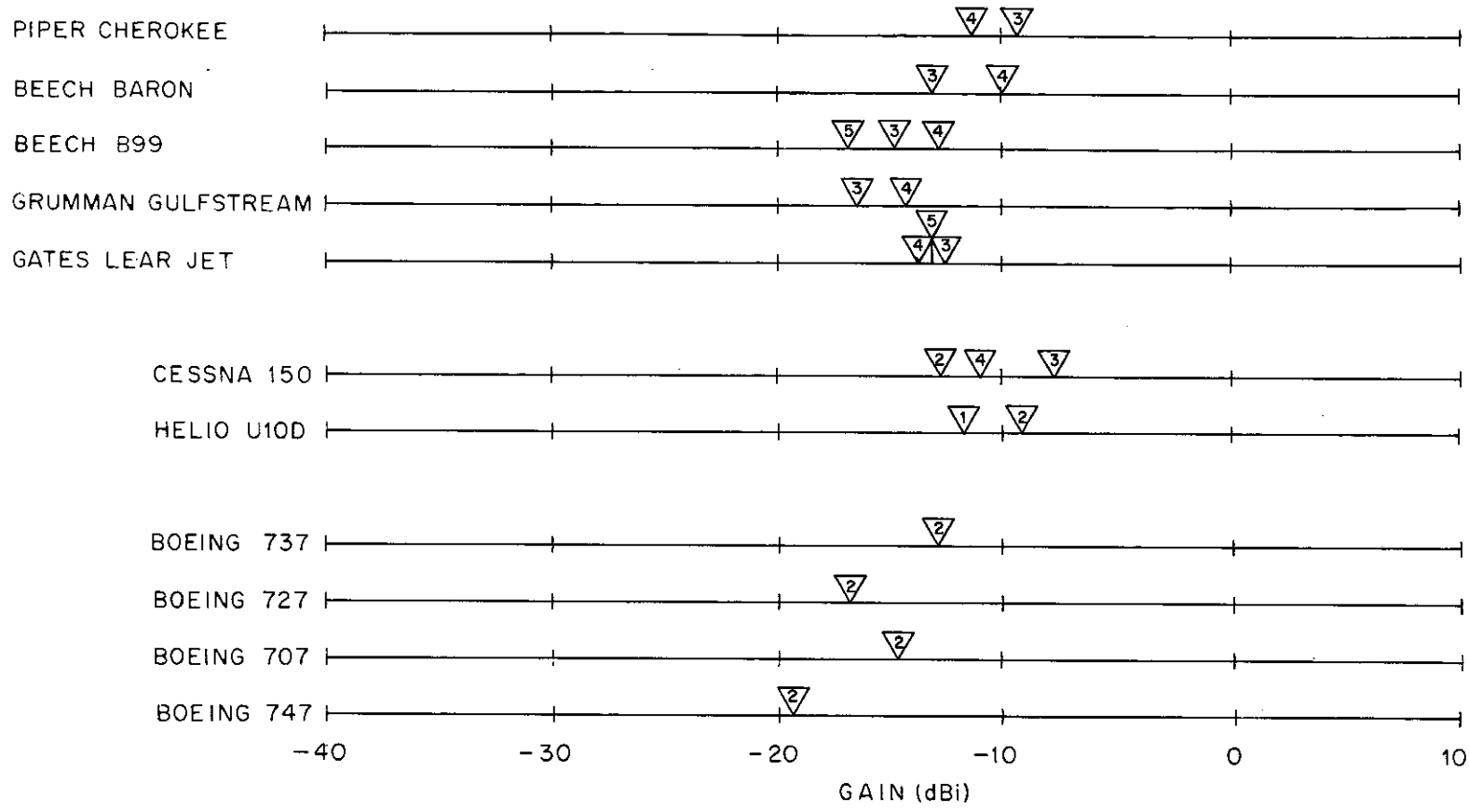
Fig. 43. 99% gain values for various aircraft in a steep roll (various antennas; gear up; flaps up).



69

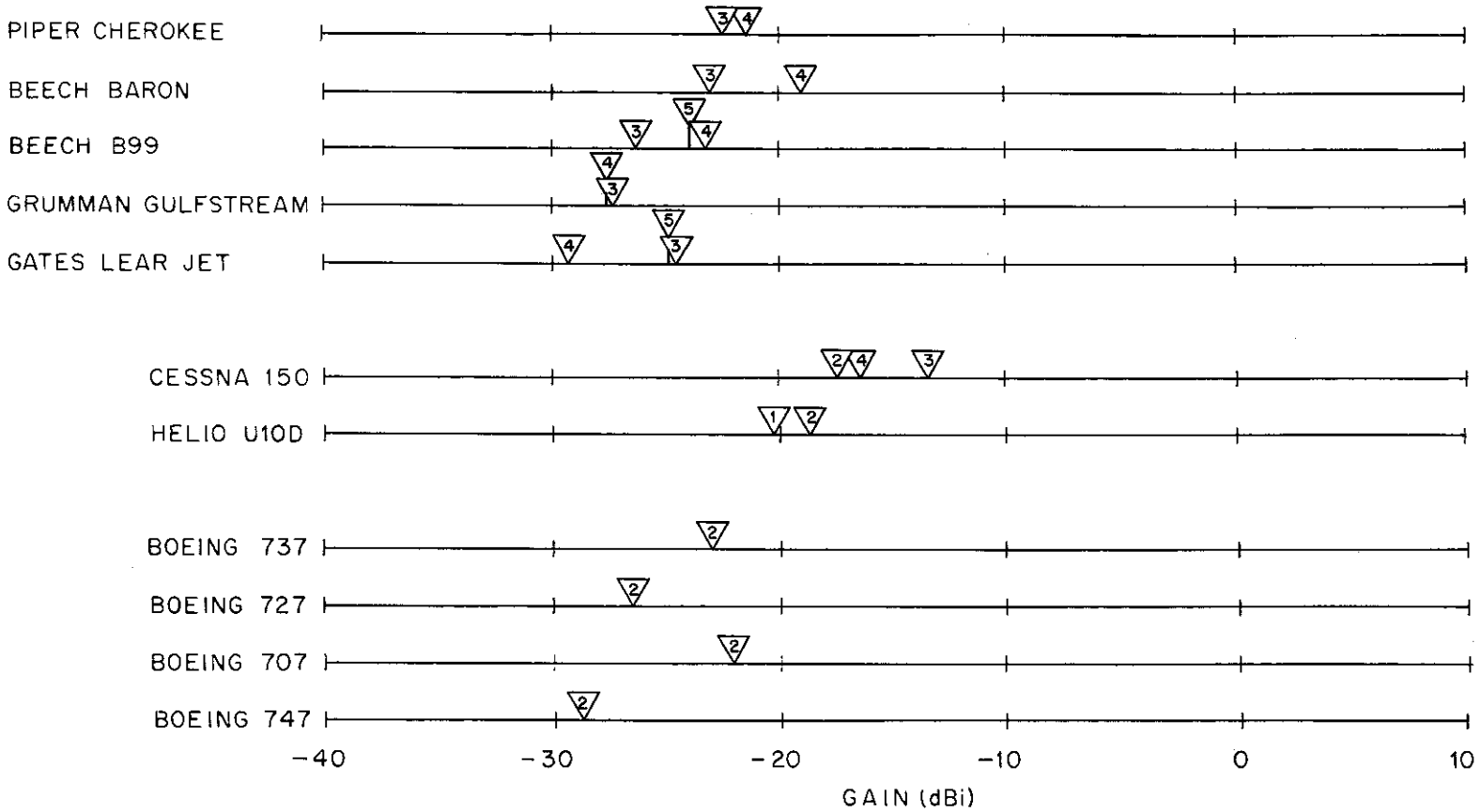
* THE NUMBER IN EACH DATA SYMBOL IS ANTENNA POSITION CODE.

Fig. 44. 99% gain values for various aircraft in a very steep roll (various antennas; gear up; flaps up).



* THE NUMBER IN EACH DATA SYMBOL IS ANTENNA POSITION CODE.

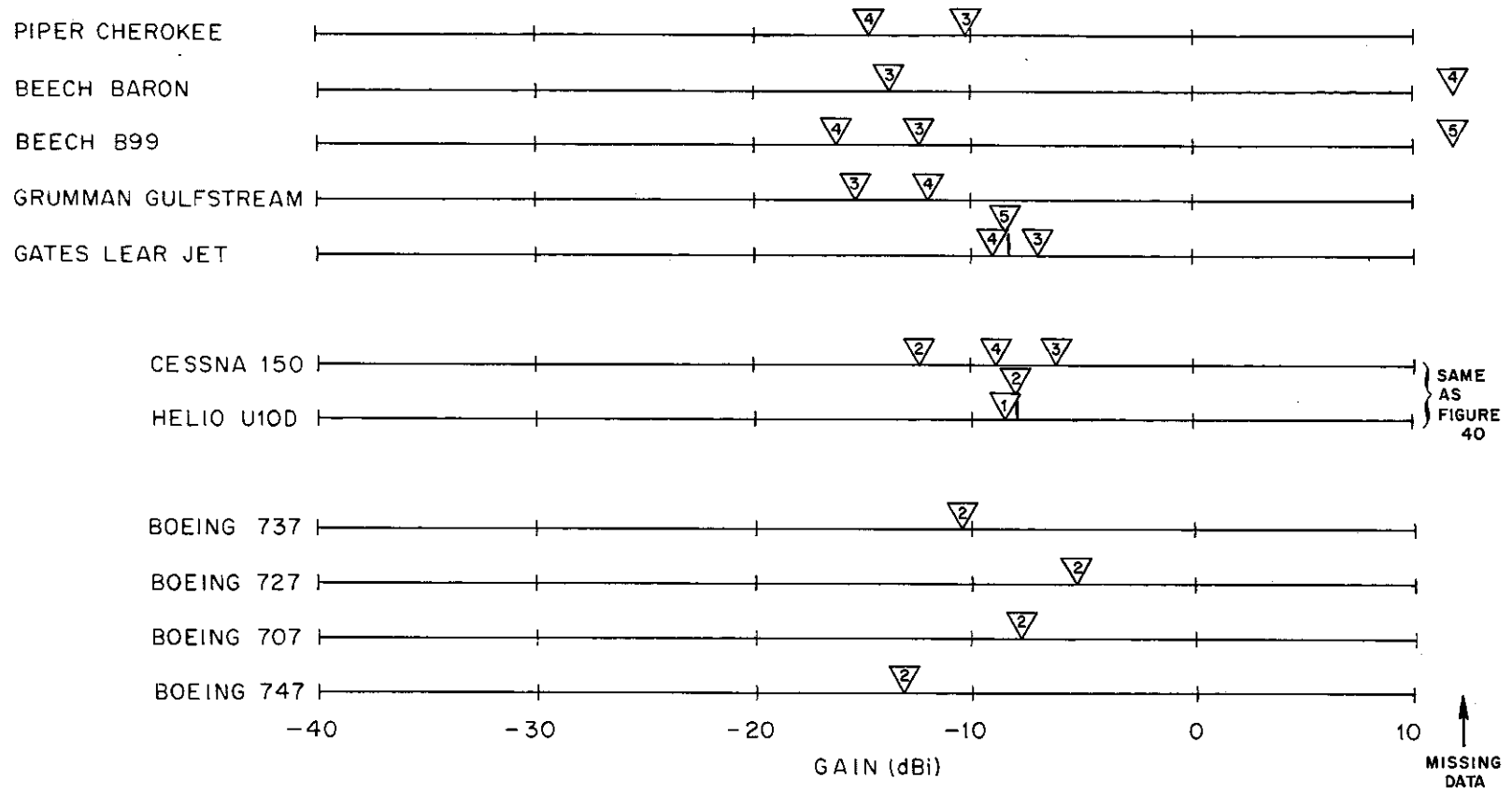
Fig. 45. 99% gain values for various aircraft in a moderate pitch (various antennas; gear up; flaps up).



* THE NUMBER IN EACH DATA SYMBOL IS ANTENNA POSITION CODE.

Fig. 46. 99% gain values for various aircraft in a steep pitch (various antennas; gear up; flaps up).

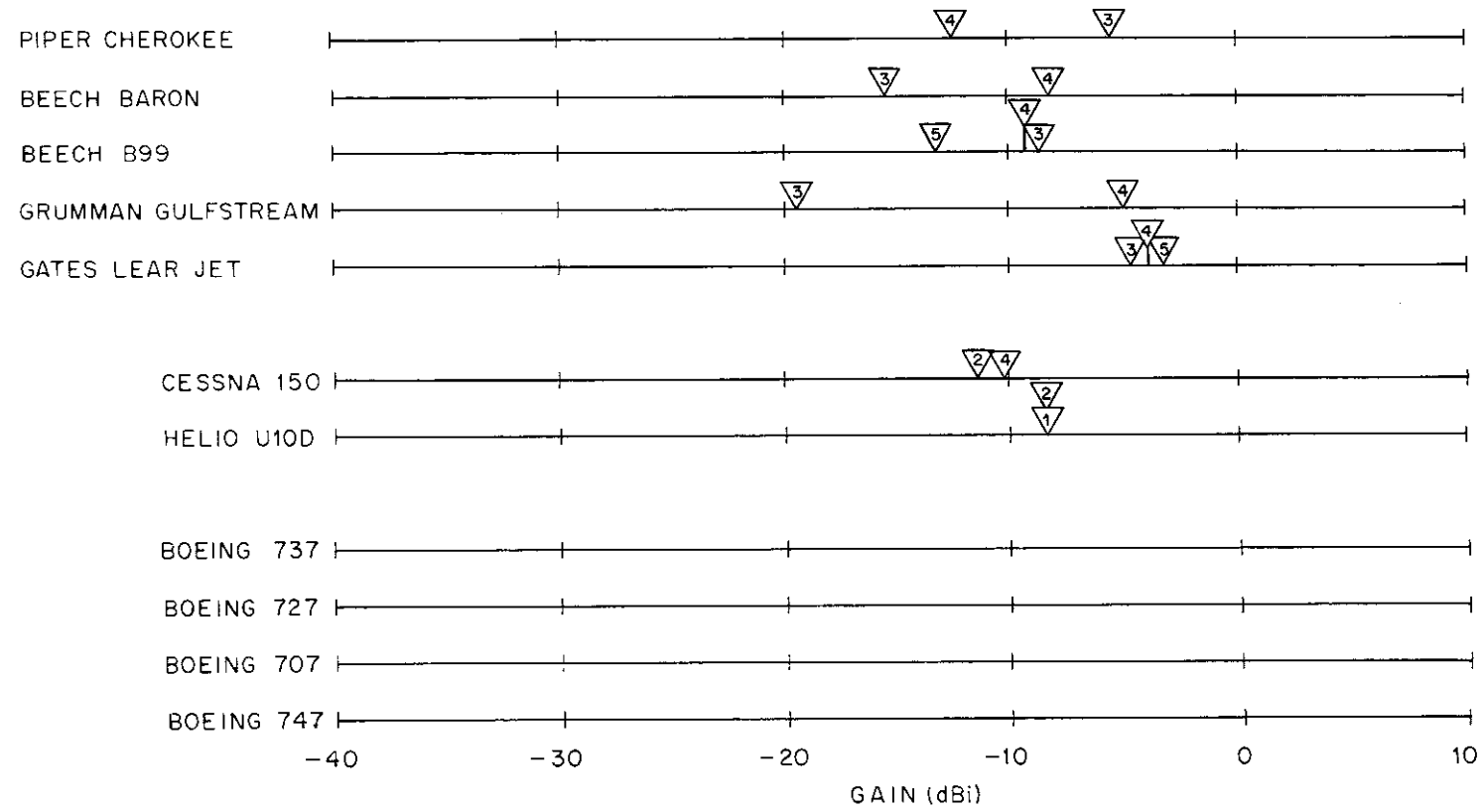
18-4-16595



* THE NUMBER IN EACH DATA SYMBOL IS ANTENNA POSITION CODE.

Fig. 47. 99% gain values for various aircraft with gear down (various antennas; level flight; flaps up).

18-4-16596



* THE NUMBER IN EACH DATA SYMBOL IS ANTENNA POSITION CODE.

↑
BAD OR MISSING DATA

Fig. 48. 99% gain values for various aircraft with flaps down (various antennas; level flight; gear up).

7. SUMMARY AND CONCLUSIONS

The results presented in this report have not only confirmed intuitive feelings about aircraft antenna patterns, but have provided a more quantitative picture useful in evaluating L-band beacon antenna installations. The relationships of the aircraft structural features to the patterns and the statistical nature of the pattern data under varying flight conditions have been examined and consistent physical explanations given where possible. It is recognized, however, that typical aircraft structures are complicated and that the use of aircraft models to observe "fine grained" effects is limited. The following conclusions have been drawn in this light:

- (1) The extension of flaps has little effect on the antenna pattern.
- (2) The landing-gear struts cause low gain values at some aspect angles in a manner consistent with interference and diffraction theory. The proximity of the struts to the antenna is therefore an important consideration.
- (3) For small, general-aviation aircraft with antennas mounted on the bottom of the fuselage under the wings, a low-wing aircraft has significantly lower gain values than a high-wing aircraft when the aircraft banks in a manner which points the aircraft antenna away from the ground antennas. Moving the antenna forward or backward on the fuselage may introduce other problems including signal blockage in the forward direction.
- (4) For large aircraft on which the antenna may be located forward from the wings, the fuselage is the primary shielding obstruction.

During banking maneuvers the gain distribution for a large aircraft exhibits less low gain values than for a small, high-wing aircraft and for a small low-wing aircraft if the antenna on the large aircraft is forward of the wings.

- (5) During pitch maneuvers the fuselage shields the antenna and more low gain values occur than during level flight. The larger size aircraft produces a greater number of these low gain conditions.
- (6) For best overall performance the antenna should be mounted on the fuselage centerline.

These conclusions are based on a small sample of common aircraft types and provide a means for making more reasonable estimates of performance for other aircraft. Such methodology has heretofore been lacking.

APPENDIX A

PHOTOS AND DRAWINGS OF AIRCRAFT
SHOWING
ANTENNA AND LANDING GEAR LOCATIONS



Fig. A-1. Piper Cherokee Arrow, three-quarter view.

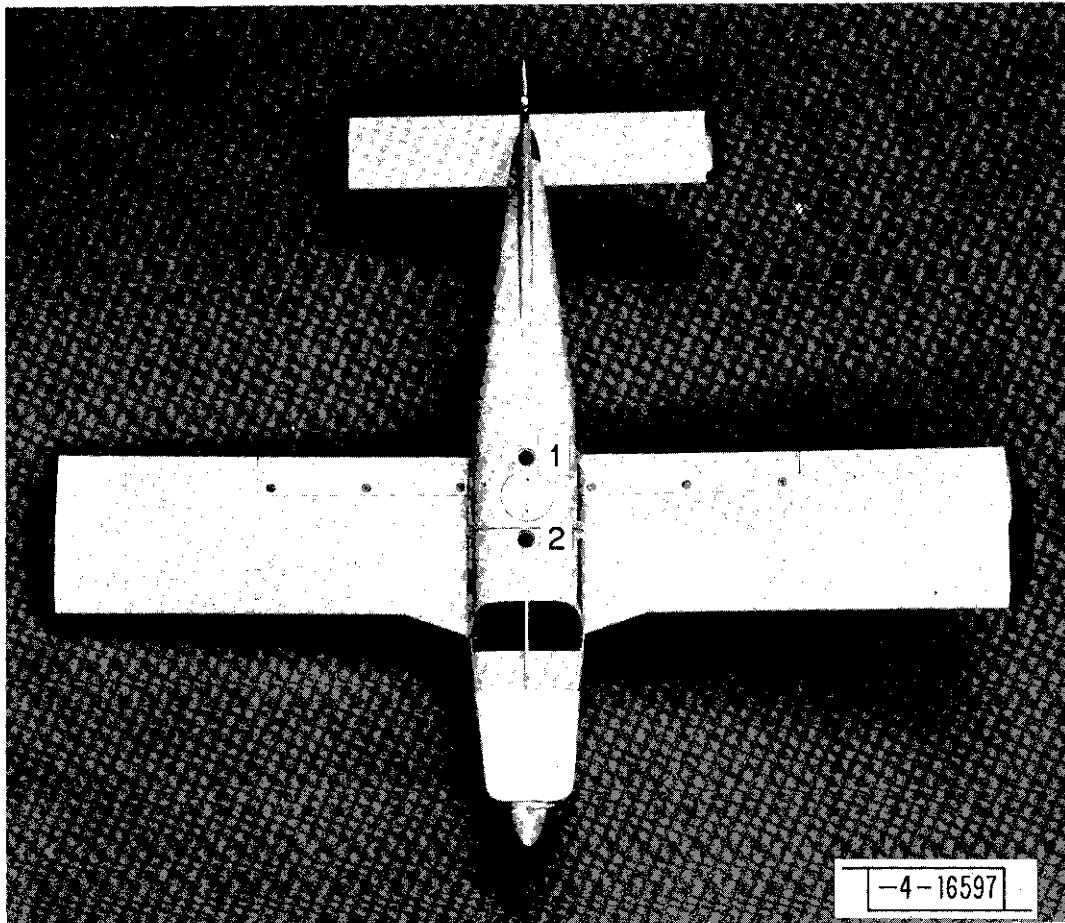


Fig. A-2. Piper Cherokee Arrow, top view showing antenna positions 1 and 2.

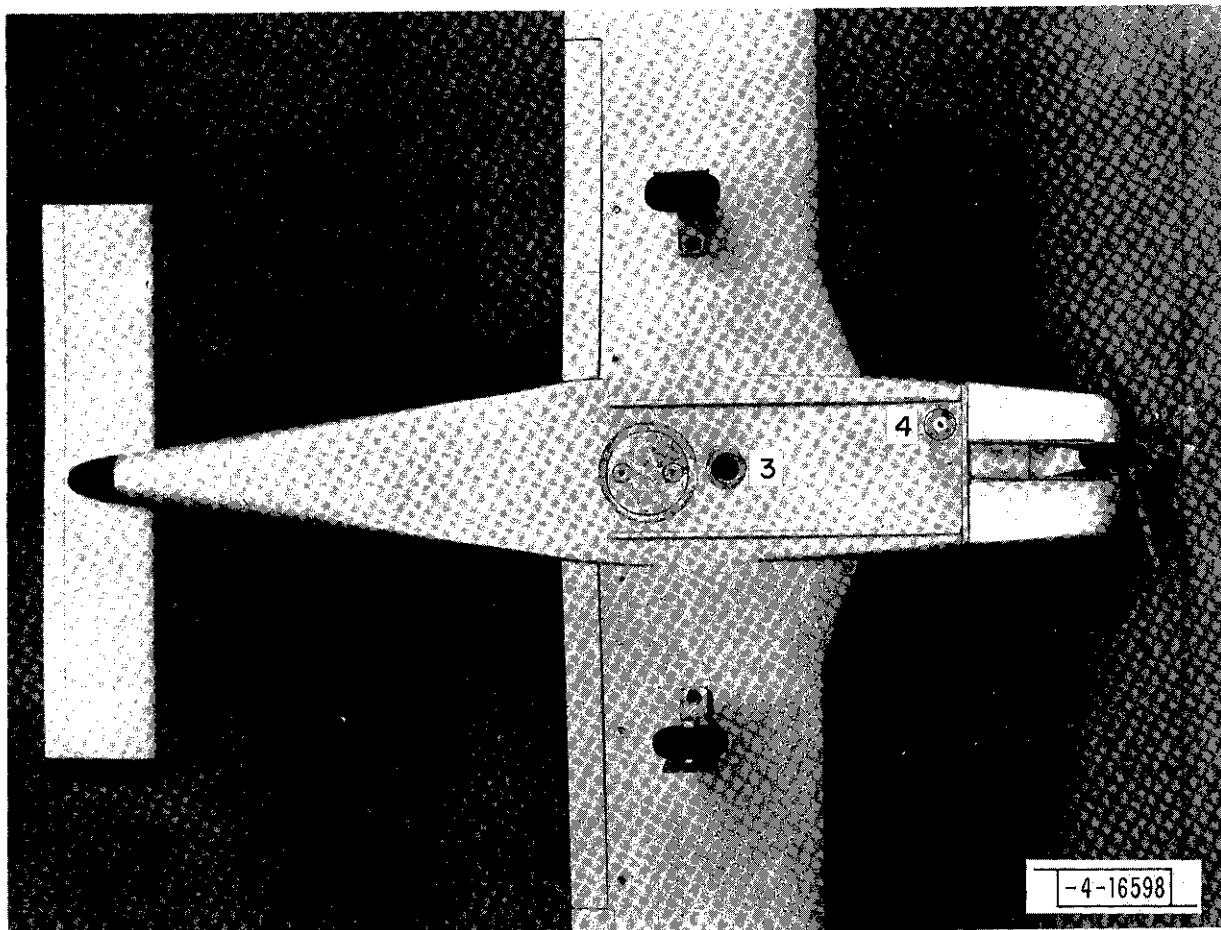


Fig. A-3. Piper Cherokee Arrow, bottom view showing antenna positions 3 and 4.

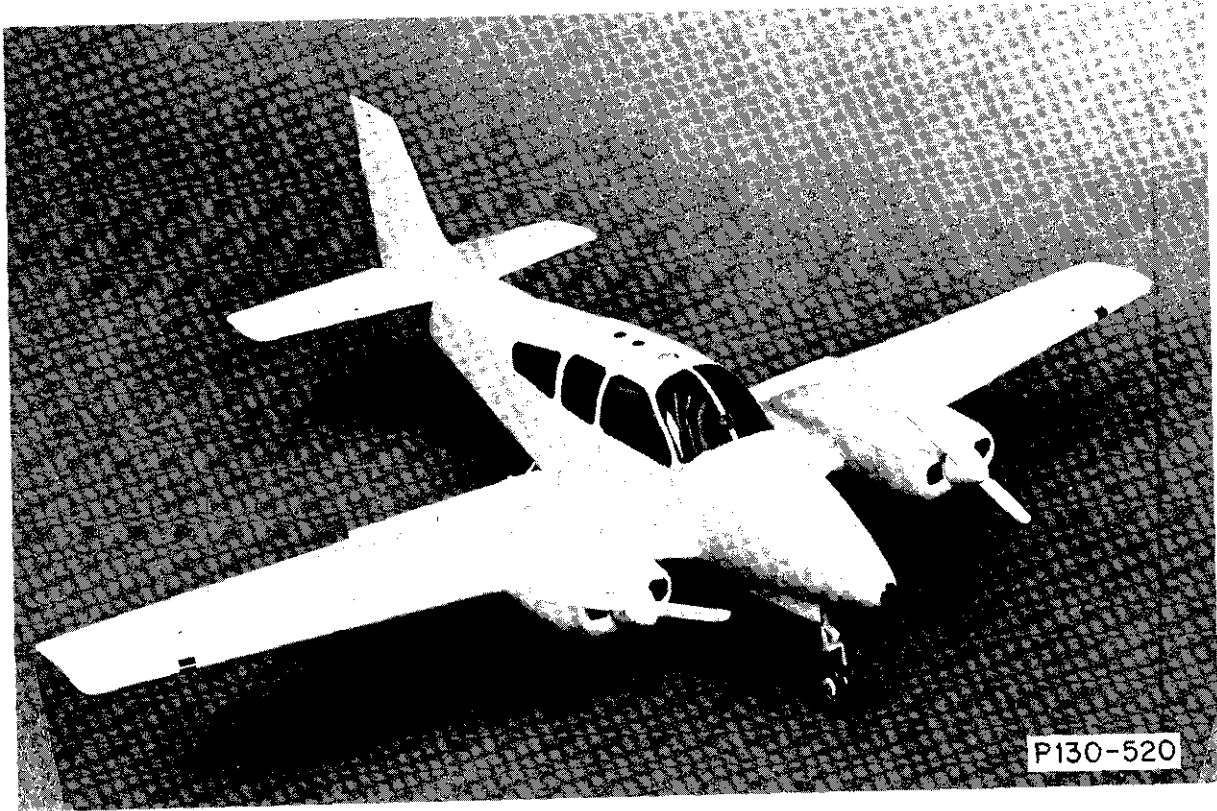


Fig. A-4. Beechcraft Baron, three-quarter view.

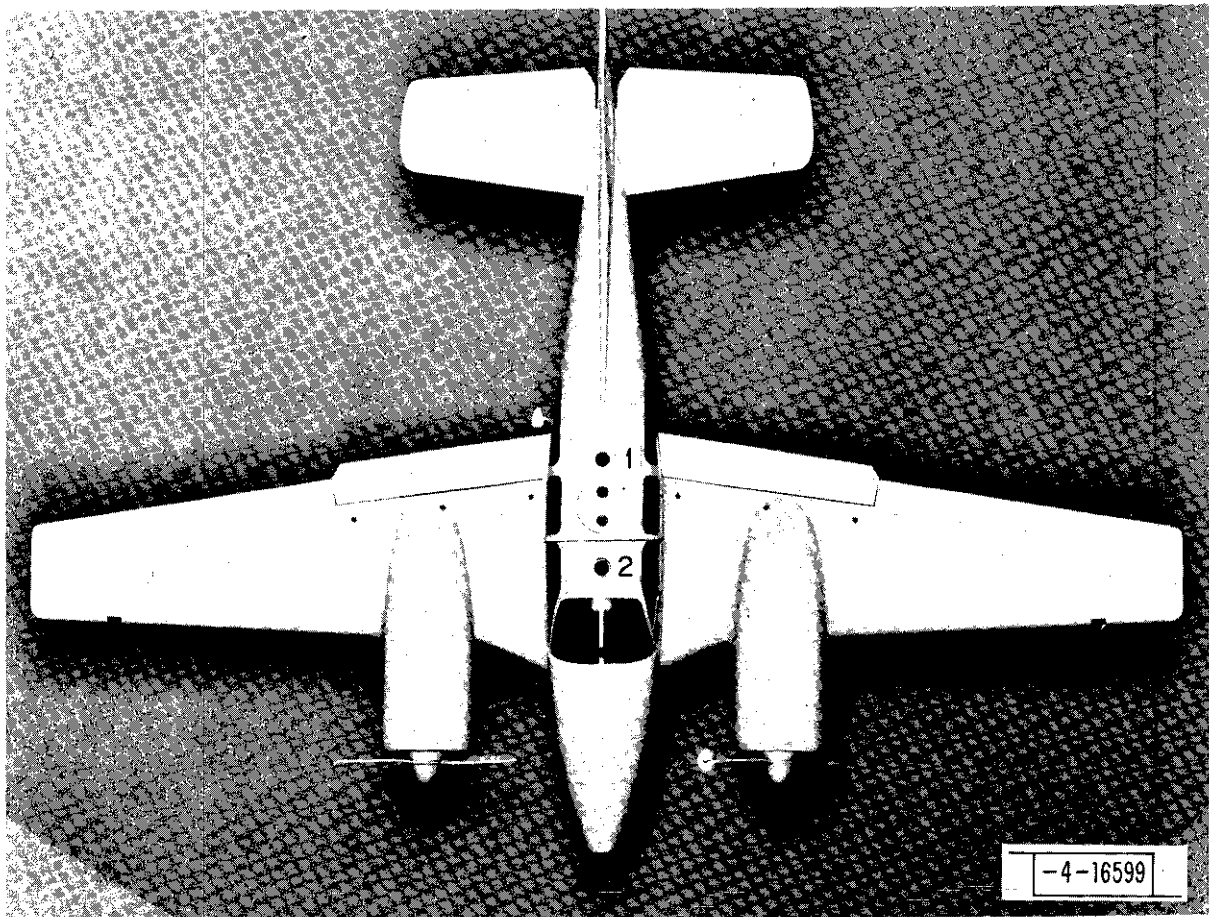


Fig. A-5. Beechcraft Baron, top view showing antenna positions 1 and 2.

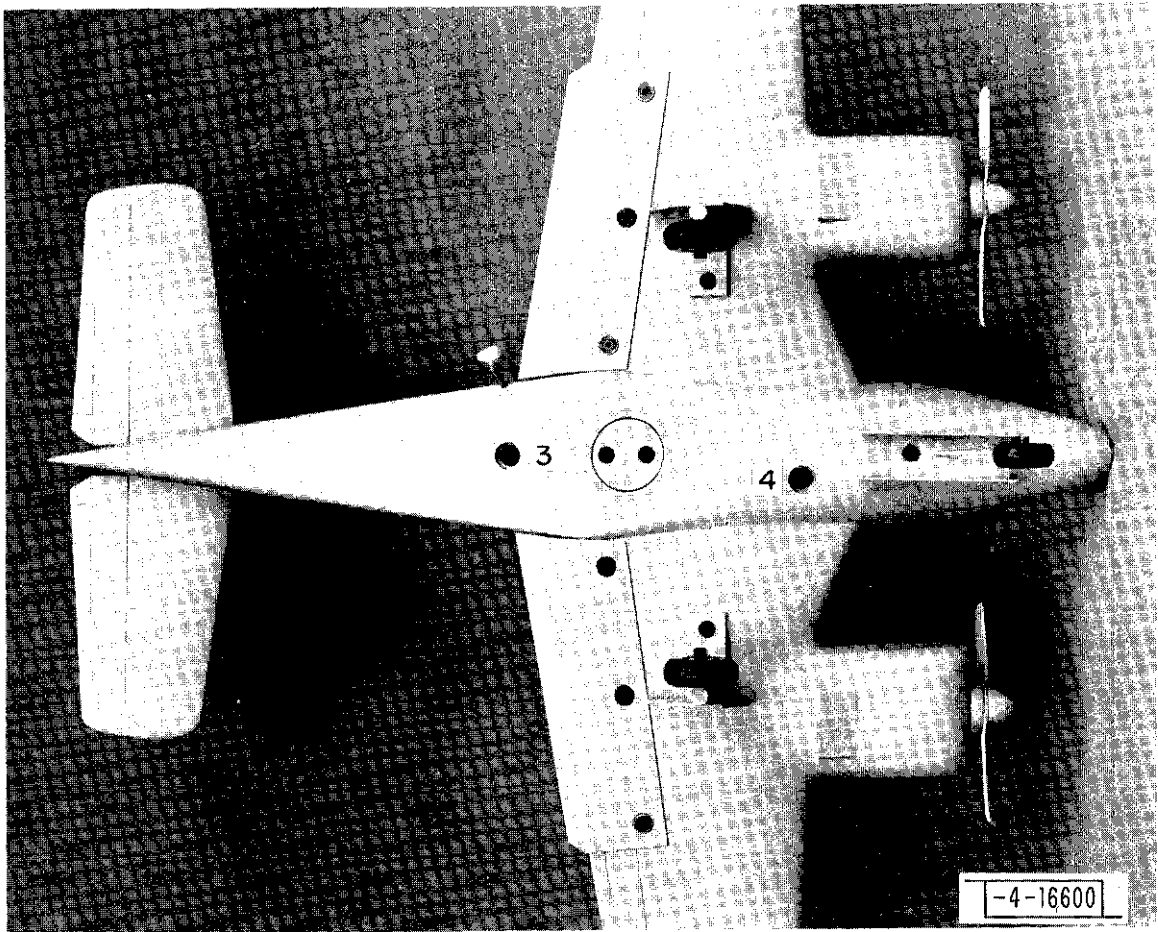


Fig. A-6. Beechcraft Baron, bottom view showing antenna positions 3 and 4.



Fig. A-7. Beechcraft B99, three-quarter view.

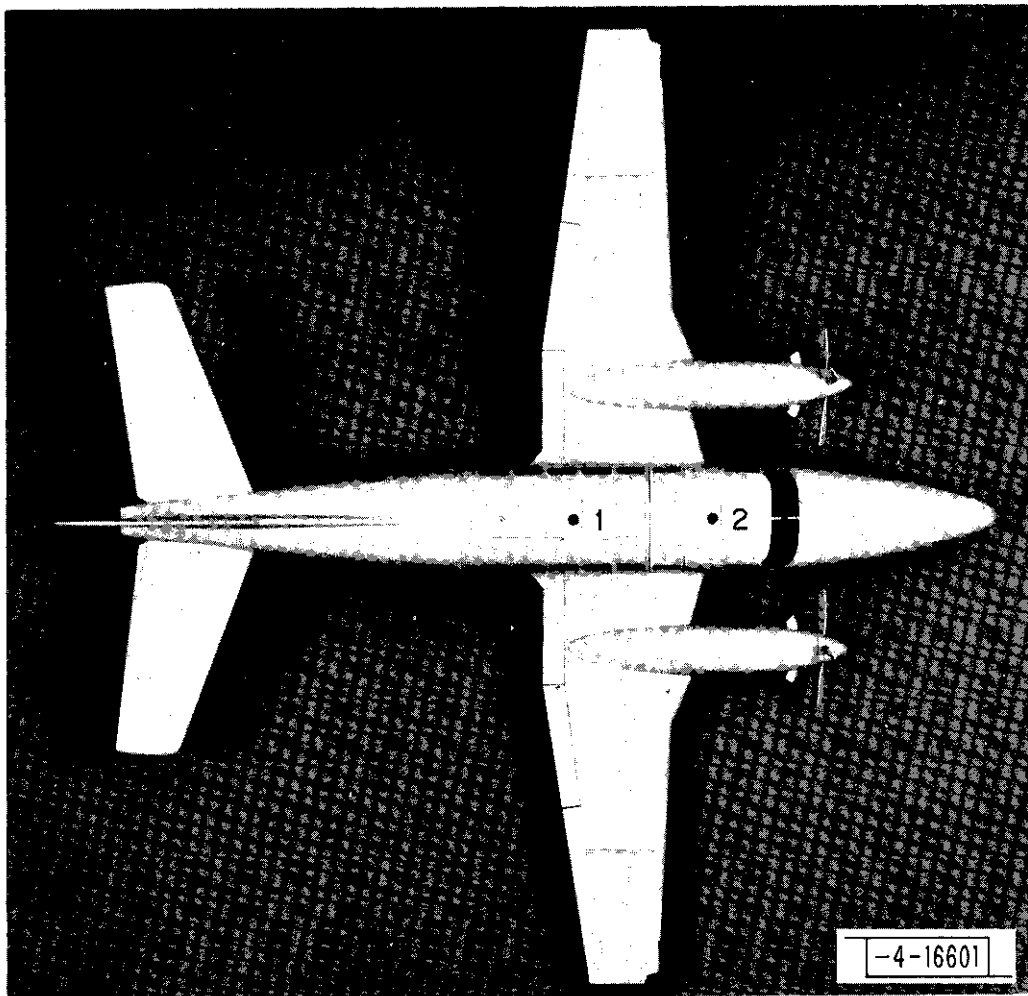


Fig. A-8. Beechcraft B99, top view showing antenna positions 1 and 2.

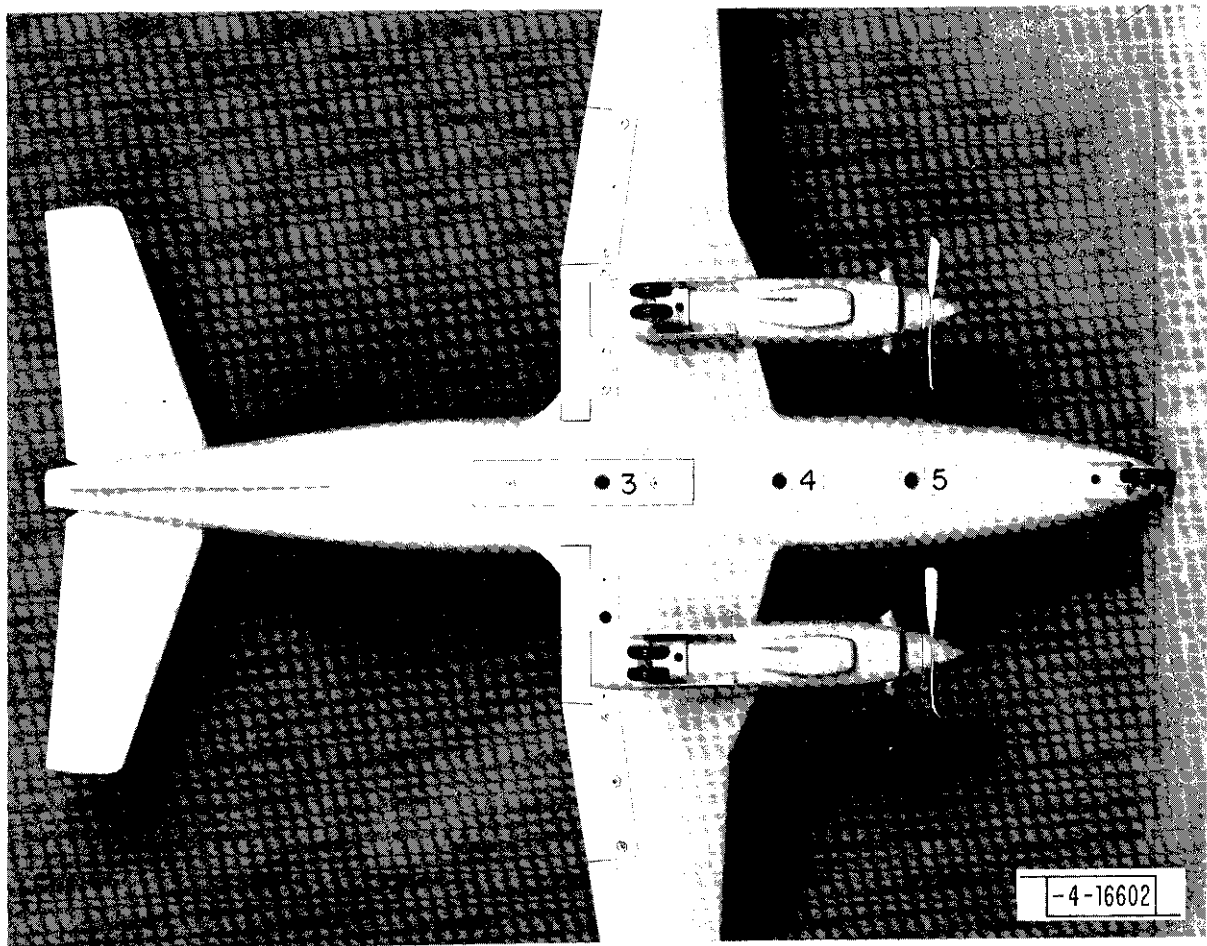


Fig. A-9. Beechcraft B99, bottom view showing antenna positions 3, 4 and 5.

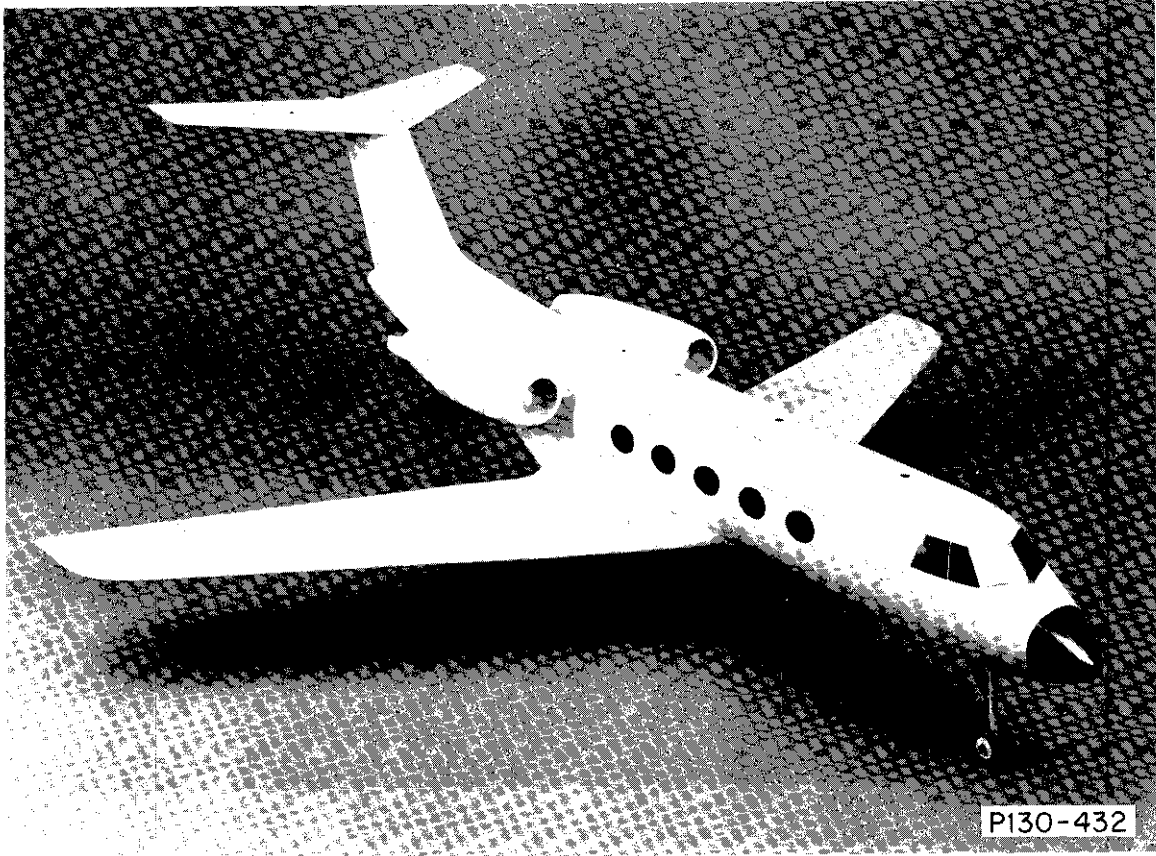


Fig. A-10. Grumman Gulfstream, three-quarter view.

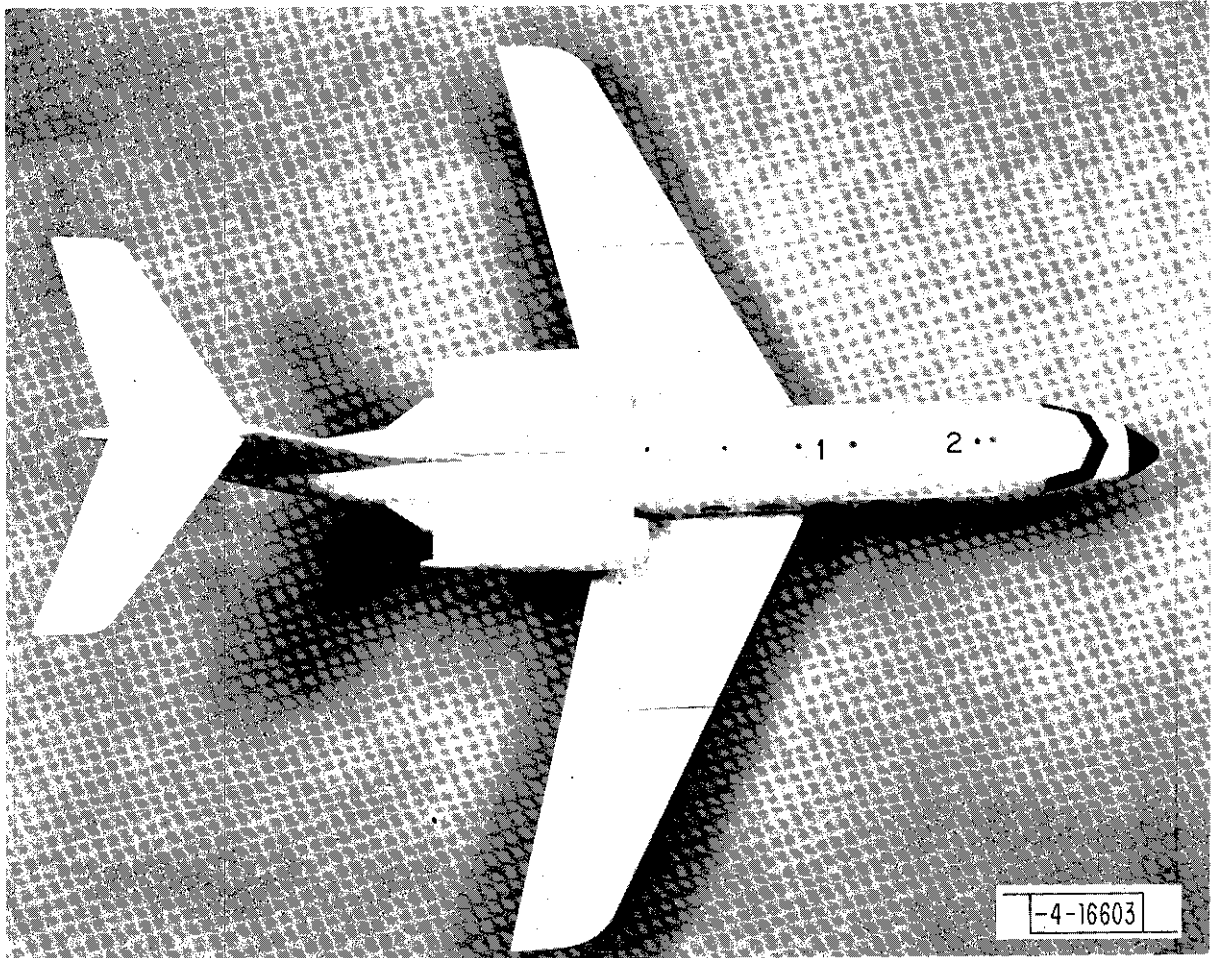


Fig. A-11. Grumman Gulfstream, top view -- showing antenna positions 1 and 2.

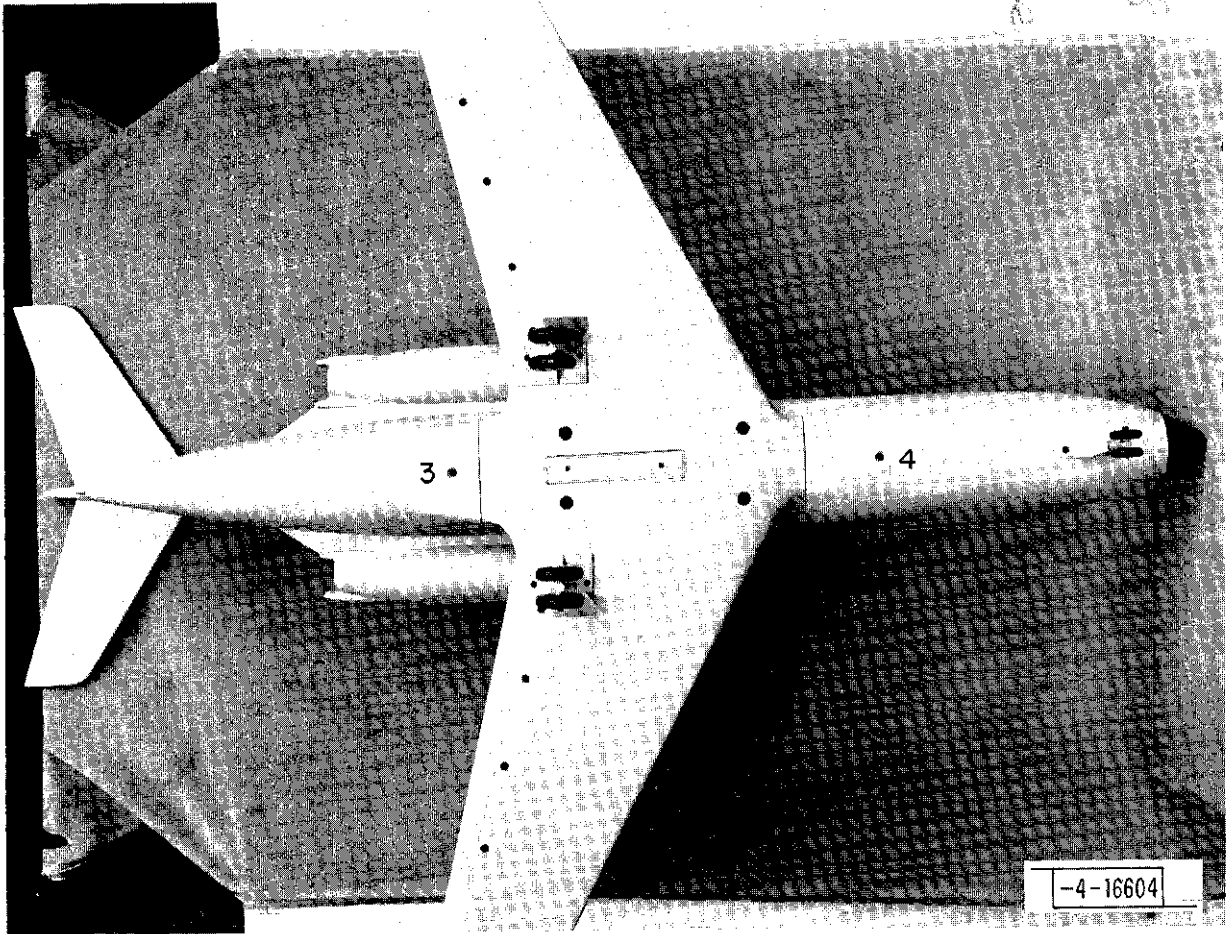


Fig. A-12. Grumman Gulfstream, bottom view showing antenna positions 3 and 4.



Fig. A-13. Gates Lear Jet, three-quarter view.

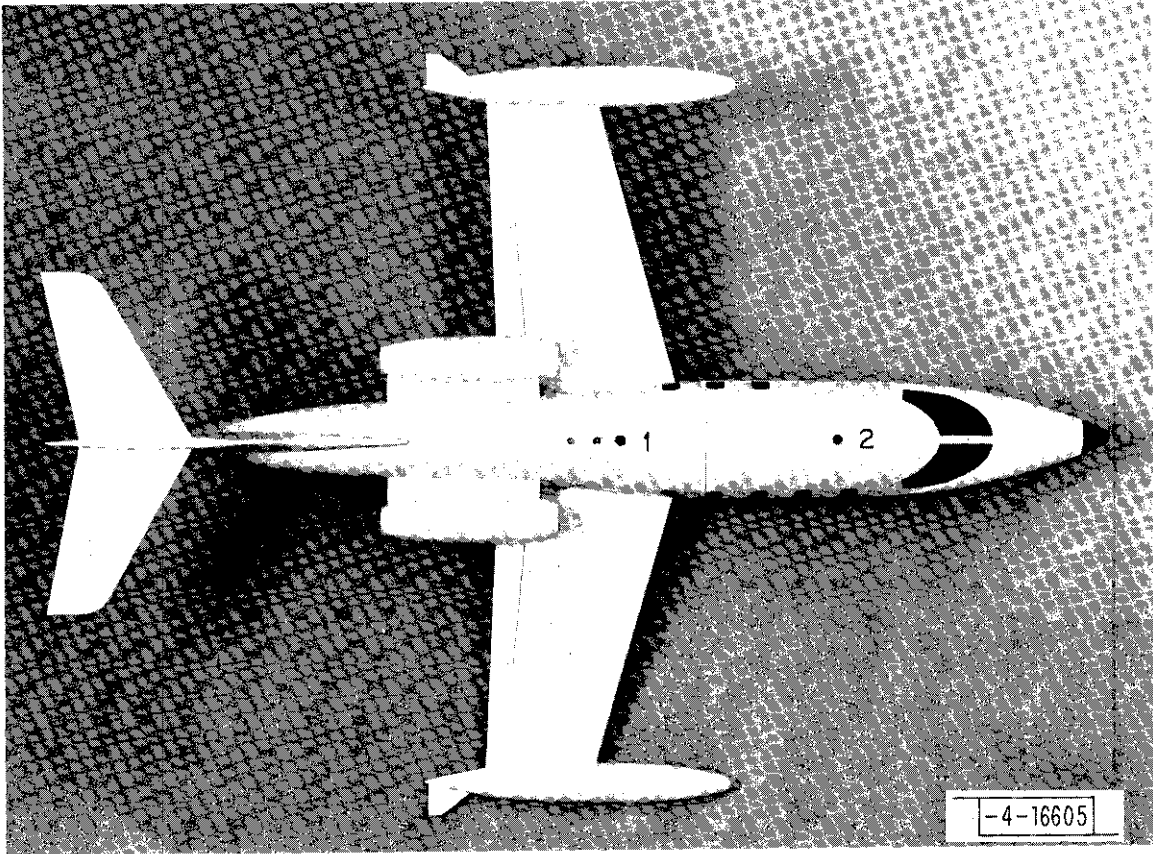


Fig. A-14. Gates Lear Jet, top view showing antenna positions 1 and 2.

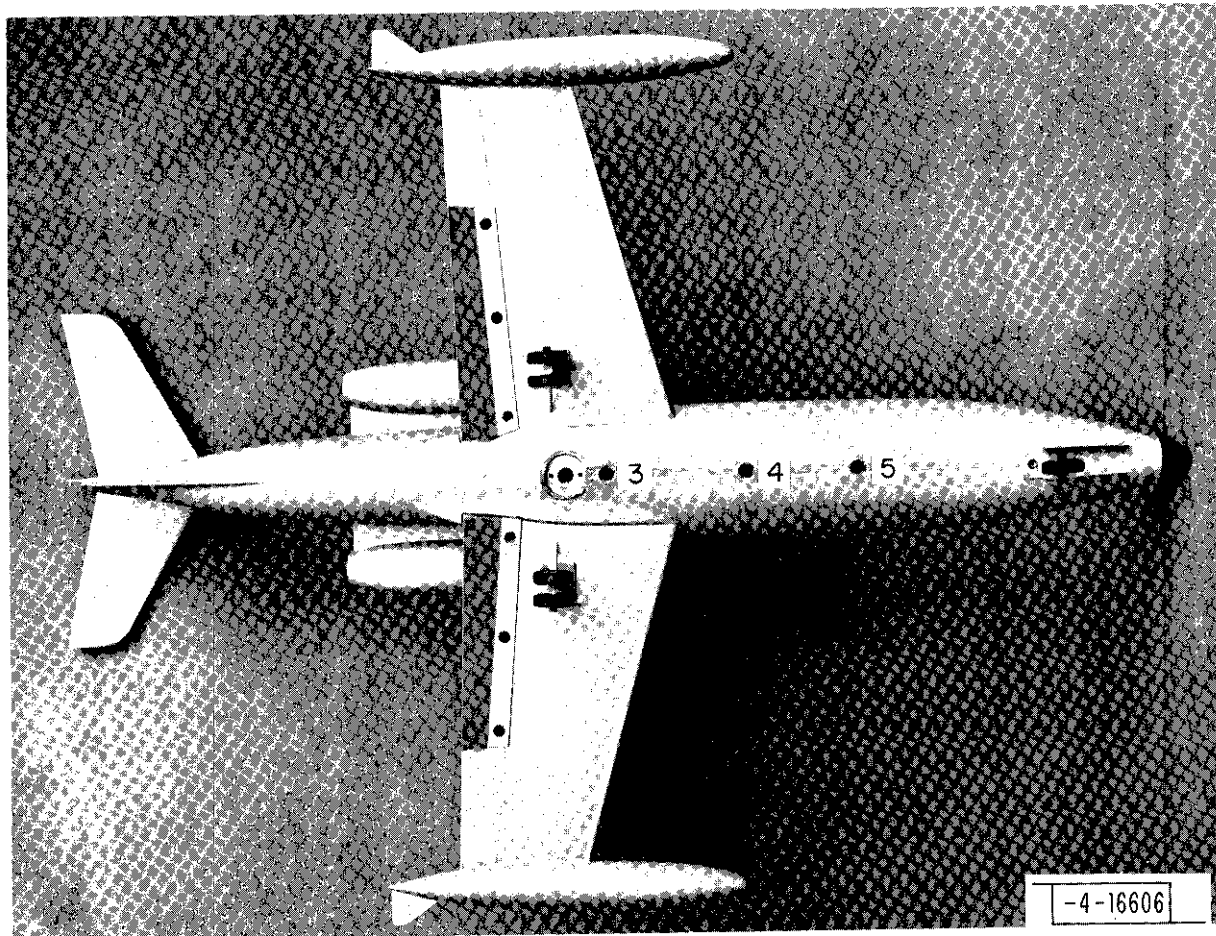


Fig. A-15. Gates Lear Jet, bottom view --
showing antenna positions 3, 4 and 5.

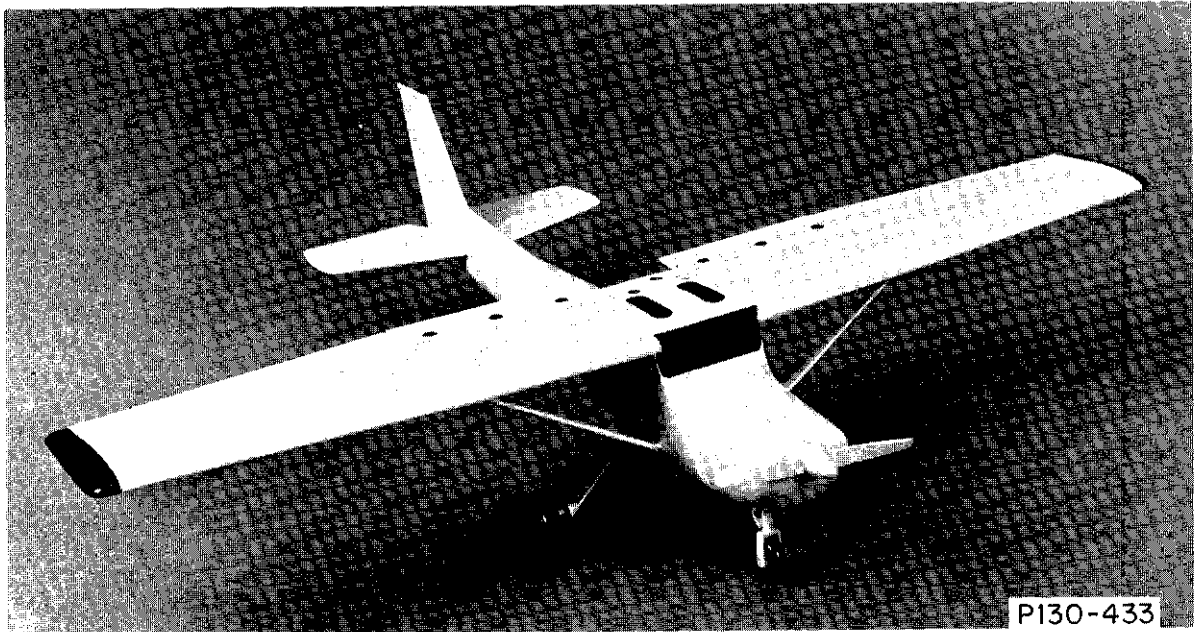


Fig. A-16. Cessna 150, three-quarter view.

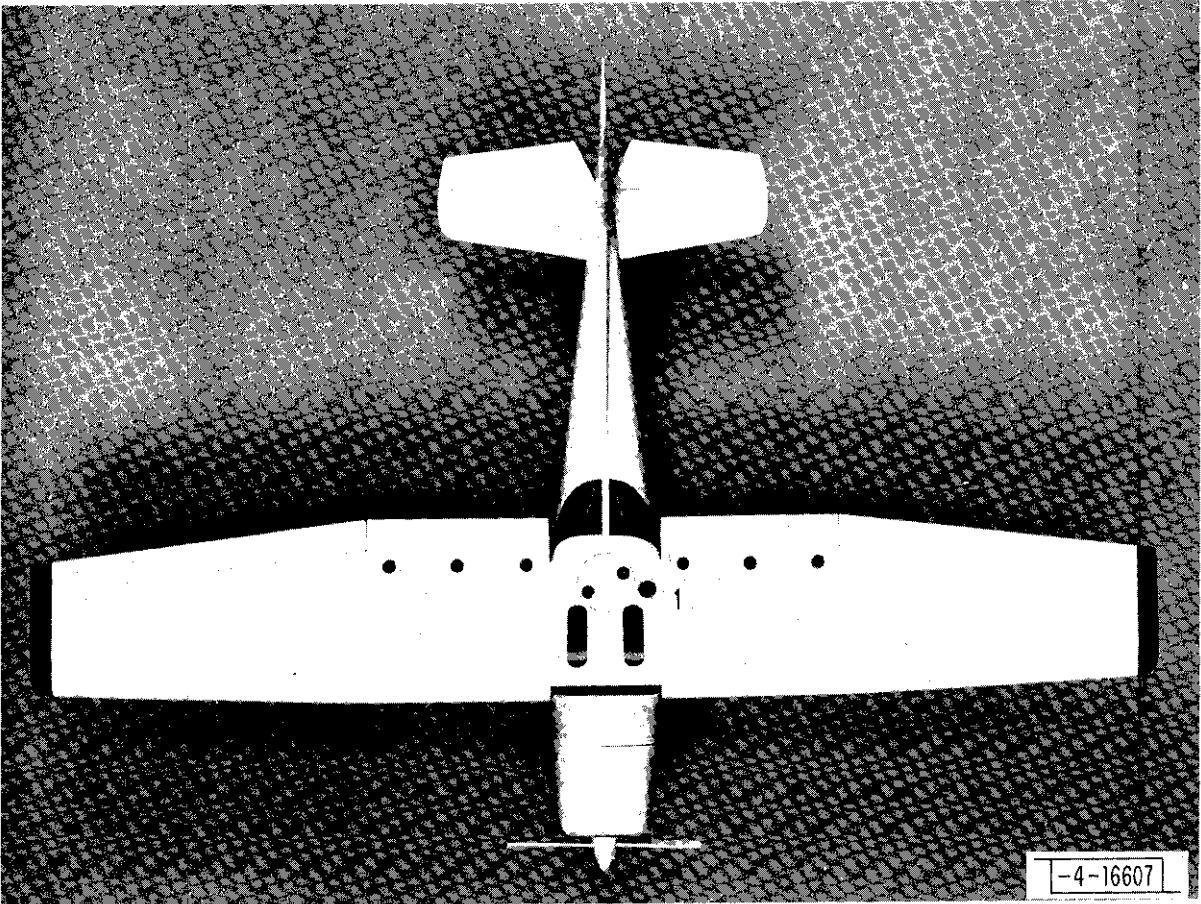


Fig. A-17. Cessna 150, top view showing antenna position 1.

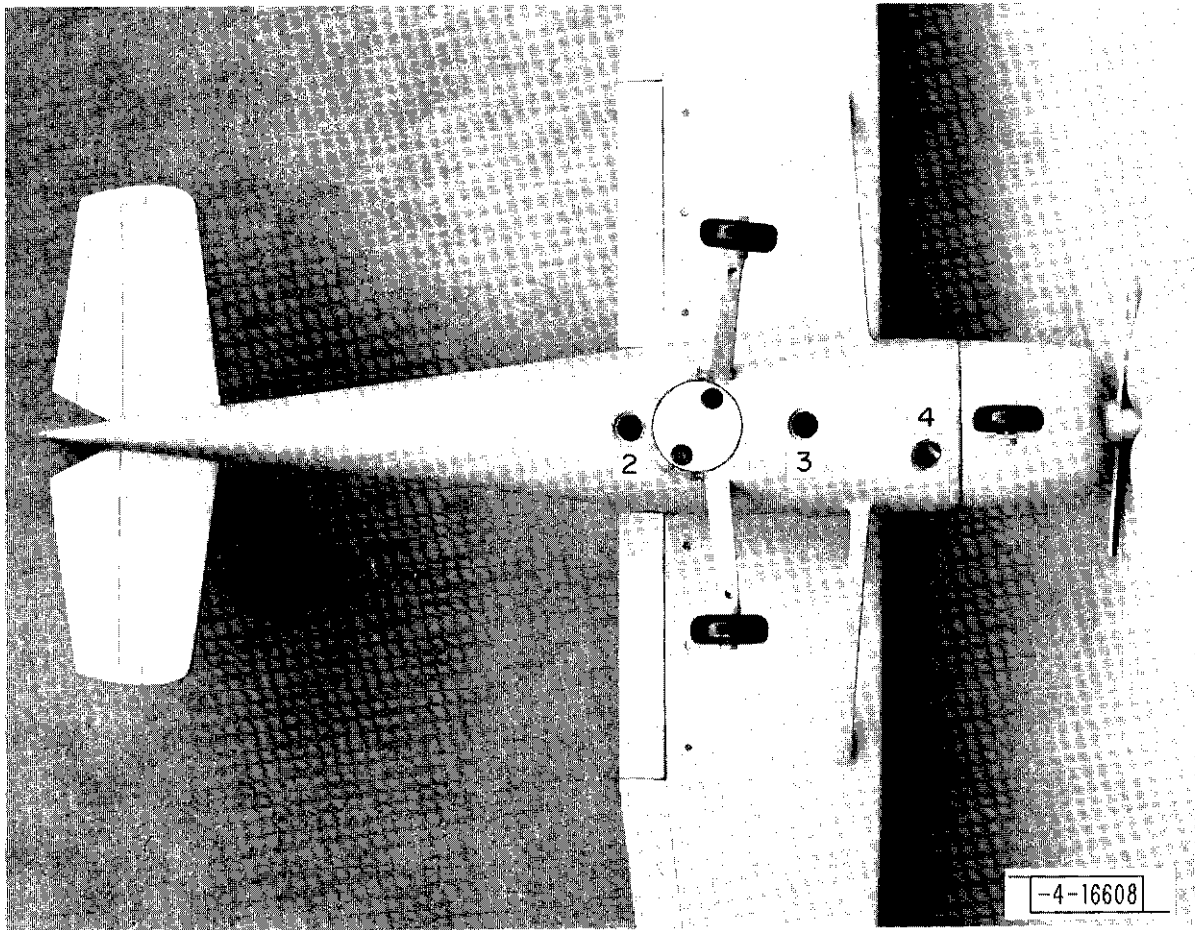


Fig. A-18. — Cessna 150, bottom view showing antenna positions 2, 3 and 4.

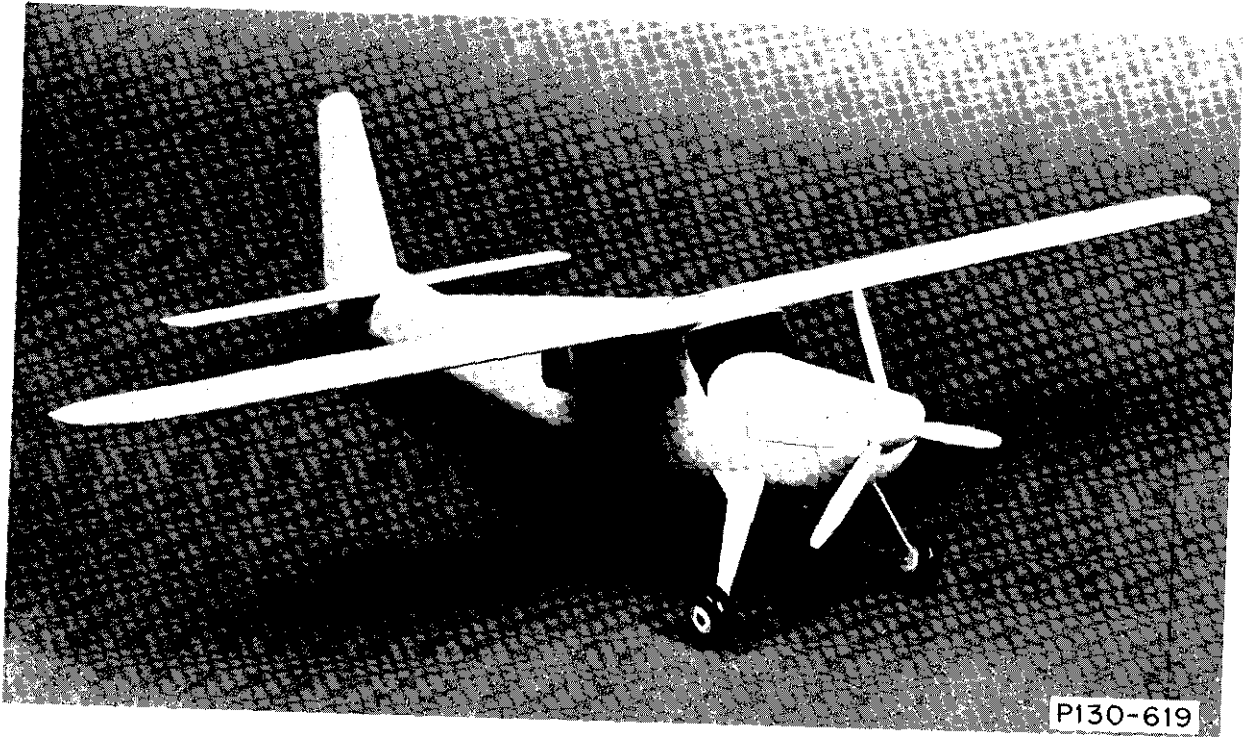


Fig. A-19. Helio V10D, three-quarter view.

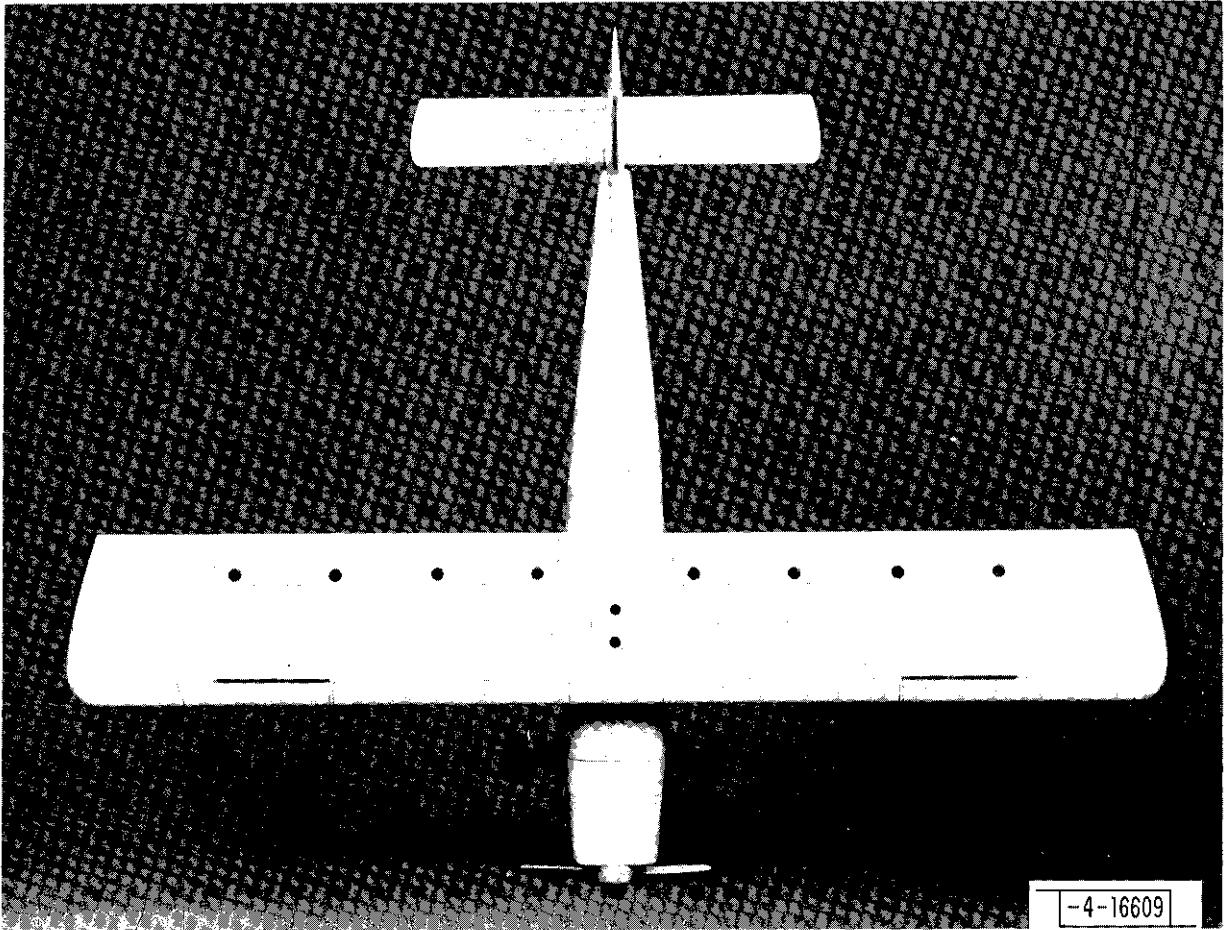


Fig. A-20. Helio V10D, top view

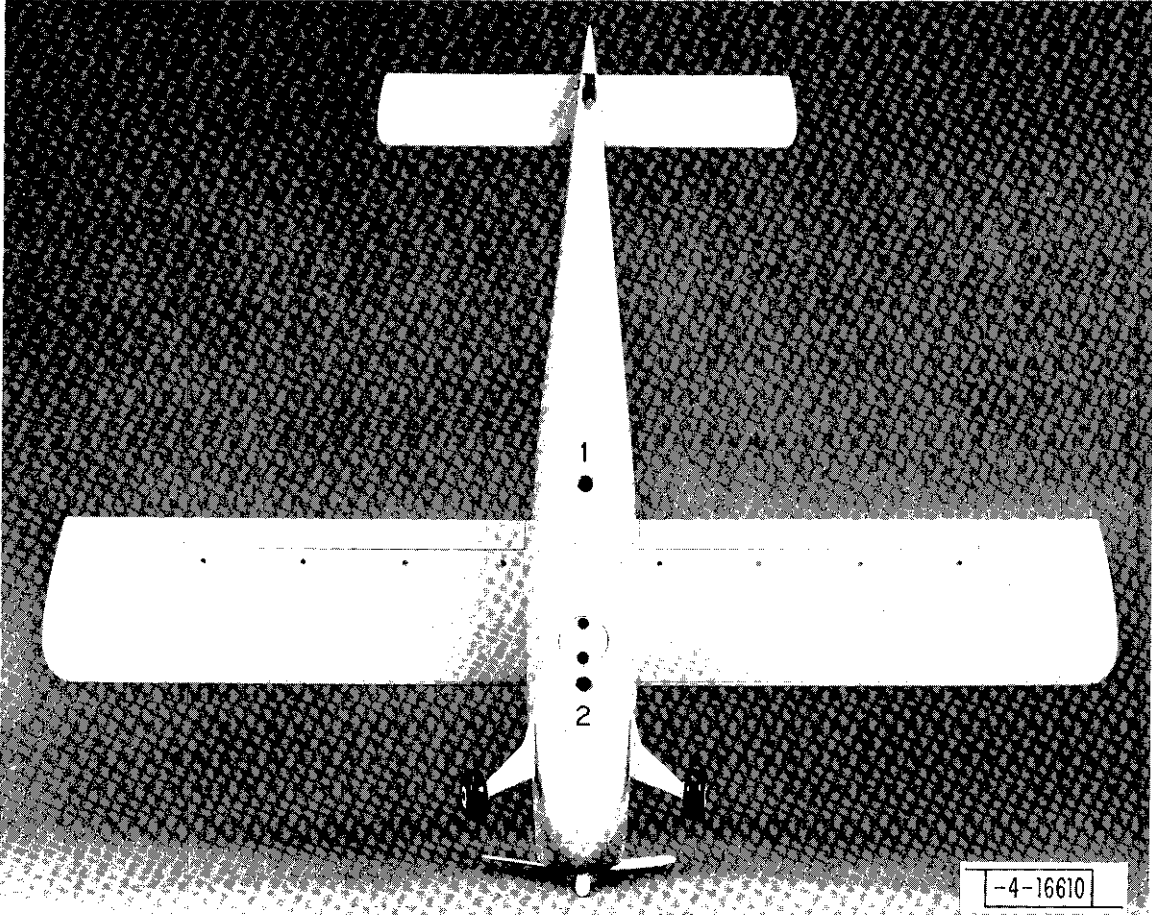


Fig. A-21. Helio V10D, bottom view showing antenna positions 1 and 2.

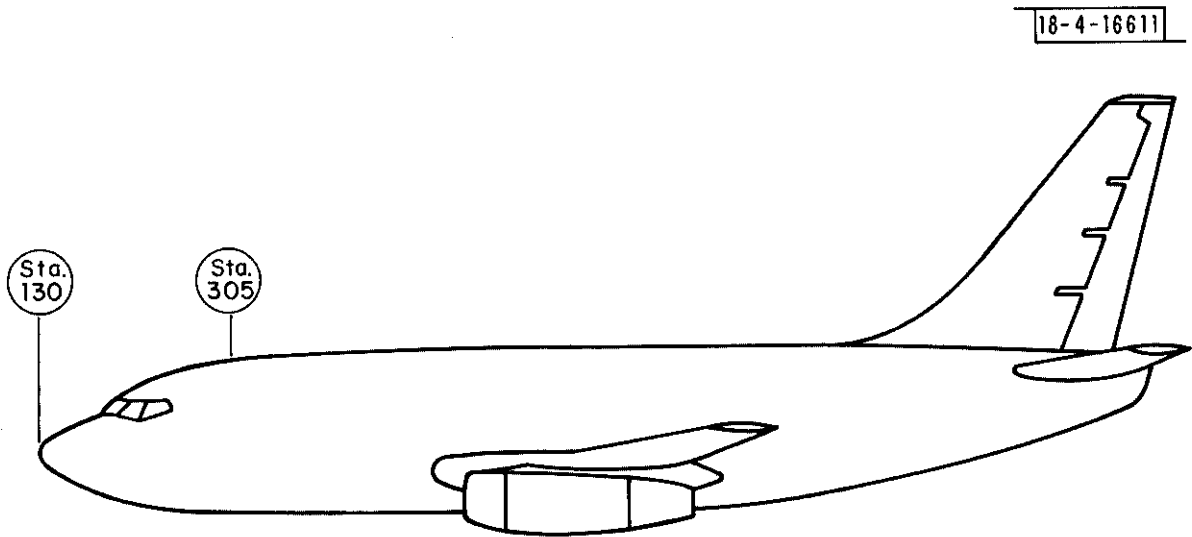


Fig. A-22. Boeing 737, side view showing station position of antennas 1 and 2.

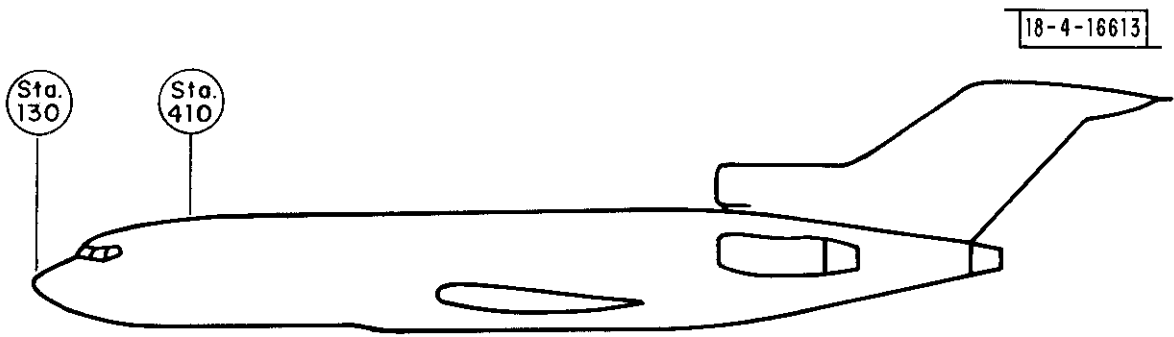


Fig. A-24. Boeing 737, side view showing station position of antennas 1 and 2.

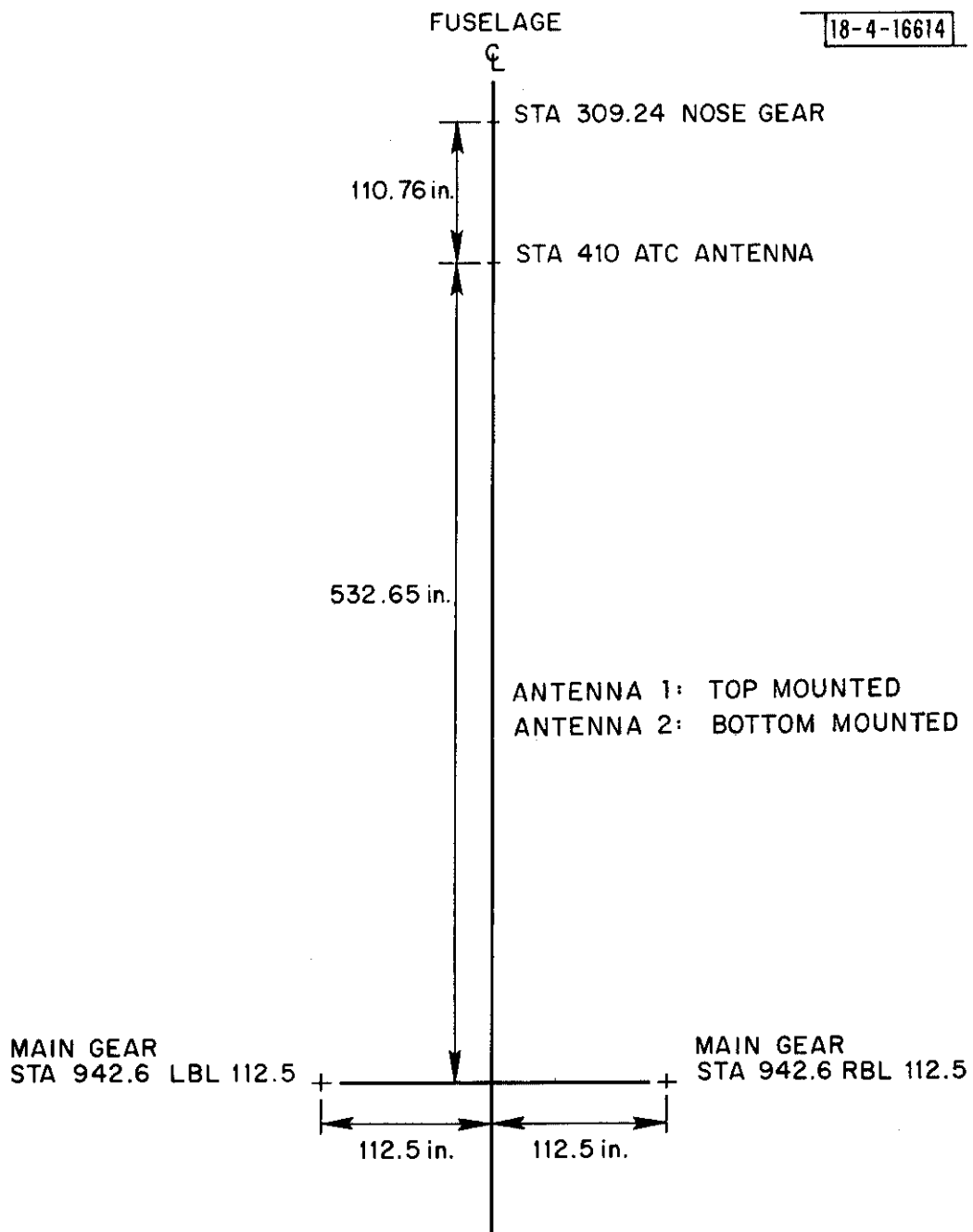


Fig. A-25. Boeing 727, relative positions of landing gear to antenna station.

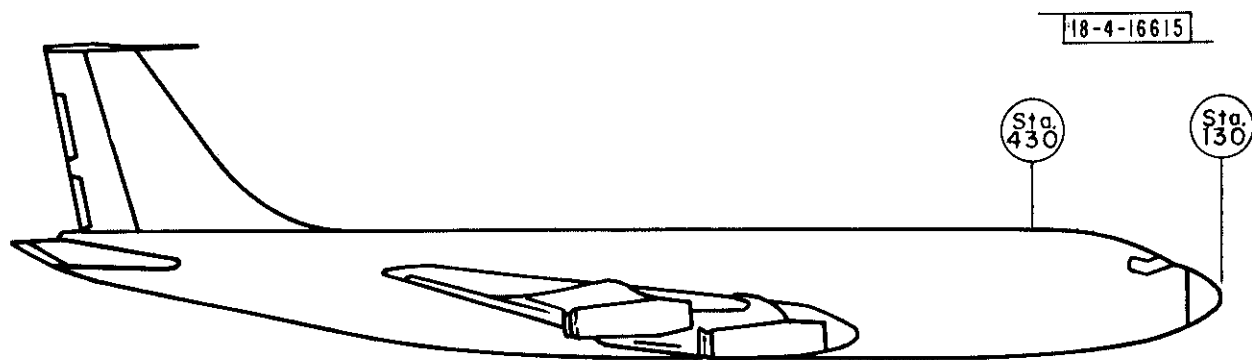


Fig. A-26. Boeing 707, side view showing station position of antennas 1 and 2.

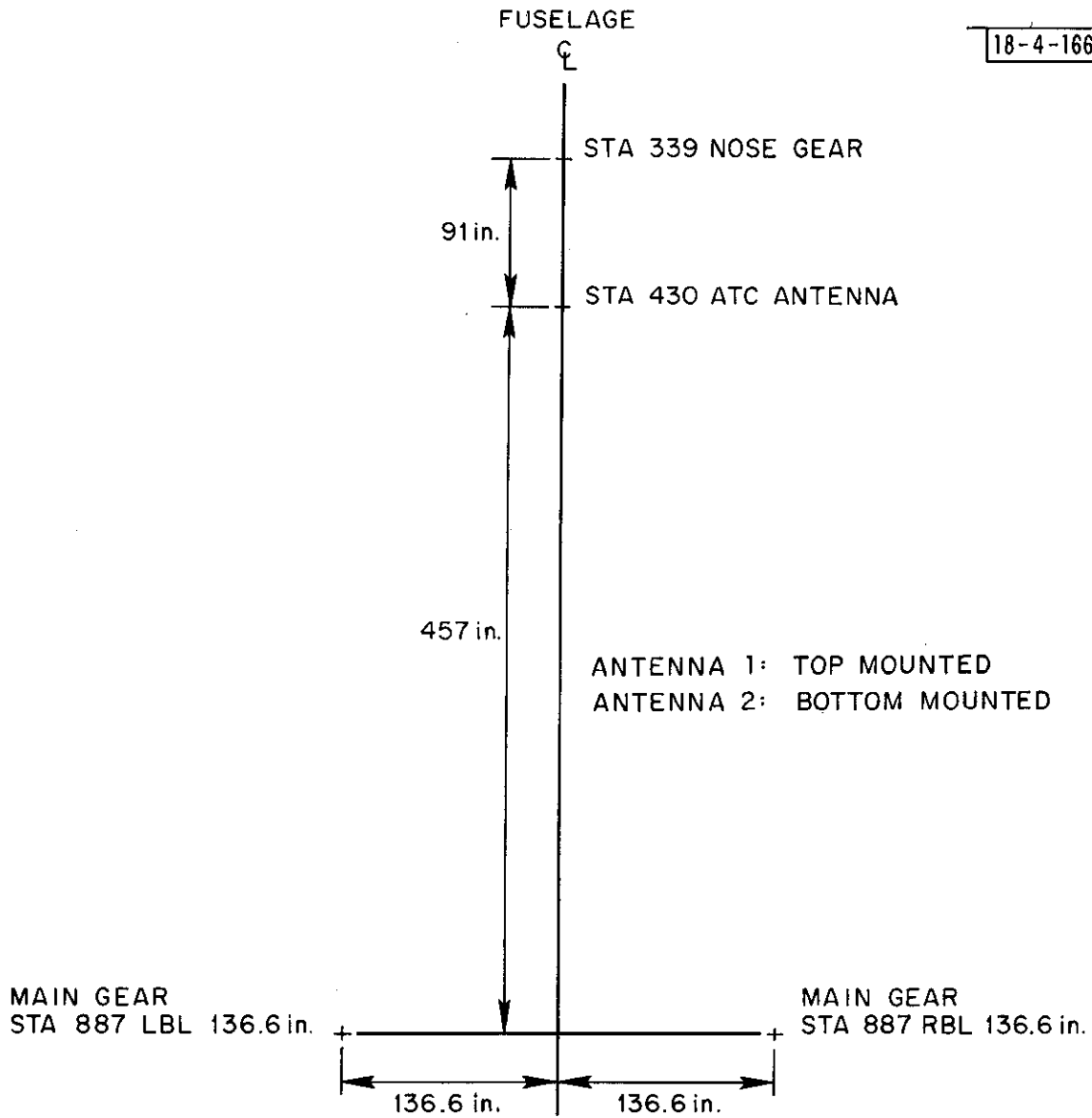


Fig. A-27. Boeing 707, relative positions of landing gear to antenna station.

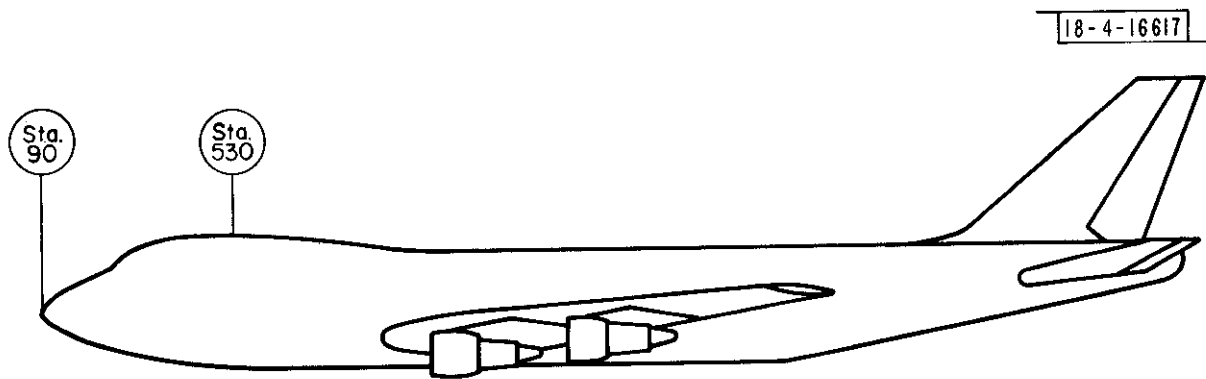


Fig. A-28. Boeing 747, side view showing station position of antennas 1 and 2.

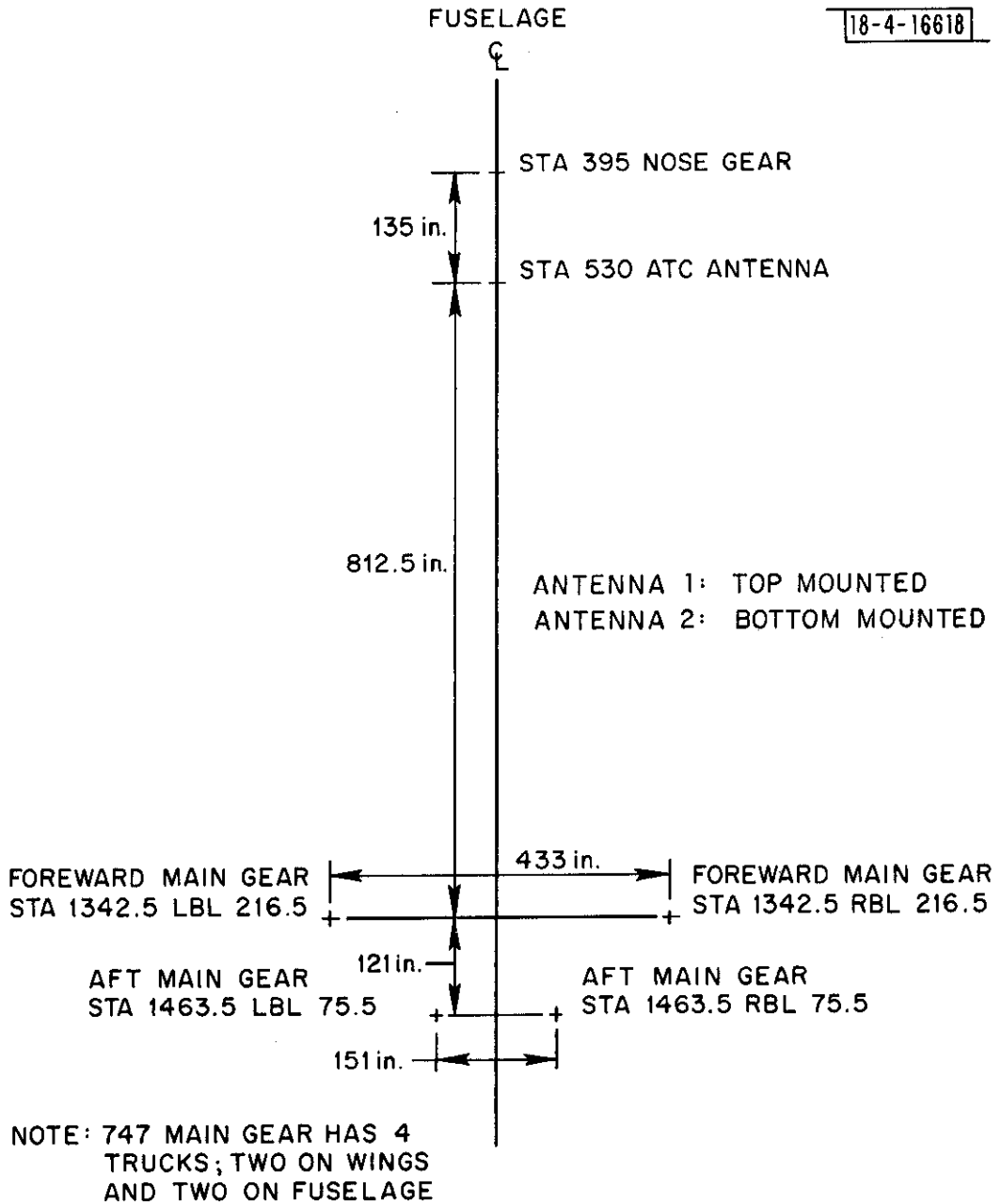


Fig. A-29. Boeing 747, relative positions of landing gear to antenna station.

APPENDIX B

AIRCRAFT-GROUND SENSOR COORDINATE RELATIONSHIPS

The Cartesian coordinate system for determining the aspect angles to the ground station is fixed to the aircraft. Let that system be labelled X_a, Y_a, Z_a . In addition to that system, let there be another coordinate system X_f, Y_f, Z_f , which has the same origin but whose orientation is fixed in airspace at the aircraft location. The positive Z_f -axis of this system points through the aircraft location from the center of the earth. The X_f and Y_f axes define a plane which is parallel to the earth tangent plane below the aircraft and whose orientation is fixed by pointing the positive Y_f axis north. These two coordinate systems are related by the three angles which describe the aircraft attitude: heading, pitch and roll. The three attitude angles are defined in the following manner:

- (a) Heading is a clockwise rotation about the Z_f axis;
- (b) Pitch is an upward rotation of the Y_a axis from the X_f, Y_f plane;
- (c) Roll is a counter-clockwise rotation about the Y_a axis.

These definitions are shown pictorially in Fig. B-1.

Now let the polar angles of a line joining the common origin of these coordinate systems and a ground sensor be defined as ξ and β , measured from the Z and X axes, respectively. The aircraft at the origin of this coordinate system is on a heading of γ degrees east of north, in a roll of ρ degrees ($\rho > 0$ for starboard turn), and at a pitch angle of Ψ degrees ($\Psi > 0$ for a climb). We wish to determine the angles θ and ϕ , as defined in Fig. 1 of the report, for the line of sight between the aircraft and the ground sensor.

18-4-16619

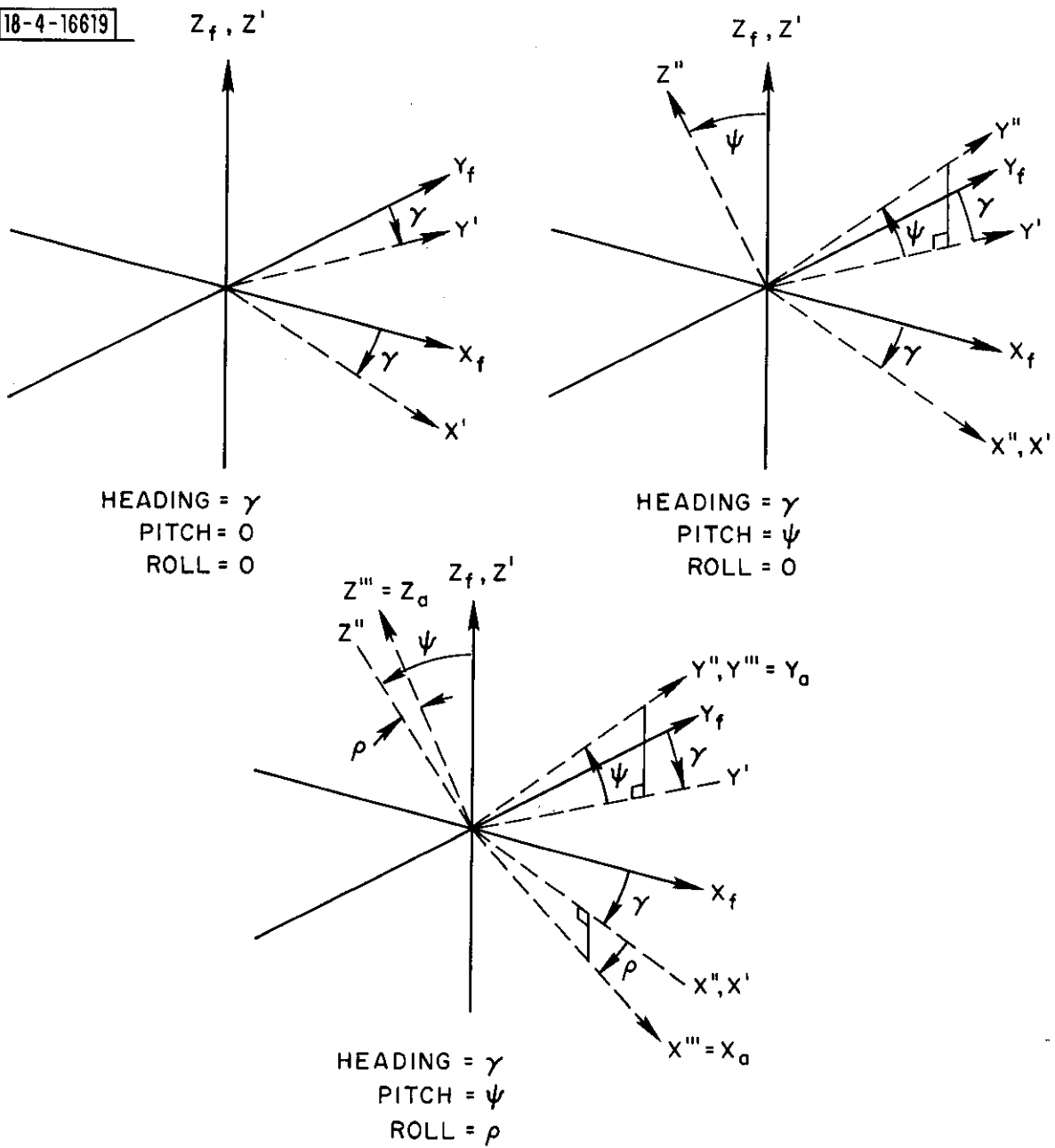


Fig. B-1. Coordinate rotations during maneuvers.

Initially a unit vector in the direction the line of sight to the sensor has the value:

$$\underline{u}_f = \begin{pmatrix} \sin \xi & \cos \beta \\ \sin \xi & \sin \beta \\ \cos \xi \end{pmatrix}$$

If the coordinates are now rotated about the Z_f axis by γ , an $X'Y'Z'$ coordinate system is established and the unit vector is now:

$$\underline{u}' = R_{\gamma} \underline{u} \quad \text{where } R_{\gamma} = \begin{bmatrix} \cos \gamma & -\sin \gamma & 0 \\ \sin \gamma & \cos \gamma & 0 \\ 0 & 0 & 1 \end{bmatrix}$$

If this coordinate system is rotated about the new X' axis by Ψ , a new value of u is obtained.

$$\underline{u}'' = R_{\Psi} \underline{u}' \quad \text{where } R_{\Psi} = \begin{bmatrix} 1 & 0 & 0 \\ 0 & \cos \Psi & \sin \Psi \\ 0 & -\sin \Psi & \cos \Psi \end{bmatrix}$$

Finally, rotated by ρ around the new Y'' axis:

$$\underline{u}''' = R_{\rho} \underline{u}'' \quad \text{where } R_{\rho} = \begin{bmatrix} \cos \rho & 0 & -\sin \rho \\ 0 & 1 & 0 \\ \sin \rho & 0 & \cos \rho \end{bmatrix}$$

The final unit vector will have the following coordinates:

$$\underline{u}''' = \underline{u}_a = \begin{pmatrix} \sin \theta & \cos \varphi \\ \sin \theta & \sin \varphi \\ \cos \theta \end{pmatrix}$$

Multiplying the matrices, \underline{u}_a is obtained:

$$\underline{u}_a = R_\rho R_\Psi R_\gamma \underline{u}$$

$$\underline{u}_a = \left\{ \begin{array}{l} \cos \rho \sin \xi \cos (\gamma + \beta) + \sin \rho \sin \Psi \sin \xi \sin (\gamma + \beta) - \sin \rho \cos \Psi \cos \xi \\ \cos \Psi \sin \xi \sin (\gamma + \beta) + \sin \Psi \cos \xi \\ \sin \rho \sin \xi \cos (\gamma + \beta) - \cos \rho \sin \Psi \sin \xi \sin (\gamma + \beta) + \cos \rho \cos \Psi \cos \xi \end{array} \right\}$$

Notice that if $\gamma = \rho = \Psi = 0$, the original vector is obtained as it should be.

Finally, using these results the desired solution for θ and φ is obtained:

$$\cos \theta = \sin \rho \sin \xi \cos (\gamma + \beta) - \cos \rho \sin \Psi \sin \xi \sin (\gamma + \beta) + \cos \rho \cos \Psi \cos \xi$$

and

$$\tan \varphi = \frac{\cos \Psi \sin \xi \sin (\gamma + \beta) + \sin \Psi \cos \xi}{\cos \rho \sin \xi \cos (\gamma + \beta) + \sin \rho \sin \Psi \sin \xi \sin (\gamma + \beta) - \sin \rho \cos \Psi \cos \xi}$$

APPENDIX C

EFFECT OF DEPRESSION ANGLE ON RADIATION STATISTICS

It is reasonable that a bottom-mounted aircraft antenna should be shielded less during maneuvers when the ground station is more directly beneath the aircraft. This fact is demonstrated by computing the statistical distribution of gains as the value of δ (depression angle, see Fig. 20) is increased as shown in Fig. C-1. In this figure the gain values marking the worst 1%, 10% and 20% of the geometric conditions are plotted as δ changes in half-degree steps. In the report a value of 1° is used because it approximates a worst condition. A value of zero would have been unrealistic since, by Fig. C-2, the aircraft disappears over the horizon before δ reaches zero.

This improvement of the gain distribution does not continue until the aircraft is overhead because cross polarization losses become very large as the dipole stub on the aircraft is looked at closer to end-on.

The use of a top-mounted antenna only would, of course, give even poorer results as δ is increased from zero, especially during level flight conditions when the entire airframe shields the antenna.

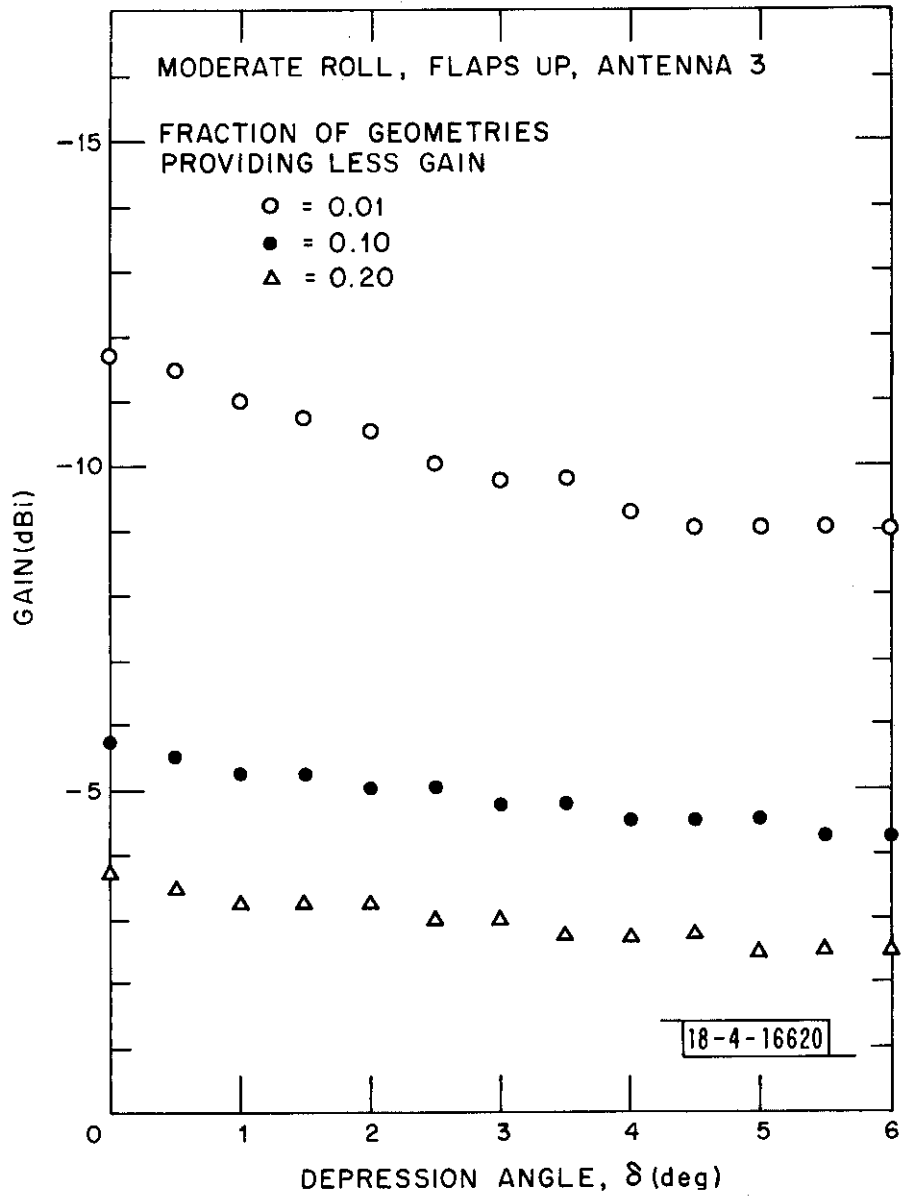


Fig. C-1. Gain distribution improvement as a function of depression angle for Cessna 150.

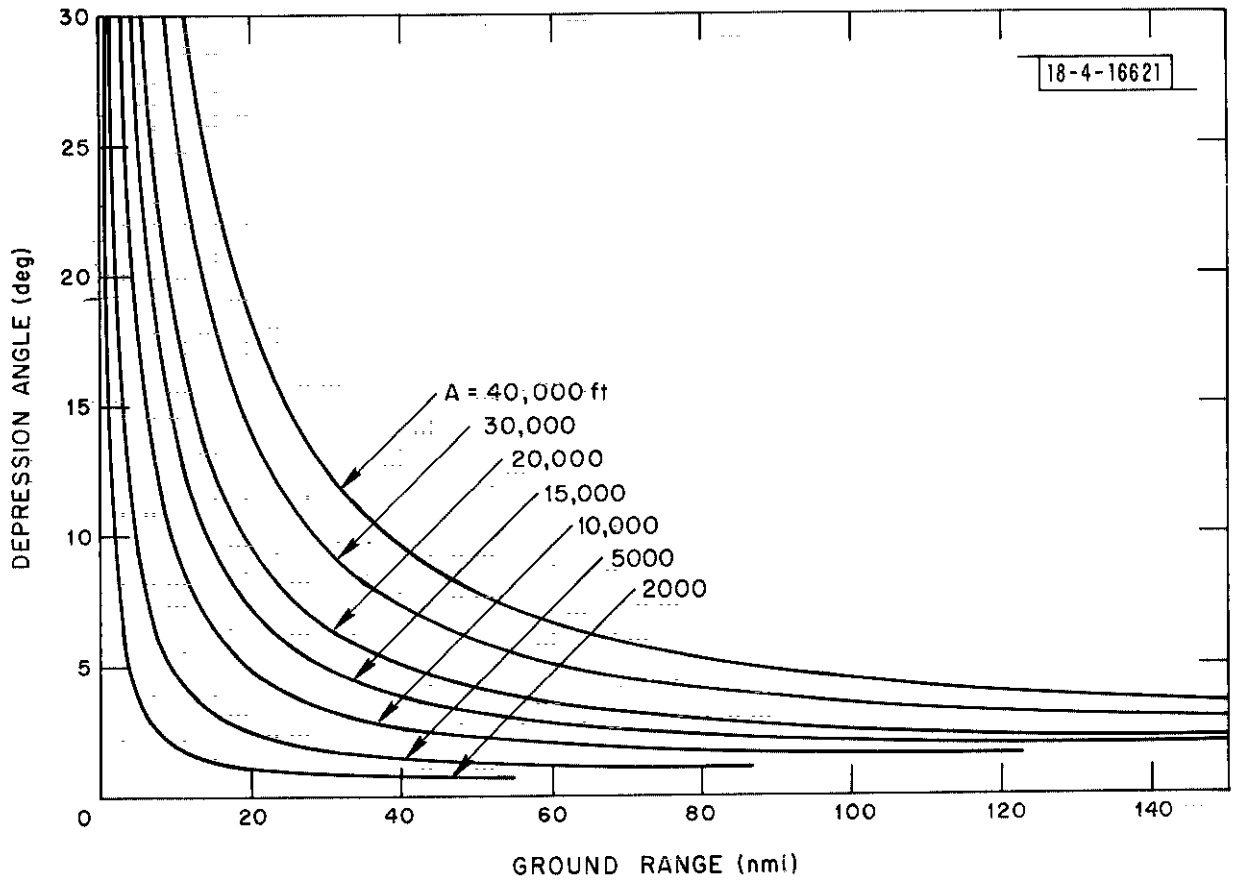


Fig. C-2. Depression angle versus ground range for aircraft at various altitudes.